Avdelningen för Konstruktionsteknik
Lunds Tekniska Högskola
Box 118
221 00 LUND

Division of Structural Engineering
Faculty of Engineering, LTH
P.O. Box 118
S-221 00 LUND
Sweden

Analysis of suspended bridges for isolated communities

- *With emphasis on wind stability*

Analys av lätta hängbroar för isolerade samhällen

- *Med fokus på vindstabilitet*

Viktor Hermansson & Jonas Holma

2015

Rapport TVBK-5243
ISSN 0349-4969
ISRN: LUTVDG/TVBK-15/5243+88p

Examensarbete
Examinator: Professor Roberto Crocetti, LTH
Handledare: Anders Klasson, LTH
Handledare: Ivar Björnsson, LTH
Handledare: Karl Lundstedt, SKANSKA
Handledare: Gustav Svensson, SKANSKA
Juni 2015

Abstract

Light suspended bridges are often used to connect villages or trail systems in geographical areas with lacking infrastructure and demanding topology. Different international non-profit organizations in collaboration with local promoters are building these bridges with the purpose of connecting isolated communities with health care and education.

The design and construction of these bridges has by and large relied on engineering judgment and design conservatism coupled with past experiences of similar construction projects. An interest to engage in the designing of similar bridges has been shown from staff at the Division of Structural Engineering at the Faculty of Engineering of Lund University. This master thesis aims therefore to provide more sophisticated models of suspended bridges as material for future work.

Suspended bridges are suitable to use for long spans, both due to low construction cost and to efficient material usage. They can also most often be built without advanced tools or machinery. The bridges studied in this thesis are intended for pedestrians and animals which result in a very slim design.

Recommendations mainly from the development organization Helvetas will be compared to the Eurocode to investigate if these creates overly conservative designs. These comparisons will be made with both hand calculations, the finite element software Brigade/Plus and data from existing bridges.

Vibrations and sways due to wind can be a major problem for light suspended bridges. Due to their small dead load in combination with a low lateral stiffness, the sways and vibrations can be very large in comparison with more common pedestrian bridges. This could lead to temporary inoperability or in worst case structural failure. With the models made in Brigade/Plus, wind effects can be analyzed and suitable measures or restrictions can be proposed.

Key words: Suspended bridge, wind loads, dynamic response, vibrations, cables, FE-analysis, modal superposition.

Sammanfattning

Lätta hängbroar används ofta för att sammankoppla samhällen i områden med bristande infrastruktur och krävande topologi. Dessa broar byggs genom samarbete mellan internationella hjälporganisationer och lokala initiativtagare med syftet att tillgängliggöra sjukvård och utbildning.

Designen på de broar som byggs bygger ofta på empiriska erfarenheter. Intresse för att engagera sig i dimensionering av liknande broar har visats från personal på Avdelningen för Konstruktionsteknik vid Lunds Tekniska Högskola. Denna uppsats syftar därför på att skapa en mer precis dimensionering av dessa broar som underlag för framtida arbete.

Lätta hängbroar är en mycket materialeffektiv konstruktion som kan överbrygga långa spann till ett relativt lågt pris. De kan dessutom oftast byggas utan avancerade verktyg eller maskiner. De broar som studeras är alla avsedda för gångtrafik från människor och djur vilket medför en slank design.

Rekommendationer från främst organisationen Helvetas jämförs med Eurocode för att utreda om dessa skapar onödigt robusta konstruktioner. Dessa jämförelser sker med både handberäkningar, finita element-programmet Brigade/Plus samt data från existerande broar.

Vibrationer och svängningar orsakade av vind kan innebära ett stort problem för lätta hängbroar. På grund av deras låga egentyngd samt deras låga styvhet i transversell riktning kan dessa svängningar bli mycket stora i jämförelse med mer vanliga gångbrotyper. Detta kan leda till att bron blir tillfälligt obrukbar eller i värsta fall blåser sönder. Med de modeller som byggs upp i Brigade/Plus kommer vindeffekter att kunna analyseras och lämpliga åtgärder eller begränsningar föreslås.

Nyckelord: Hängbro, vindlaster, dynamisk respons, vibrationer, kablar, FE-analys, modal superpositionering

"What would be the best bridge? Well, the one which could be reduced to a thread, a line, without anything left over; which fulfilled strictly its function of uniting two separated distances."

Pablo Picasso

Preface

This master thesis is the final phase of our five year Master Program in Civil Engineering at the Faculty of Engineering, LTH, at Lund University. As always in the start of a project, this thesis had a very wide objective, which during the last months has made us humble to how much we still have to learn. However, this has been the most intensive and educational time during our time at the university.

The subject of this thesis was proposed by the Division of Structural Engineering and the thesis has been carried out at Skanska AB in Malmö.

There are many people we would like to thank, especially our examiner Professor Roberto Crocetti and our supervisors Anders Klasson and Ivar Björnsson at the Division of Structural Engineering for all your ideas and support, and Karl Lundstedt and Gustav Svensson at Skanska Malmö for all the good advice and for letting us be a part of your team for half a year.

We would also like to thank Helvetas and Bridges to Prosperity for providing us with helpful material, and Scanscot Technology for their Brigade/Plus support.

Finally we would like to thank our families and friends for all their support during these years, and last, but by no means least, all our classmates in whose company these years have been fantastic.

Lund June 2015

Viktor Hermansson & Jonas Holma

Innehållsförteckning

1 Introduction

1.1 Background

Cable supported bridges are widely used because of their ability to overcome large spans. The term cable supported bridges includes many different types of bridges, for example suspended-, suspension- and cable stayed bridges. This thesis will focus on the designing and construction of suspended bridges.

Figure 1.1 A suspended bridge (With permission from Bridges to Prosperity)

The suspended bridge contains load carrying cables for the walkway and also often for the handrails. Because of its natural shape the main use is as a pedestrian bridge. The reason for the widely use of suspended bridges in aid projects around the world is that the structure is relatively simple and have shown to be convenient for construction in rural areas since it can cross large span in combination with being material efficient and therefore quite cheap. A suspended bridge can most often be built without the use of heavy machinery and it requires very little maintenance.

Suspended bridges has a typical span smaller than 200 meters, but spans up to 350 meters exist, for example the 337 meter long Arroyo Cangrejillo Pipeline Bridge in Argentine (OPAC Consulting Engineers, 2015) and the 344 meter long Kusma-Gyadi Bridge in Nepal (Ekantipur, 2015). Longer spans are usually pure suspension bridges but can also be a combination, i.e. a suspension bridge with very short pylons, for example the 406 meter long Highline179 in Ruette, Austria. Almost all bridges with spans of this magnitude are stabilized in their lateral direction with so-called windguys to prevent wind induced movements. A suspended bridge fitted with windguys can be seen in Figure 1.2.

Suspended bridges can also be uses as road bridges, so-called stress ribbon bridges, but in these cases the deck is made much stiffer and the suspended cables or ribbons are often pre-stressed.

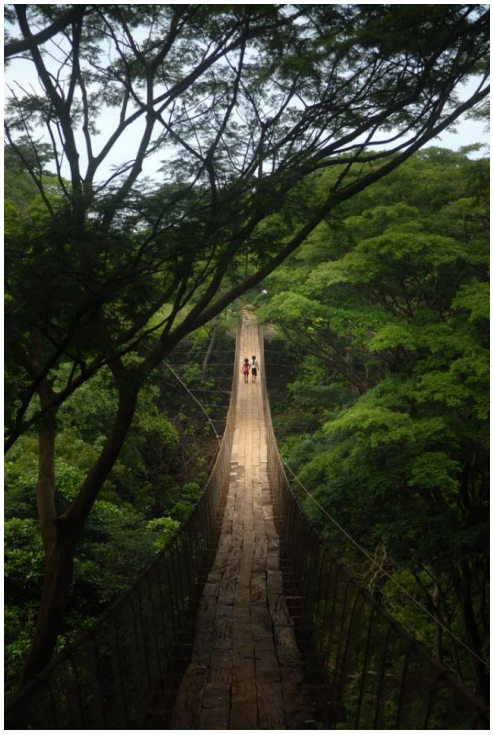

Figure 1.2 A suspended bridge with visible windguy arrangement below (With permission from Bridges to Prosperity)

The Suspension bridge has taller towers at the supports which gives a larger sag and a more effective transfer of vertical loads. The cable and the deck are connected with vertical hangers. The deck can be made more or less stiff. Suspension bridges have the advantage of having a horizontal walkway or traffic path, but it can even take a convex shape if the designer finds this more preferable. The two bridge types are shown in Figure 1.3 and Figure 1.4 below.

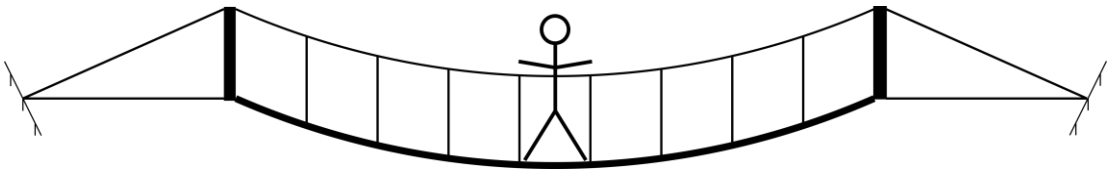

Figure 1.3 Suspended bridge

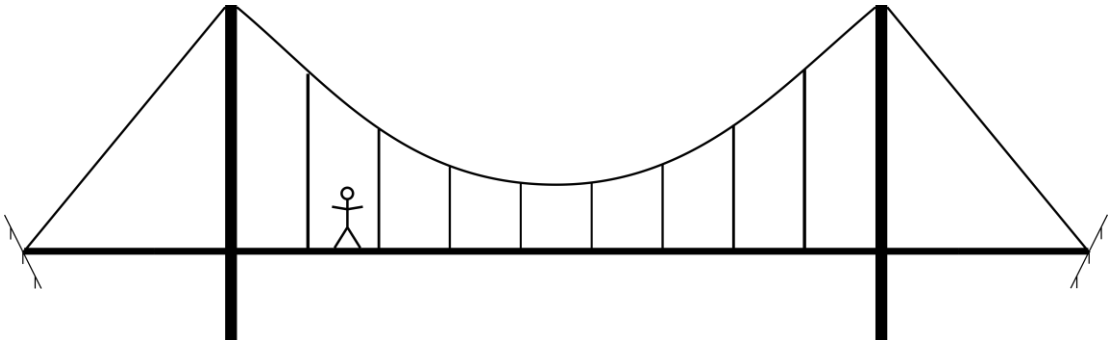

Figure 1.4 Suspension bridge

1.2 Aim

The general aim of this thesis is to highlight suspended bridges and make their design and structural behavior more understandable for both the general reader of this thesis and, especially, for future designers of these type of bridges.

The differences between designing according to Helvetas or Eurocode will be investigated since this can result in a different design criteria and therefore lead to more material efficient and cheaper bridges.

An investigation of the wind stability of light suspended bridges will be made. The aim of this investigation is to formulate design criteria for windguys, i.e. when and why they should be used?

Hand in hand with the wind stability goes the dynamic behavior of suspended bridges. A study of the natural frequencies and appurtenant modes and how they are affected by the sag and the span of the bridge will be done.

Another aim of this thesis is to create a design guide in Excel which can be used to design suspended bridges according to both Helvetas and Eurocode. This guide will make a fast and accurate design of the bridge main cables possible. A careful comparison between the results from the design guide and result from finite element models will be done to validate both methods.

1.3 Limitations

It's only the bridge structure, i.e. the structure between the saddles at the two abutments that will be analyzed and discussed in this thesis. Everything else, for example design of abutments, slope stability and technical survey etc, will be left for further investigations. The focus of this thesis is on the main bearing elements which leads to that no connectors will be investigated.

The type of wind stabilization system used is windguys that are symmetrically designed around the midpoint of the bridge. Other types of stabilization systems (which obviously exists) will not be investigated thoroughly.

Vertical dynamic response due to pedestrian traffic will also be out of scope for this thesis.

1.4 Outline

This thesis is divided into 9 different chapters.

Chapter 1 contains an introduction to suspended bridges and a short presentation of the thesis.

Chapter 2 contains background theory of all the forthcoming chapters. Statics and dynamics of the singe cable, loads and an introduction to the finite element software Brigade/Plus.

Chapter 3 contains a description of the reference bridge.

Chapter 4 contains both static and dynamic analyses of the single cable.

Chapter 5 contains a static analysis of suspended bridges. This includes hand calculations compared to finite element models, stress distribution between cables, displacements and the connection between span and cable diameters.

Chapter 6 contains a dynamic analysis of suspended bridges. This includes displacements and accelerations due to a wind impulse and the determination of natural frequencies.

Chapter 7 contains the conclusions from this thesis.

Chapter 8 contains all the references.

Chapter 9, the annex, contains a design guide and pictures of natural frequency modes.

2 Background theory

2.1 History of suspended and suspension bridges

The model of suspending a rope as main load carrying element has been used for a very long time. The Incas connected its 39 000 km long networks of roads with suspended bridges made of ropes (BBC, 2015). An example of such a bridge can be seen in Figure 2.1.

Figure 2.1 A replica of a traditional Inca rope bridge (Dylan Thuras; Atlas Obscura, 2015)

However, the first cable supported structure with drawn iron wires was built in 1823 in Geneva (Gimsing, 1997). The main types used today are cable-stayed bridges with typical spans up to 1100 meters and suspension bridges with typical spans between 1000 and 2000 meters. For example the current world record holder for suspended bridges is the Akashi Kaikyō Bridge in Japan with a main span of 1991 meter. Bridges with longer spans are planned, for example the Messina strait bridge, and if this bridge ever to be built, its main span will have a length of 3.3 kilometers (COWI, 2015).

2.2 Description of a typical suspended bridge

As mentioned in the introduction, the span of the suspended bridges this thesis concerns seldom exceeds 200 meters. For these bridges the design are often very similar. The two main foundations are placed on each side of the span and the elevation of them can be either the same (level bridge) or it can differ (inclined bridge). These main foundations are usually designed as gravity foundations even if anchorage rods may be used if the space for gravity foundations is limited. The cables can be attached either adjustable or nonadjustable to the main foundations. Both the handrail and the lower cables acts as load-bearing elements and they are connected with hanger rods throughout the bridge. The hanger rods are connected at top to the handrail

cables and at the bottom to the cross-beams. The cross-beams are bolted to the main cables and supports the walkway deck. If there is need for wind stabilization, windguys can be added to the structure. A visualization of the bridge described above can be seen in Figure 2.2 below.

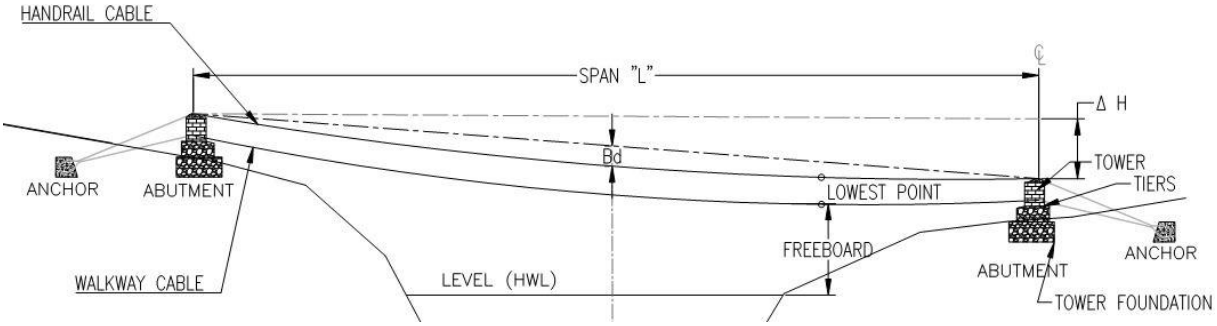

Figure 2.2 A typical suspended bridge

2.3 Suspended bridges in aid projects

As described in the introduction suspended bridges are widely used in aid projects around the world. Communities, that for several months every year are isolated due to impassible rivers, can with a suspended bridge be provided with a safe route to education, health care and economic possibilities. The construction of a suspended bridge requires a large community participation. Community participation during construction includes transport of materials, collection of locally available materials such as sand, stones and wood and site clearing and excavation. Since the community will be both the owner and user of the bridge, it will also be responsible for the long time bridge maintenance and repair

2.4 Helvetas and Bridges to Prosperity

Helvetas and Bridges to prosperity are two organizations that designs and builds bridges to connect isolated communities. Both organizations aims to provide better and safer access to health care, education and economic opportunities for these communities.

Helvetas Swiss Intercooperation is an aid organization that works in more than 30 countries (Helvetas, 2015). Since 1972, Helvetas has been involved in trail bridge building in Nepal, and later on in other countries as well. This work has, in collaboration with other organizations, ended up in the Short Span Trail Bridge Standard (SSTBS) and the Long Span Trail Bridge Standard (LSTBS). These two manuals gives guidance for the construction of suspended and suspension bridges. Both the Short Span Trail Bridge Standard and especially the Long Span Trail Bridge Standard will be used in this thesis.

Bridges to Prosperity is an American aid organization with focus on bridge building in rural and isolated areas. Bridges to Prosperity was founded in 2001 and they work mostly in Central America, South America and Africa. The manual from Bridges to Prosperity are based on the manuals from Helvetas, with some modifications.

2.5 Cables

2.5.1 Types of cables

Parallel wire cables

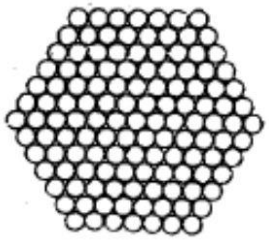

Figure 2.3 Parallel wire cable

Parallel wire cables, as seen in Figure 2.3, are the most widely used cables in suspension bridges. They consist of a number of wires, laid parallel and straight throughout the whole length of the cable. These cables are constructed by in situ spinning or by assembling a number of preformed parallel wire strands. The void ratio of parallel wire cables after compaction is generally 18-22 % (Ryall, Parke, & Harding, 2000). The stiffness of a parallel wire cable is around E=200 MPa (LTH, Structural Engineering, 2014)

Spiral cables

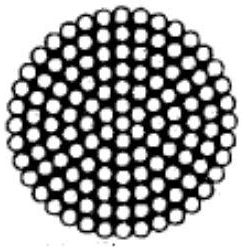

Figure 2.4 Spiral cable

Spiral cables, as seen in Figure 2.4, consist of a straight center core wire with multiple layers of round steel twisted around it. Each layer of wires is twisted in the opposite direction to the preceding layer. The twist of the wires result in a 15-25 % decreased stiffness and the cable strength is reduced to around 90 % of the sum of the breaking strength of the individual wires (Ryall, Parke, & Harding, 2000). The stiffness of a spiral cable is around E=150 MPa (LTH, Structural Engineering, 2014).

Locked coil cables

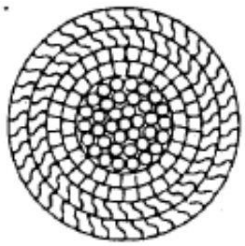

Figure 2.5 Locked coil cable

Locked coil cables, as seen in Figure 2.5, are very similar to spiral cables. They consist of, just like spiral cables, a straight center core wire with multiple layers of round steel twisted around it. They differ in that the final layers of wire consist of Z-shaped wires. These wires lock into each other and create a smooth exterior surface. The Z-shaped wires also minimize the void space in the cross-sectional area. The compact outer layers of the cable make protective wrapping unnecessary, but they make inspection and maintenance of the inner strands difficult (Ryall, Parke, & Harding, 2000). The stiffness of locked coil cables is around E=160 MPa (LTH, Structural Engineering, 2014).

Wire rope / Strand rope

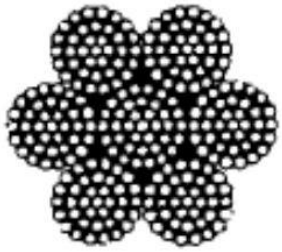

Figure 2.6 Wire rope / Strand rope

Wire rope, as seen in Figure 2.6, usually consists of 6 spiral cables twisted around a core strand, but the number can vary a lot. The core could be made of either steel or synthetic material. Wire ropes are very flexible which makes them suitable for cranes, ski lifts etc. The flexibility depends on the choice of material of the core. A ropewith a synthetic core is more flexible than a rope with a steel core but it’s

more sensitive to crushing than the steel core rope. Wire rope is not usually used in bigger suspension bridges since the other types of cables mentioned above are more suitable for this purpose (LTH, Structural Engineering, 2014). However, in this dissertation wire rope will be used as main load carrying element since it's the most common solution for suspended bridges in rural and remote areas. Wire rope is a mass fabricated standard product which makes it more affordable and more available in areas where this type of bridges are built. The stiffness of wire rope varies a lot, but the wire rope that will be used in this dissertation has a Young's modulus of around E=110 GPa (Helvetas, 2004).

Wire rope is elastic and it will stretch or elongate when it's subjected to a tensile force. This stretch can be divided into three different phases which depends on the magnitude of the force and the lifetime-situation of the cable.

Phase 1 – Constructional extension

When a wire rope is subjected to a load for the first time, the helically-laid wires will act in a constricting manner which will lead to a compression of the core and a more tight contact of all the rope elements. The constructional extension depends on the core material, the wire construction and the steel quality. Ropes with fiber core extends more than ropes with steel core. This is because the steel cannot compress as much as the synthetic core. Because of these different factors it's hard to set at definite value of the constructional extension. Approximate values is 0.25 % - 0.5 % for a rope with steel core and 0.75 % - 1 % for a rope with synthetic core (Hanes Supply, 2015).

Phase 2 – Elastic extension

Following phase 1, an elastic extension resulting mostly from recoverable deformation on the metal will occur. The manner of this extension complies approximately with Hooke's law which makes it possible to quite easy calculate the elastic extension. It's important to note that the Young's modulus of a wire rope is only an approximation because of the non-homogenous cross section. This "apparent" Young's modulus can be obtained from the manufacturer or by making a modulus test on an actual wire rope sample.

Phase 3 – Permanent extension

Just as any other metallic structural member, wire rope has a yield point. If the tensile stress in the wire rope exceeds the yield stress, permanent extension will occur.

Beyond these three types of extensions, both thermal extension, extension due to rotation and extension due to wear can appear, but they won't be taken into consideration in this thesis.

2.5.2 Cables as load bearing element

In a comparison between using a single cable or beam as load-carrying elements for transversal load, the two show different behavior. Due to its low bending stiffness, a cable works in almost pure tension whilst a beam carries load by combining compression and tension in its cross section. For simplicity it's assumed that the cable has no bending stiffness and can therefore only transfer load by tension. For the cable it means that the geometrical configuration is of absolute importance, i.e. the sag. A straight cable is unable to carry any transversal load. With a cable there will also be a horizontal reaction at the supports in Figure 2.7 which often is larger than the vertical reaction. The beam will only be subjected to a vertical reaction at the supports.

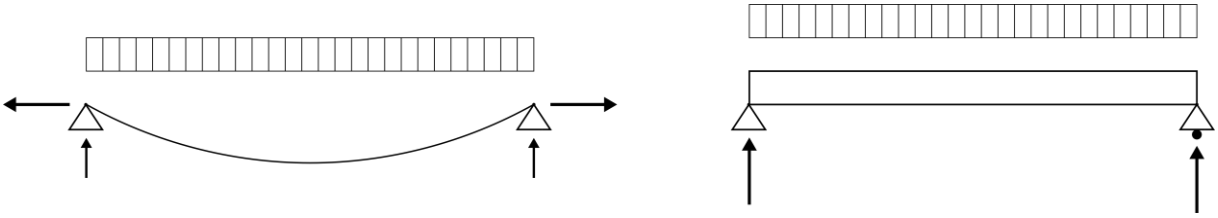

Figure 2.7 Support reactions for a cable and a beam

The advantage in using cables compared to beams is material efficiency. This is because the cables transfer load in the most efficient way, pure tension. Gimsing (Gimsing, 1997) illustrated this by comparing a cable with a sag of 3 meters and a beam for the same load case, see Figure 2.8.

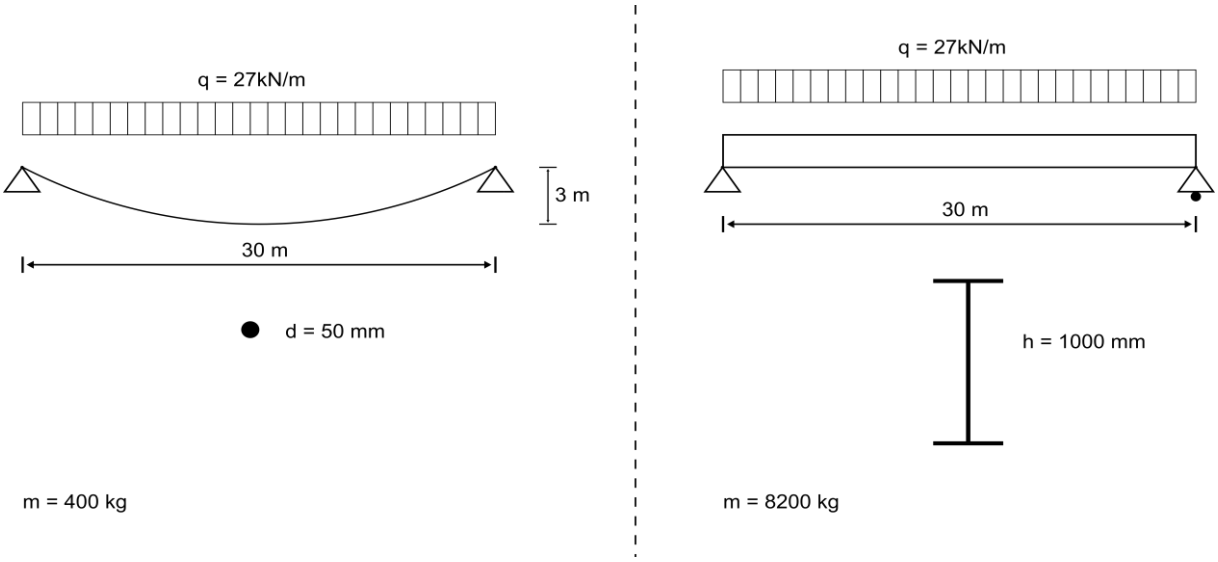

Figure 2.8 A cable and a beam designed for a uniform load, 27 kN/m, over a 30 meter span

For this given load case and span the amount of structural material used with a cable as load-carrying elements is substantial less than with a beam, which can be seen in Figure 2.8 above.

A cable is showing more geometrical change due to different loading than a beam because a cable follows the funicular shape of the loading applied to it. A few examples of different loading on a single cable are illustrated in Figure 2.9.

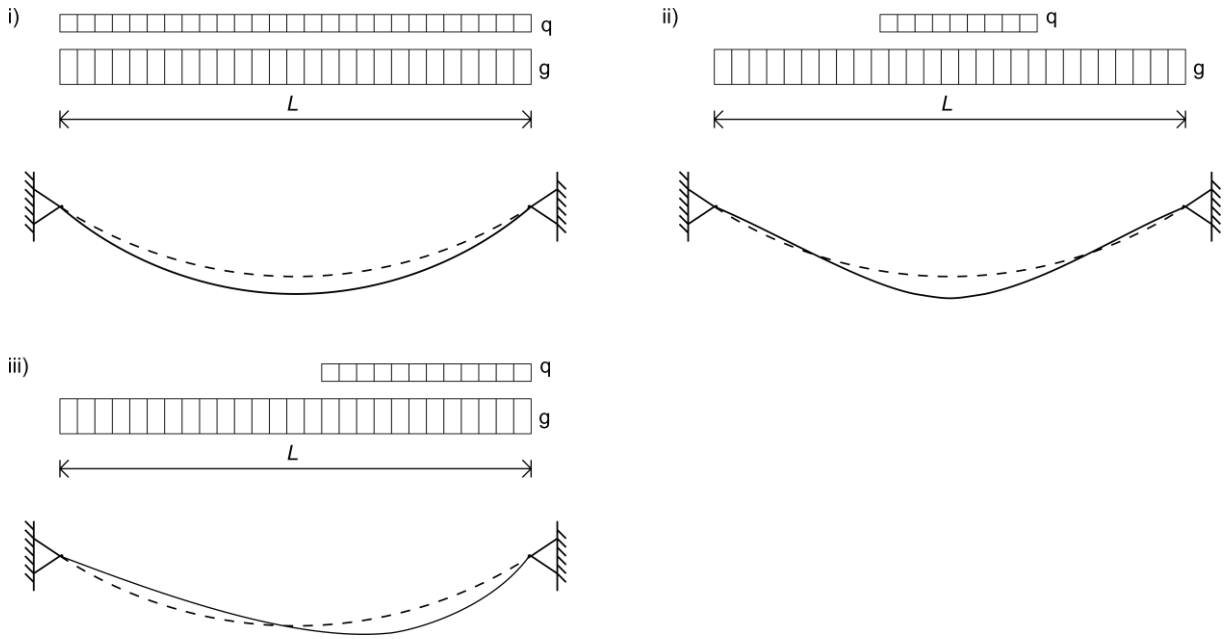

Figure 2.9 Deflection of a cable subjected to i) uniform load, ii) partial live load and iii) asymmetric live load

2.6 Statics

The stress-strain behavior of cables is, due to its cross-section with much void, not linear. When cables are loaded, the void between the strands decreases with a change in the cross-sectional area as result. This will lead to both permanent and temporary deformations. Permanent deformations often arises in the beginning of the lifetime of a cable. The reason for this is when the cable is subjected to a load, a strain hardening takes place when the void between the strands closes. This will lead to an increased axial stiffness and permanent elongations. Besides the permanent deformations there will always be elastic deformations in the cable as well.

Since cables are subjected to large deformations, it's necessary to formulate the equilibrium conditions in the deformed shape of the cable. This is done by analyzing a cable element (Figure 2.10 ii)) of an arbitrary cable. This will eventually lead to the formulation of the ***cable equation***.

The cable spans between the points A and B in Figure 2.10 i) and it has a constant axial stiffness EA, a bending stiffness EI→0 and an initial length L. The cable is subjected to a vertical line load q.

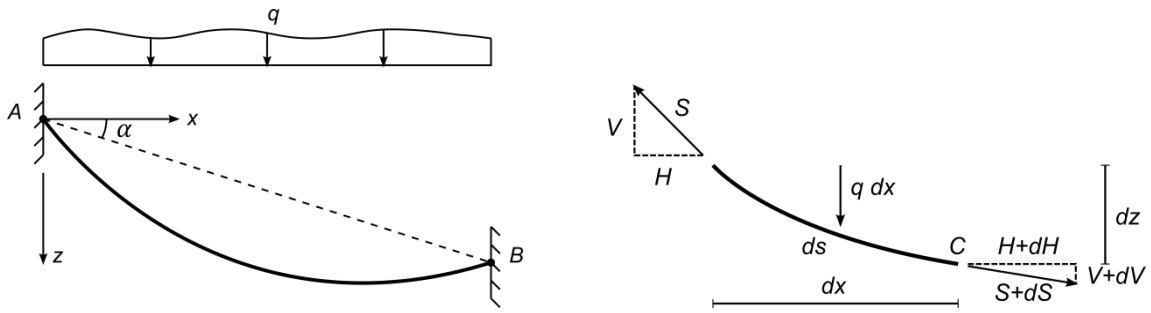

Figure 2.10 i) Static system ii) Cable element

Equilibrium from Figure 2.10 ii)

Horizontal equilibrium:

$$-H + (H + dH) = 0 \qquad \Longrightarrow \qquad dH = 0 \tag{2.1}$$

The horizontal force in the cable is constant.

Vertical equilibrium:

$$-V + (V + dV) + q \cdot dx = 0 \qquad \Longrightarrow \qquad q = -\frac{dV}{dx} \tag{2.2}$$

Moment around point C:

$$q \cdot dx \cdot \frac{dx}{2} + H \cdot dz - V \cdot dx = 0 \qquad since \quad q \cdot dx \cdot \frac{dx}{2} \approx 0$$

$$\Longrightarrow \qquad V = H\frac{dz}{dx} = -Hz' \qquad \Longrightarrow \qquad q = -\frac{dV}{dx} = -Hz'' \tag{2.3}$$

The cable force *S* is given by:

$$S = \sqrt{H^2 + V^2} = \sqrt{H^2\left(1 + \frac{V^2}{H^2}\right)} = H\sqrt{1 + z'^2} \tag{2.4}$$

The differential cable length *ds* is derived in a similar manner:

$$ds = \sqrt{dx^2 + dz^2} = \sqrt{dx^2\left(1 + \frac{dz^2}{dx^2}\right)} = dx\sqrt{1 + z'^2} \tag{2.5}$$

When the equilibrium for the cable element is formulated, the results can be used in the moment equilibrium for the deformed cable below.

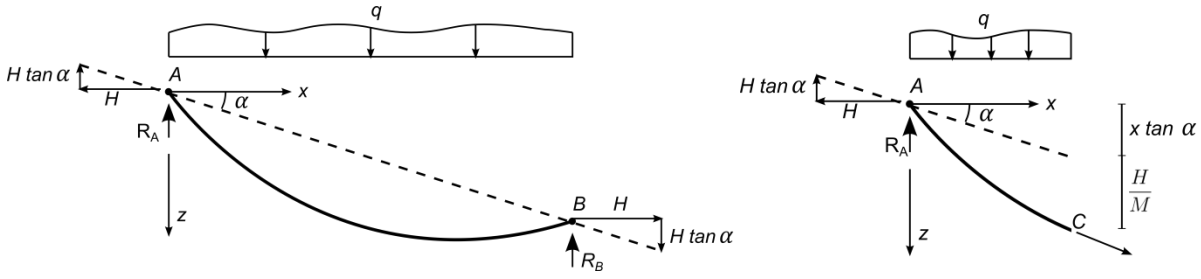

Figure 2.11 i) Cable in deformed shape ii) Cut for moment equilibrium

Moment equilibrium around point C in Figure 2.11 ii).

$$H \cdot z - H \cdot x \cdot \tan(\alpha) - R_A x + \int_0^x q \cdot x \cdot dx = 0 \tag{2.6}$$

The third and fourth term in the equation above is equal to the moment $\bar{M}$ in a simply supported beam with the length *L* subjected to a vertical line load *q*.

$$Since \quad R_A \cdot x + \int_0^x q \cdot x \cdot dx = \bar{M} \qquad \Rightarrow \qquad z = x \cdot \tan(\alpha) + \frac{\bar{M}}{H}$$

$$\Rightarrow \qquad z' = \tan(\alpha) + \frac{\bar{V}}{H}$$

$$\Rightarrow \qquad z'' = -\frac{q}{H} \tag{2.7}$$

The length of the cable *s* in its deformed shape is given by the *cable equation:*

$$\int_0^l ds = \int_0^l \sqrt{1 + z'^2}\, dx = L\left(1 + \alpha_T \cdot T - \frac{\sigma_0}{E}\right) + \int_0^l \frac{S}{E \cdot A} ds \tag{2.8}$$

The length of the deformed cable is the sum of the original length L, the thermal deformation, the pre-stress deformation and the elastic strain. The last part of the cable equation, the elastic strain, is given by:

$$\int_0^l \frac{S}{E \cdot A} ds = \int_0^l \frac{S \cdot \sqrt{1 + z'^2}}{E \cdot A} dx = \int_0^l \frac{H\sqrt{1 + z'^2} \cdot \sqrt{1 + z'^2}}{E \cdot A} dx = \frac{H}{E \cdot A} \int_0^l (1 + z'^2) dx =$$

$$= \frac{H}{E \cdot A} \int_0^l \left(1 + \left(\tan(\alpha) + \frac{\bar{V}}{H}\right)^2\right) dx = \frac{H \cdot L}{E \cdot A} + \frac{H}{E \cdot A} \int_0^l \left(\tan(\alpha) + \frac{\bar{V}}{H}\right)^2 dx \quad (2.9)$$

The cable equation can therefore be written as:

$$\int_0^l ds = \int_0^l \sqrt{1 + z'^2}\, dx =$$

$$= L\left(1 + \alpha_T \cdot T - \frac{\sigma_0}{E}\right) + \frac{H \cdot L}{E \cdot A} + \frac{H}{E \cdot A} \int_0^l \left(\tan(\alpha) + \frac{\bar{V}}{H}\right)^2 dx \quad (2.10)$$

The cable equation can be solved in an iteratively way. Start with estimating a value of *H*, then the cable curve *z(x)* can be calculated. With *H* and *z(x)* known, it's possible to solve the cable equation. If the result isn't accurate enough, repeat the calculations with a better estimate of *H* (Marti, 2012).

2.7 Dynamics of cables

2.7.1 Dynamic behavior of the single cable

Cables are, due to their small mass per unit length and their small bending stiffness, very sensitive to oscillations. To explain the dynamic behaviour of a single cable, it's necessary to compare the vibrations in an inextensible taut string compared to the vibrations in a sagging cable.

The first natural vibration modes for the inextensible taut string can be seen in Figure 2.12. The first natural frequency ω_1 can be found with the formula:

$$\omega_1 = \frac{\pi}{L}\sqrt{\frac{T}{m}}\ rad/s \quad (2.11)$$

Where T is the tension force in the string
m is the mass per unit length of the string
L is the length between the supports

The natural frequency ω_i for modes of higher order is given by:

$$\omega_n = \frac{n \cdot \pi}{L}\sqrt{\frac{T}{m}}\ rad/s \qquad where\ n = 1, 2, 3, \ldots \tag{2.12}$$

Since the first mode is symmetric, symmetric modes are characterized by odd numbers and nonsymmetrical modes by even numbers. Example of the first four modes can be seen in Figure 2.12. Note that this is just a theoretical example. It's a good estimation for a vertical string, but for a horizontal string gravity always affects it with a sag and a curvature as result (Gimsing, 1997).

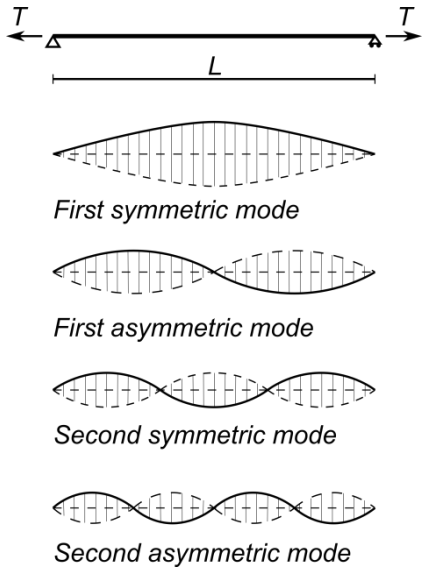

Figure 2.12 The first 4 vibration modes for the taut string

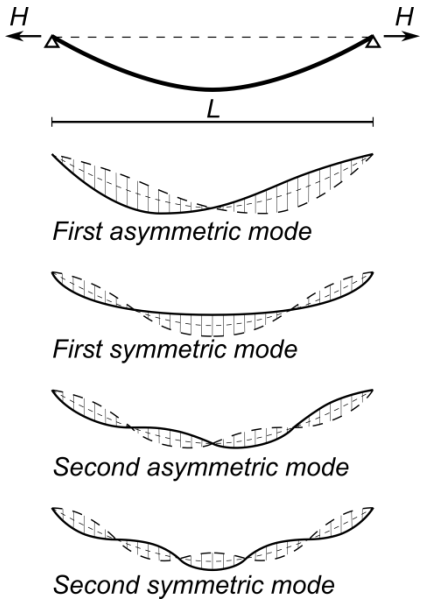

Figure 2.13 The first 4 in-plane vibrations modes for the sagging cable

For a cable with a sag and suspended between two points, two types of vibrations are possible. The first type is called sway vibration. Sway vibration is an out of the vertical plane vibration and it can be seen in Figure 2.15.

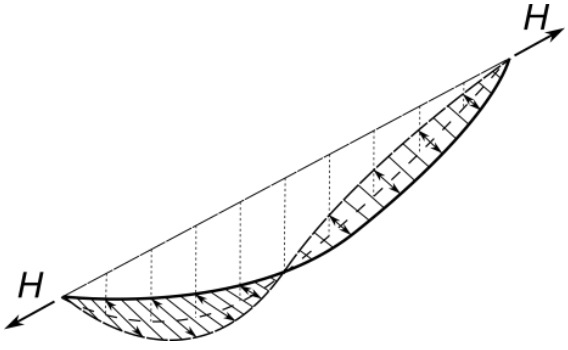

Figure 2.15 Sway vibration out of the vertical plane. Notice the arrows

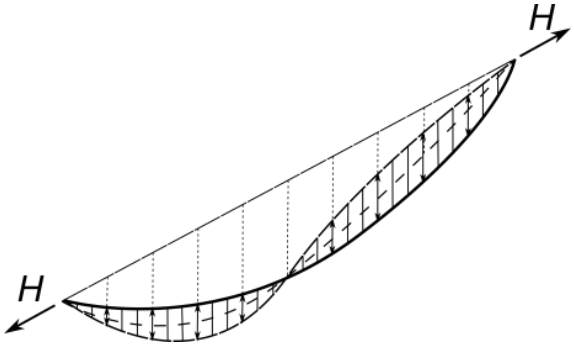

Figure 2.14 In-plane vibration. Notice the arrows

Similar to the taut string, the natural frequencies for the sway vibration are given by:

$$\omega_n = \frac{n \cdot \pi}{L}\sqrt{\frac{H}{m}}\ rad/s \qquad where\ n = 1, 2, 3, \ldots \tag{2.13}$$

Where H is the horizontal tension force in the string

For the in-plane vibration, as seen in Figure 2.14, the first four vibration modes will look like the ones in Figure 2.13. The in-plane vibration can be either symmetric or asymmetric just like the earlier examples, but since the cable has a sag and is considered inextensible, the first symmetric mode with only one half wave, as seen for the taut string, cannot exist. Instead, the first mode for the in-plane vibration is asymmetric. The asymmetric vibration modes for a sagging cable are given by (Irvine, 1974):

$$\omega_n = \frac{2 \cdot n \cdot \pi}{L}\sqrt{\frac{H}{m}}\ rad/s \qquad where\ n = 1, 2, 3, \ldots \tag{2.14}$$

where the first two asymmetric modes can be seen in Figure 2.13.

The symmetric in-plane modes for an inextensible cable can be found by solving the following equation (Irvine, 1974):

$$\tan\left(\frac{\beta \cdot L}{2}\right) = \frac{\beta \cdot L}{2} \qquad where\ \beta = \omega \cdot \sqrt{\frac{m}{H}} \tag{2.15}$$

The first two roots found for (2.15) are:

$$(\beta \cdot L)_{1,2} = 2{,}86\,\pi, \qquad 4{,}92\,\pi \tag{2.16}$$

Higher roots can quite accurately be found with (Irvine, 1981):

$$(\beta \cdot L)_n = (2 \cdot n + 1) \cdot \pi \cdot \left(1 - \frac{4}{((2 \cdot n + 1)^2 \cdot \pi^2)}\right) \qquad where\ n = 3, 4, 5, \ldots \tag{2.17}$$

The natural frequencies for an inextensible sagging cable are therefore:

$$\omega_1 = \frac{2{,}86 \cdot \pi}{L}\sqrt{\frac{H}{m}}\ rad/s \tag{2.18}$$

$$\omega_2 = \frac{4{,}92 \cdot \pi}{L}\sqrt{\frac{H}{m}}\ rad/s \tag{2.19}$$

$$\omega_n = \frac{(2 \cdot n + 1) \cdot \left(1 - \frac{4}{((2 \cdot n + 1)^2 \cdot \pi^2)}\right) \cdot \pi}{L} \sqrt{\frac{H}{m}} \frac{rad}{s} \qquad where\ n = 3, 4, 5, \ldots \tag{2.20}$$

As mentioned many times in the text above, the analyzed cables are all assumed to be inextensible. However, this is not the case for real cables. In reality, cables are always flexible and often their supports to. The pylons in a suspension bridge are for example always flexible. As seen in the previous examples the sag of the cable or string affects the order of the first natural frequencies. The relationship between the geometry, the elasticity and the order of the first natural frequencies can be seen in Figure 2.16. The abscissa P_{ge} is a parameter that governs the dynamic behaviour of the current cable. As seen in Figure 2.16, the value of P_{ge}decides the order of the symmetric and the asymmetric modes. A low value of P_{ge} indicates that the cable in question has a small sag and/or a small axial stiffness, for example the taut string seen in

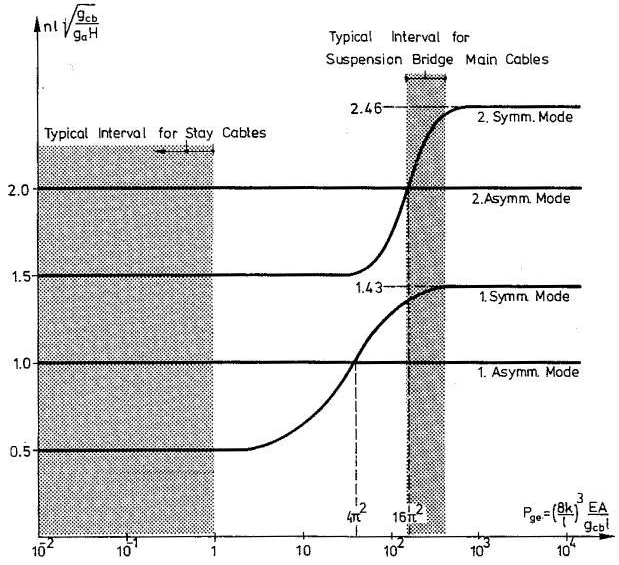

Figure 2.16 The first four natural frequencies for a sagging cable. With permission from (Gimsing, 1997).

Figure 2.12 and a stay cable in a cable stayed bridge. For higher values of P_{ge}, the behavior of the cable looks more like the sagging cable in Figure 2.13 with a reversed order of the modes compared to the taut string. P_{ge} is given by (Gimsing, 1997) (Irvine, 1981):

$$P_{ge} = \left(\frac{8 \cdot f}{L}\right)^3 \cdot \frac{E \cdot A}{g_a \cdot m \cdot L} \tag{2.21}$$

Where
- f is the sag of the cable
- E is the Young's modulus of the cable
- A is the cross sectional area of the cable
- g_a is the acceleration due to gravity
- m is the mass per unit length of the string
- L is the length between the supports

As seen in Figure 2.16, three important cases can now be considered:

I. If $P_{ge} < 4\pi^2$

The frequency of the first symmetric in-plane mode is less than the frequency of the first asymmetric in-plane mode and it has no internal nodes along the span.

II. If $P_{ge} = 4\pi^2$

The frequency of the first symmetric in-plane mode is at this "cross-over point" equal to the frequency of the first asymmetric in-plane mode.

III. $P_{ge} > 4\pi^2$

The frequency of the first symmetric in-plane mode is higher than the frequency of the first asymmetric in-plane mode. The first symmetric in-plane mode has two internal nodes along the span

As also seen in Figure 2.16, if $4\pi^2 \leq P_{ge} \leq 16\pi^2$, both the first and the second symmetric mode has two internal nodes. When $P_{ge} = 16\pi^2$, the frequency of the second asymmetric mode is equal to the frequency of the second symmetric mode. $P_{ge} = 16\pi^2$ is therefore the second "cross-over point". This pattern repeats for higher values of P_{ge}.

As seen in Figure 2.16, the natural frequencies for the asymmetrical modes don't change when the cable is considered extensible. However, the natural frequencies for the symmetrical modes depend on P_{ge} and are given by:

$$\tan\left(\frac{\beta \cdot L}{2}\right) = \frac{\beta \cdot L}{2} - \frac{4}{P_{ge}}\left(\frac{\beta \cdot L}{2}\right)^3 \tag{2.22}$$

This equation can be used for all values of P_{ge}. For example, if the cable is considered inextensible, i.e. $P_{ge} \to \infty$, equation (2.22) will be equal to equation (2.15).

As a summary, start with deciding P_{ge} of the cable and find out the order of the symmetric and asymmetric modes. Then calculate the out of plane frequencies with equation (2.13), the frequencies for the asymmetric modes with equation (2.14) and finally the frequencies for the symmetric modes with equation (2.22).

2.8 Wind effects

Wind loads can affect a bridge in different ways. Some bridges doesn't become affected in a noticeable way, while other bridges, especially cable supported bridges, can start sway or vibrate quite heavily. These motions are often a problem for the serviceability of the bridge, but they can in some cases be a risk for the structural capacity of the bridge. Below some wind phenomena that's been reported from bridges are presented. Not all are relevant for the suspended bridges this thesis are concerning, but their existence is important for a bridge engineer to know.

2.8.1 Buffeting

Vibrations due to buffeting are a phenomenon created by wind turbulence. The natural fluctuation in wind velocity gives an inconsistent load over time on the structure, just like the sway of trees and bushes encountered in high winds. Buffeting actions can occur in both lateral, vertical and torsional modes of vibration of a bridge structure and the magnitude depends on the shape of the bridge deck (Storebaelt Publications, 1998). When the frequency of the wind load is approaching the natural frequency of the structure, resonance occur. Buffeting does not generally cause structural failure but it can cause problems with serviceability of the structure. It can also lead to fatigue problems in local elements.

2.8.2 Flutter

For wind induced vibrations the flutter phenomenon is maybe the most severe problem for slender bridges and can cause failure with catastrophic consequences. The wide known collapse of the Tacoma Narrows bridge in 1940 was caused by single degree freedom flutter (Storebaelt Publications, 1998). This instability problem happens when the aerodynamic damping becomes negative. The energy transfer from the airflow exceeds the energy dissipation by structural damping. This is true for a system with one degree of freedom i.e. pure torsional motion, also known as stall flutter. With coupled vibration modes, torsional and vertical, classical flutter can occur even when all aerodynamic damping terms are positive (Dyrbye & Hansen, 1997).

2.8.3 Vortex shedding

With airflow acting on blunt bodies, vortices are shed from the sides. These vortices are created periodically and creates therefore alternating aerodynamic pressure. When the frequency of the shifting aerodynamic pressure coincide with one of the torsional vibration modes of the structure, resonance will occur. The main direction of the forces are transversal to the airflow. The vibrations caused by these forces are often too small to cause any damage to a bridge but they can cause an uncomfortable feeling among the users of the bridge (Ryall, Parke, & Harding, 2000)

2.8.4 Galloping

Galloping is a wind induced phenomena where the vibration is perpendicular to the wind direction. Similar to stall flutter but with the movement in the transversal degree of freedom. Galloping is typical for light structures with little damping and usually for non-circular bodies. It is dependent on the velocity of the wind acting on the body. A known galloping scenario is with ice-accreted cables. Due to the change of shape of the cable it loses aerodynamic stability.

2.9 Comfort criteria

Due to the shape and stiffness of a suspended bridge, vibrations and sway will occur in a stronger manner than in regular bridges and buildings. These vibrations will occur in both vertical, lateral and torsional direction, but the main focus will be laid on the lateral sway of the bridge since this is the direction in which the largest displacement due to wind will occur. Vibrations due to pedestrian traffic will also occur, but these vibrations are assumed to cause less comfort problems than the vibrations caused by the wind, and will therefore be considered out of scope for this thesis. The thesis will also not consider dampers as a possible solution for reducing vibration due to economic reasons.

At first, before any comfort criteria has been given, one must first note that large accelerations or deformations sometimes has to be accepted due to, for example, achieve a low construction cost or due to a low frequency of use. In those cases the best comfort criteria can be as simply as a warning sign. However, there's still reason to investigate more sophisticated comfort criteria.

There has been many studies made that covers the human perception of horizontal vibrations in different structures. Unfortunately, most of this work has focused on horizontal vibration in buildings and not in bridges. (Zivanovic et al, 2005). Even if this ratio isn't preferable, some valuable information is given. The most fundamental fact of horizontal vibrations is that each pedestrian has its own perception and that this is based on many different factors. According to (Heinemeyer et al, 2009), this is some of the aspects that affect the human assessment of vibrations on a bridge:

- The number of people using the bridge
- The frequency of use
- The surrounding landscape and the height above ground
- The motion of the human body
- The exposure time
- The expectation of vibrations. If a person expects a bridge to vibrate, the acceptance of vibrations is greater.

This is some of the non-quantifiable aspects that affect the perception of vibrations. Even if the perception is individual, some general criteria must be given. It exist different recommendations for deciding a maximum size of the vibrations. The most common way to estimate the level of comfort is to measure the peak value of the acceleration the bridge is subjected to. This has been done by different scientific reports and standards.

2.9.1 Eurocode

Eurocode 0, SS-EN 1990, appendix A2 gives the following suggestions for the peak value of the acceleration, also known as critical acceleration of the bridge (SIS, 2010):

- 0.7 m/s^2 for vertical vibrations
- 0.2 m/s^2 for horizontal vibrations under normal use
- 0.4 m/s^2 for horizontal vibrations under exceptional crowd conditions

These peak values should be checked if the natural frequency of the superstructure is less than 5 Hz for vertical vibrations and less than 2,5 Hz for lateral and torsional vibrations.

The national annex can give other recommendations than the ones given above. However, the Swedish annex for example, gives no further comfort criteria.

The critical accelerations for a given frequency can be translated into displacement and velocity with equation (2.23) and equation (2.23).

$$a = f^2 \cdot u \tag{2.23}$$

$$a = f \cdot v \tag{2.24}$$

2.9.2 Sétra

Sétra, the French Technical Department for Transport, Roads and Bridges Engineering and Road Safety, suggest that three different comfort levels with corresponding maximum accelerations should be used for both vertical and lateral vibrations. For lateral vibrations the following acceleration ranges are suggested (Sétra, 2006):

- 0 – 0,15 m/s^2 for range 1, maximum comfort
- 0,15 – 0,30 m/s^2 for range 2, mean comfort,
- 0,30 – 0,80 m/s^2 for range 3, minimum comfort
- > 0,80 m/s^2 for range 4, unacceptable discomfort

Sétra also recommends a maximal acceleration of 0,1 m/s^2 to avoid "lock-in" effects, i.e. when a pedestrian adjust its walking frequency so it enters in phase with the bridge motion and becomes a negative damper. A famous example of a bridge subjected to the "lock-in" effect is the Millenium Bridge in London (Sétra, 2006). This recommendation, however, will not be taken into consideration since it's unnecessary due to the amount of crossing pedestrians and also because it's probably impossible to achieve such a low maximum acceleration.

2.9.3 JRC- and ECCS-report

The Design of Lightweight Footbridges for Human Induced Vibrations by (Heinemeyer et al, 2009) is a JRC- (European Commission Joint Research Centre) and ECCS-report (The European Convention for Constructional Steelworks). The report is a guideline for dynamic behavior of light-weight steel structures. The recommendations given is this report are very

similar to the ones suggested by Sétra. The following recommendations are suggested (Heinemeyer et al, 2009):

- $< 0{,}10\ m/s^2$ for comfort class 1, maximum comfort
- $0{,}10 - 0{,}30\ m/s^2$ for comfort class 2, medium comfort,
- $0{,}30 - 0{,}80\ m/s^2$ for comfort class 3, minimum comfort
- $> 0{,}80\ m/s^2$ for comfort class 4, unacceptable discomfort

As seen above it's only the limit for comfort class 1 that divides these recommendations from the ones given by Sétra.

2.9.4 ISO 10137

Bases for design of structures – Serviceability of buildings and walkways against vibration

ISO 10137 is a guideline for the serviceability of buildings and walkways against vibrations, made by the International Organization for Standardization (ISO). Instead of 3-4 different ranges/comfort classes, ISO uses a diagram that gives the maximum allowable acceleration for a given frequency. This diagram should be used with four different loading scenarios and, depending on the load scenario, the base curve of the diagram should be multiplied with a certain factor. The load scenarios are according to ISO 10137:

- Load scenario 1: A single person walking over the bridge while another person is standing at the mid-span
- Load scenario 2: A pedestrian flow of eight to fifteen walks across the bridge. The number of persons depends on the length and width of the bridge.
- Load scenario 3: A stream with significantly more than 15 person walks across the bridge
- Load scenario 4: Exceptional crowd load, for example an opening ceremony.

These load scenarios are more important for vertical vibrations since it's only for these the multiplying factor varies. For vertical vibrations the multiplying factor is 30 for load scenario 1 and 60 for load scenario 2-4, but then another diagram than Figure 2.17 should be used.

For horizontal vibrations the multiplying factor is 60 for every load scenario and this factor will be multiplied with the acceleration value in Figure 2.17 below. This will give a maximal allowed horizontal acceleration of 0.216 m/s^2 for frequencies < 2 Hz and for example 0,54 m/s^2 for a frequency of 5 Hz.

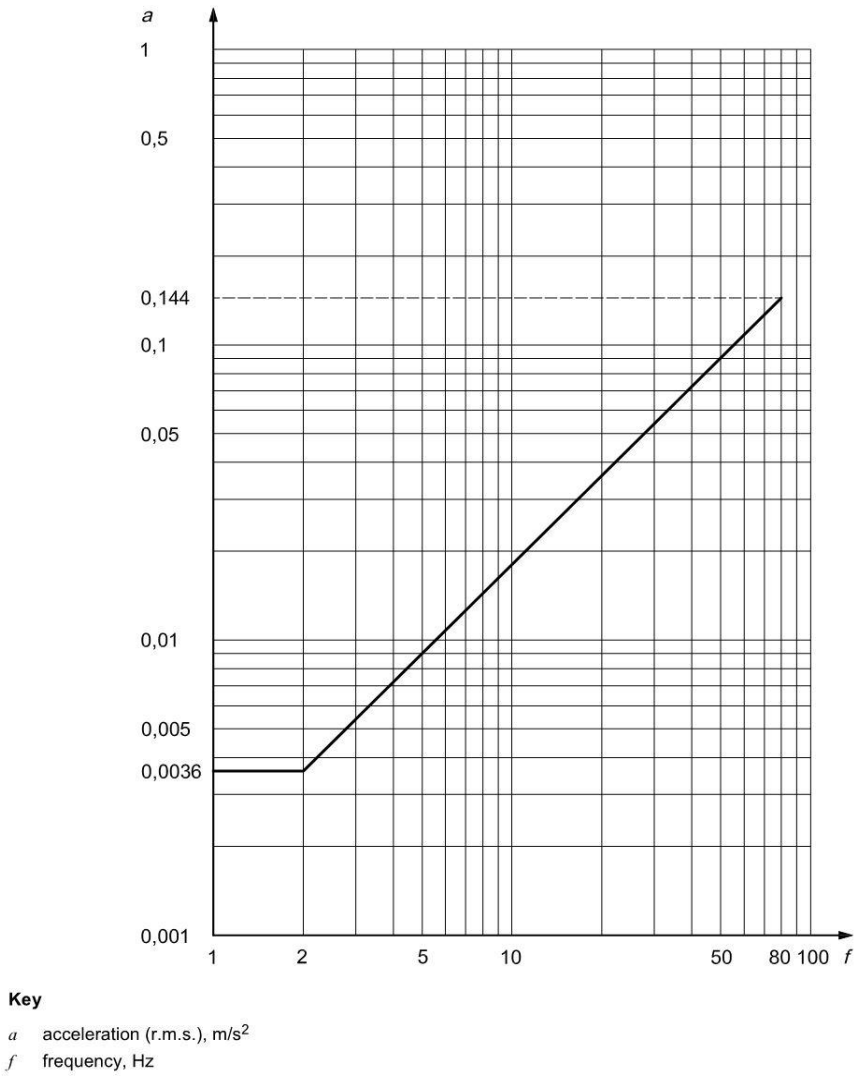

Figure 2.17 Horizontal vibration according to ISO 101 37. With permission from SIS

One important thing to notice is that this acceleration recommendation from ISO isn't, according to (Zivanovic et al, 2005), based on published research pertinent to footbridge vibrations. Therefore it can be questioned if these recommendations are relevant for footbridges.

2.9.5 Nakamura

Maybe the most interesting study made on horizontal vibration in footway bridges are done by (Nakamura, 2003). In the report *Field measurements of lateral vibration on a pedestrian suspension bridge*, Nakamura investigates the lateral dynamic behavior of a 320 meter long pedestrian suspension bridge. The report focus on lateral vibrations caused by the footsteps of the users and not the wind induced vibrations. However, since accelerations have been measured, this report is a very important comparison since the dynamic behavior of the tested bridge is very alike the suspended bridges studied in this master thesis. This bridge is stabilized by windguys in the lateral direction which decreases the amplitude of the vibrations.

The perception of the vibrations varied between the pedestrians but some general grades of discomfort due to a certain acceleration could be identified:

0,3 m/s^2: Pedestrians are able to feel the vibrations. Some of them become uncomfortable but most of them can walk normally.

0,75 m/s^2: Some of the pedestrians find it difficult to walk normally and some must use the handrails from time to time.

1,35 m/s^2: Pedestrians often loses their balance and some of them have to stop temporarily to support themselves with the help of the handrail. Some of the elderly people aren't able to walk at all.

2,1 m/s^2: This acceleration occurred on the London Millennium Bridge where it was reported that many people were unable to walk and that many people felt unsafe.

Nakamura suggest that 1,35 m/s^2 is a suitable serviceability limit. This corresponds to a girder amplitude of 45 mm and a velocity of 0,25 m/s for the bridge in the study. The acceleration and the velocity seems reasonable for comparison with the bridges in this thesis, but the amplitude will most likely be at least ten times bigger.

2.9.6 Summary and suggestions

As seen in the sections above, the acceleration limits varies a bit between the different standards and reports. Even if it's always preferable that the maximum acceleration of a bridge doesn't exceeds the maximum comfort classes, the main focus here will be to suggest a maximum allowable acceleration for suspended bridges. The maximum lateral accelerations recommended by the different standards and reports can be seen in Table 2.1 below:

	Eurocode	**Sétra**	**JRC/ECCS**	**ISO 10137**	**Nakamura**
Max acceleration m/s^2	0,4	0,8	0,8	0,22 – 0,54	1,35

Table 2.1 Maximum allowed lateral accelerations

Since Nakamuras report is focused on pedestrian bridges and especially suspension bridges, this recommendation seems adequate as a reference for the suspended bridges this master thesis will focus on.

2.10 Loads

2.10.1 Wind loads on bridges

As discussed in earlier chapters, cable supported bridges are very flexible structures and therefore it becomes important to analyze the movement of the bridge due to wind. Different phenomena caused by wind induced vibrations are buffeting, flutter, vortex shedding and galloping. The total wind load on a bridge deck can divided into three parts according to (2.25).

$$F_{tot} = F_q + F_t + F_m \tag{2.25}$$

The term F_q denotes the mean wind load, F_t the turbulent wind load, and F_m is the motion-induced wind load. For bigger cable supported bridges these three loads must be considered. For the trail bridges in this report only the first part, the mean wind load F_q, is taken into account.

2.10.2 Static wind loads

Eurocode

Wind loads in Eurocode are given by SS_EN 1991-1-4. Unfortunately SS_EN 1991-1-4 doesn't give guidance on cable supported bridges, i.e. suspended bridges, suspension bridges and cable stayed bridges. Neither the Swedish annex, the British annex, the German annex nor the Danish annex gives any guidance on cables supported bridges. However, as a guideline the simplified method described in SS_EN 1991-1-4 8.3.2 will be used since it´s alike the methods used by both Helvetas and Bridges to Prosperity. The vertical load component of the wind load is neglected by both Helvetas and Bridges to Prosperity and will therefore be neglected in this chapter. One can question if Eurocode as design code is appropriate for these types of bridges since they most likely will be built in places where Eurocode isn't a standard. However, due to the authors knowledge of Eurocode, this seems as the most effective and reliable way to verify the size of the wind loads given by Helvetas and Bridges to Prosperity.

The first step in determining the wind load/force is to calculate the basic wind velocity w_b at 10 meter above ground of terrain category II. w_b is a function of wind direction and time of year and it´s given by:

$$w_b = c_{dir} \cdot c_{season} \cdot v_{b,0} \tag{2.26}$$

Where c_{dir} is the directional factor. Recommended value is 1.
c_{season} is the seasonal factor. Recommended value is 1.
$v_{b,0}$ is the fundamental value of the basic wind velocity 10 meters above ground of terrain category II

When w_b is decided the basic velocity pressure q_b can be calculated with:

$$q_b = \frac{1}{2} \cdot \rho \cdot v_b^2 \tag{2.27}$$

Where ρ is the density of the air. Recommended value is 1.25 kg/m^3.

The wind force acting on the long side of the bridge can be calculated with the simplified method described in SS_EN 1991-1-4 8.3.2:

$$F_w = \frac{1}{2} \cdot \rho \cdot v_b^2 \cdot C \cdot A_{ref} = q_b \cdot C \cdot A_{ref} \tag{2.28}$$

Where C is the wind load factor based on the shape of the bridge lane and the exposure to the wind

The manuals from Helvetas and Bridges to Prosperity recommends a wind speed of 160 km/h or 44.4 m/s and a reference area of 0.3 m^2/m. To make a comparison between the different wind loads possible it's assumed that the bridge used for the Eurocode wind load is situated 10 meters above ground and that the terrain beneath is flat and of category II. This will give the following value of the wind load factor:

$$C = c_e \cdot c_{f,x} = 2{,}35 \cdot 1{,}3 = 3{,}06 \tag{2.29}$$

The basic velocity pressure q_b can then be calculated:

$$q_b = \frac{1}{2} \cdot 1{,}25 \cdot 44{,}4^2 = 1{,}23\ kPa \tag{2.30}$$

With these values known the wind force can be calculated:

$$F_w = \frac{1}{2} \cdot 1{,}25 \cdot 44{,}4^2 \cdot 3{,}06 \cdot 0{,}3 = 1{,}13\ kN/m \tag{2.31}$$

When deciding the wind loads, Bridges to Prosperity refers to Helvetas where both the *Short Span Trail Bridge Standard* and the *Long Span Trail Bridge Standard* refer to the *Report on Windguy Arrangement for Suspended and Suspension Standard Bridges, Dr. Heinrich Schnetzer, WGG Schnetzer Puskas Ingenieure AG, Switzerland, 2002*. In this report they discuss the wind loads used by Helvetas. The wind speed recommended by Helvetas, 160 km/h, is considered very conservative by the authors. Instead they recommend a wind speed of 140 km/h for normal design situations which is the value recommended by the Swiss standard SIA 160. Only for bridges situated in exposed areas or very high above ground, a wind speed of 160 km/h is recommended (Schnetzer, 2002). However, both Helvetas and Schnetzer recommends a final load of 0.5 kN/m. This load is based on a reference area of 0.3 m^2/m and a wind coefficient of 1.3. Note that Helvetas recommended load is based on 160 km/h and Schnetzers on 140 km/h. Schnetzer recommends a load of 0.6 kN/m for bridges situated in exposed areas or very high above ground.

A short summary of the recommended loads can be seen in Table 2.2 below.

		Helvetas	Schnetzer	Bridges to Prosperity	Eurocode
Reference wind	**(km/h)**	160	140	160	160*
Wind pressure	**(kPa)**	1,3	1,3	1,7	1,23
Wind load	**(kN/m)**	0,5	0,5	0,3 (30 kgf/m)	1,13

Table 2.2 Wind loads

*Based on Helvetas and Bridges to Prosperity

Note that these loads are only recommendations for static wind loads. In every design situation there have to be a consideration if the size of the load is correct. Helvetas has taken gorge effects into account but the surrounding terrain must always be considered.

2.10.3 Vertical loads

The vertical loads acting on a suspended bridge, i.e. the dead load and the live load, are the most contributing factors for the design of the load carrying cables. Since recommendations from both Helvetas and Eurocode will be used, the vertical loads and load combinations from both of them will be presented. The characteristic loads are very alike for Helvetas and Eurocode, in fact it's only the live load that differs. The biggest difference between Helvetas and Eurocode is that Eurocode uses partial coefficients as enlargement factor for the current loads, both dead load and live loads. Helvetas doesn't enlarge its characteristic loads, instead a safety factor of 3 between the sum of the loads and the structural capacity is used.

2.10.3.1 Dead load

The dead load, with exception from the self-weight of the cables, doesn't differ so much between a suspension bridge designed according to Eurocode or Helvetas. Since Helvetas has great experience and knowledge in the building of suspended bridges, there is no reason for not use their recommended characteristic dead-loads for design according to both Helvetas and Eurocode. The recommended dead loads for a suspended bridge with a 1 meter wide steel deck can be seen in Table 2.3. If other dimensions or materials, for example a wooden deck, are preferd, the dead loads in Table 2.3 can be modified. The additional dead load from the main cables and possible windguy cables have to be calculated for each case. Note that the dead load from the windties, i.e. the cables between the bridge and the windguy cable, in Table 2.3 should only be used if windguys are installed.

Walkway	0,46 kN/m
Walkway support	0,22 kN/m
Fixation cables	0,01 kN/m
Wiremesh netting	0,06 kN/m
Windties (average)	0,03 kN/m

Table 2.3 Dead loads

2.10.4 Live load

Live loads are an estimation of the loads from pedestrians and wind acting on the bridge. Both Eurocode and Helvetas has recommendations for characteristic live loads, both from wind, which was presented in chapter 2.10.2, and from pedestrians.

Helvetas recommendation for pedestrian live load varies with the length of the span since the possibility of extreme overloading due to a large crown decreases with the span length (Helvetas, 2004). The live loads recommended by Helvetas can be seen in

$$For\ span\ l \leq 50\ m, \qquad q = 4\ kN/m^2 \tag{2.32}$$

$$For\ span\ l > 50\ m, \qquad q = 3 + \frac{50}{l} kN/m^2 \tag{2.33}$$

The live load recommended by Helvetas can be seen in Figure 2.18 below:

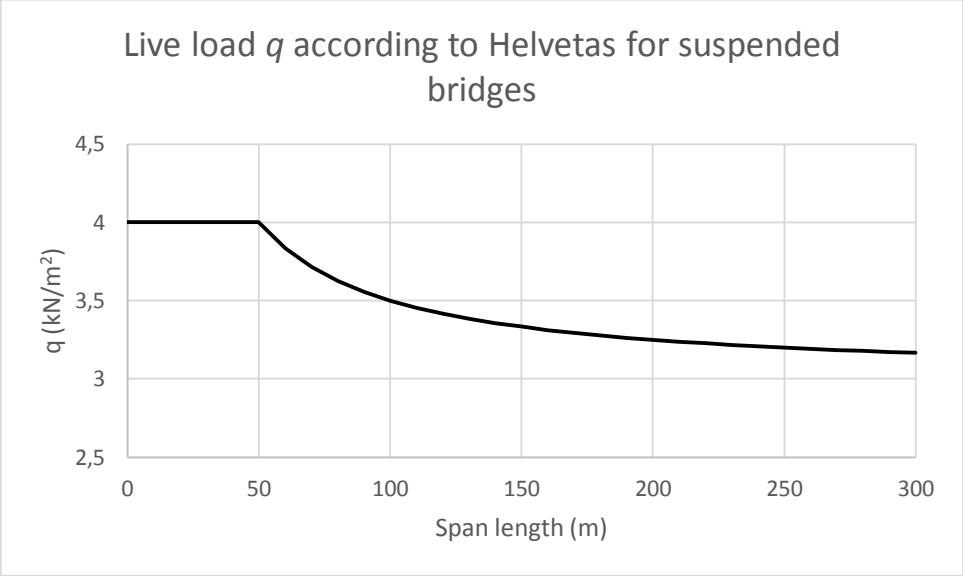

Figure 2.18 Live load according to Helvetas

Eurocode has two alternatives for crowd loading. The most common crowd load is Load Model 4, defined in SS-EN 1991-2 part 4.3.5, which is a uniformly distributed load equal to 5 kN/m^2. However, it's up to each project to define if Load Model 4 is relevant. 5 kN/m^2 is a very large load since it's equal to almost 500 kg/m^2, which is quite hard to achieve when only pedestrians are affecting the bridge. It's possible that these bridges will be used even for cattle, which isn't a problem, but some regard has to be taken to the structural capacity of the bridge, for example some limitation of the allowed number of cattle using the bridge at the same time.

If it's decided that Load Model 4 isn't relevant for the specific bridge, there is another option. The recommended load in this case is very similar to the load recommended by Helvetas, i.e. a load that depends on the length of the span. Even here it seems like the risk of over-crowding decreases with an increasing span length. The live load recommended by Eurocode is therefore:

$$For\ all\ spans\ \ q = 2 + \frac{120}{l + 30} kN/m^2, \quad where\ 2{,}5\ kN/m^2\ \leq q \leq 5\ kN/m^2 \tag{2.34}$$

The live load recommended by Eurocode can be seen in Figure 2.19 below.

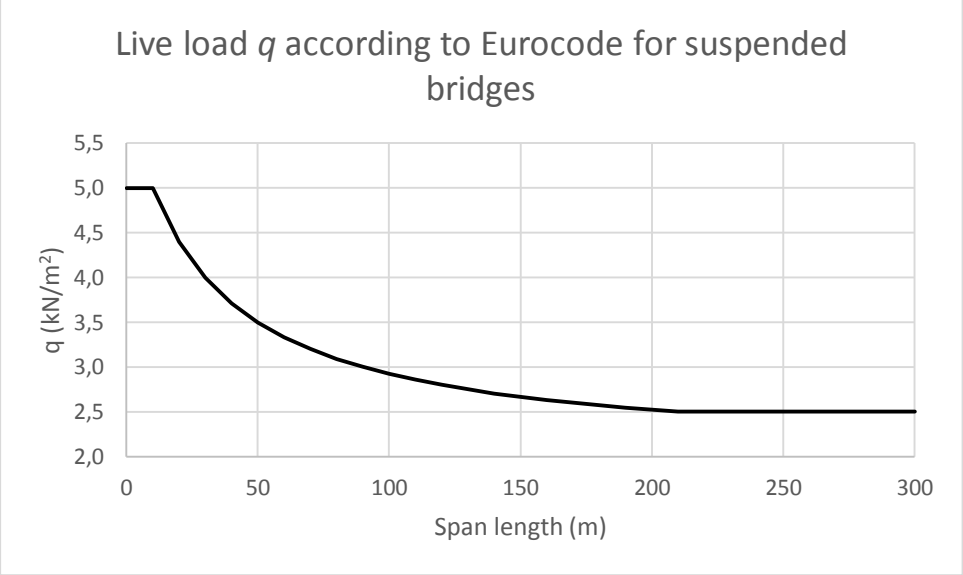

Figure 2.19 Live load according to Eurocode

2.10.5 The vertical effects from wind load

Since the wind loads are assumed to be horizontal, they won't affect a "normal" bridge in a vertical way. Suspended bridges however are easily displaced by the wind, which creates a different load situation compared to more stable bridges. The displacement increases the load that has to be transferred trough the cables to the abutments. This situation can be described with seeing the bridge as a pendulum hanging from the axial line between the abutments, which can be seen in Figure 2.20. When there's no wind load acting on the bridge, the pendulum string, representing the vertical load *S* carried by the bridge main cables, will hang vertical. The force *S* in the string will in this case be equal to the vertical force *g*. When the wind load increases the horizontal displacement *d* will also increase, creating a larger force *S* in the pendulum string and therefore a larger force in the bridge main cables. The enlarged force *S* due to the wind load is given by:

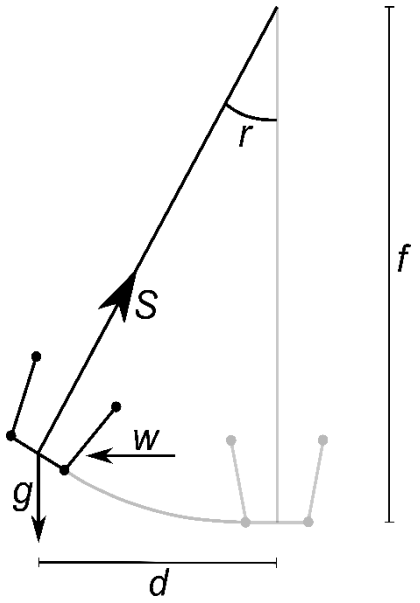

Figure 2.20 Static equilibrium for a bridge under constant wind load

$$S = \frac{g}{\cos(r)} = \sqrt{g^2 + w^2}\ \ N/m \tag{2.35}$$

2.10.6 Load combinations

When using Eurocode, designing in the ultimate limit state (ULS) and therefore load combinations 6.10a and 6.10b will be used according to SS-EN 1990 6.4.3.2. The cable strength will be designed according to equation 6.2 in SS-EN 1993-1-11.

2.11 Fatigue

According to (Schnetzer, 2002), damage on the cables due to fatigue hasn't been reported from site inspections on existing bridges without windguy arrangement. Note that the span of these bridges didn't exceed 120 meter. However, the wind displacements leads only to small cable rotations at the support which therefore makes the fatigue effects negligible on the main cables (Schnetzer, 2002). Fatigue effects on suspenders and other structural members can't be excluded, but this will not be investigated further.

One important factor to the absence of fatigue problems on the bridges examined by (Schnetzer, 2002) may be the high safety factor that Helvetas uses in their design. Since the dimension of the cables are getting bigger due to the safety factor, the stress ranges in the cables decreases, which reduces the risk of fatigue problems. If Eurocode is used in the design, it will lead to a more slender design. This will lead to higher stress ranges and an increasing risk for fatigue problems. It's important to have this in mind when using Eurocode in the design.

2.12 Brigade/Plus

As modelling software BRIGADE/Plus, or just Brigade as it will be called, has been chosen. Brigade is developed by Scanscot Technology and it´s a finite element software for structural analysis of bridges and other civil structures. Brigade includes an integrated Abaqus finite element solver and it can handle dynamic analyses and nonlinear structural models which is important capabilities when modelling cable supported structures.

Brigade/Plus will be used to determine the dynamic behavior of suspended bridges. The basic theory behind the dynamic calculations will be presented in the next chapters.

2.12.1 Equation of motion SDOF

The most simple oscillator system that can be described is mass spring system with a single degree of freedom (SDOF). The components are a mass, a spring and a viscous damper. The system is subjected to a dynamic external force, see Figure 2.21.

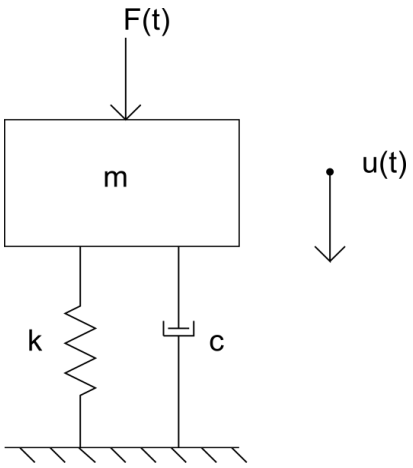

Figure 2.21 Mass spring system

F is the external force, m the mass, k the spring stiffness, c the viscous damping and u denotes the displacement. The spring force and the viscous dissipation force depending on the displacement and the velocity, will be negative with the analogy from Figure 2.21.

$$f_s = -ku - c\dot{u} \tag{2.36}$$

Newton's second law of motion with constant-mass system gives:

$$F(t) - f_s = m\ddot{u} \tag{2.37}$$

The dynamic equation of motion for the system can now be written with (2.36) in (2.37) as:

$$m\ddot{u} + c\dot{u} + ku = F(t) \tag{2.38}$$

2.12.2 Rayleigh Damping

The type of damping referred to as Rayleigh damping or classical damping is proportional to the mass and stiffness matrices according to equation (2.39). This type of damping is suitable for nonlinear analysis because of the proportionality to the stiffness matrix, which is updated with the iteration scheme.

$$C = \alpha M + \beta K \tag{2.39}$$

The modal damping factor is described in equation (2.40)

$$\xi_n = \frac{1}{2\omega_n}\alpha + \frac{\omega_n}{2}\beta \tag{2.40}$$

This shows that α will be dominant for low frequencies and β will consequently be dominant for high frequencies.

2.12.3 Newton-Raphson

Due to the geometric nonlinearities, an iterative analysis will be used. The nonlinearities comes from the relative large displacements the bridge is subjected to. The Newton-Raphson method is used in Brigade/Plus. The Newton-Raphson is a method used to solve the nonlinear equilibrium equations. The load is applied in increments and the force equilibrium for every increment is achieved with iterations with updated stiffness matrix.

2.12.4 Eigenvalue

When extracting the natural frequencies and associated modes for the bridge it can be handled as an eigenvalue problem. Considering a free vibration multi degree of freedom (MDOF) system, equation of motion will be according to equation (2.41).

$$M\ddot{u} + \mathrm{Ku} = 0 \tag{2.41}$$

Trying to find the solution according to equation (2.42).

$$u = \phi \sin(\omega t) \tag{2.42}$$

Due to the time independence of ϕ the acceleration is given by equation (2.43).

$$\ddot{u} = -\omega^2 u \tag{2.43}$$

Inserting eq. (2.43) in (2.41) the following is obtained:

$$(K - \omega^2 M)\phi = 0 \tag{2.44}$$

Where ω denotes the eigenfrequencies and ϕ the eigenmodes. This gives the fundamentals for a modal analysis.

2.12.5 Modal dynamics

A Modal dynamics analysis is an analysis based on modal superposition. The natural modes gives the most likely behavior and movement of the bridge. Before this step can be used an extraction of the natural frequencies and associated modes of the bridge needs to be done. The system will have equal number of mode shapes as the number of degrees of freedom. Due to the user defined number of frequency modes that will be extracted, the system of equations will be smaller than a full implicit analysis and therefore the calculation time will be less. The response of the bridge will be a linear set of equations. Rayleigh damping will be used on the modes extracted. The loads will be applied on the nodes.

2.12.6 Implicit dynamics

The implicit dynamics analysis can handle nonlinear problems. The implicit analysis solves the equation of motion and updates the velocities and displacements using a Newmark time integration procedure. When no numerical damping is applied, the procedure is called the trapezoidal rule. Due to the integration scheme the calculation time will be larger than the Modal dynamics analysis.

3 Reference bridge

To be able to make a more precise model, a real built bridge has to be analyzed. With help from Bridges to Prosperity, and especially Maria Gibbs, we have received dynamic measurements from a real suspended bridge.

The bridge that has been analyzed is named the Jicaro Bridge and it's situated in Nicaragua. The bridge is 64 meter long and it's a suspended bridge without wind stabilization. Its main load carrying system is composed of 5 cables with a diameter of 32 mm, 3 under the walkway and 2 as handrails. Both the deck and the crossbeams are made of wood. The bridge can be seen in Figure 3.1 below.

Figure 3.1 The Jicaro Bridge

Since these measurements are a part of Maria Gibbs PhD-project, we are not able to publish results from these. However, we have been able to calibrate our model from these measurements. The structural damping have been measured and some natural frequencies have been identified. One must note that these measurements are done with quite few accelerometers, which of course affects the results and that these result only validates the model for this single case. But overall, these measurements has been very valuable for our models.

4 Analysis of the single cable

4.1 Evaluation of sag

The dynamic behavior of a suspended bridge is very affected by its sag. In some literature, for example (Schnetzer, 2002), the natural frequencies for a suspended bridge is plotted against the length of its span with a fixed sag/span-ratio. An example of this, made with hand calculations, can be seen in Figure 4.1.

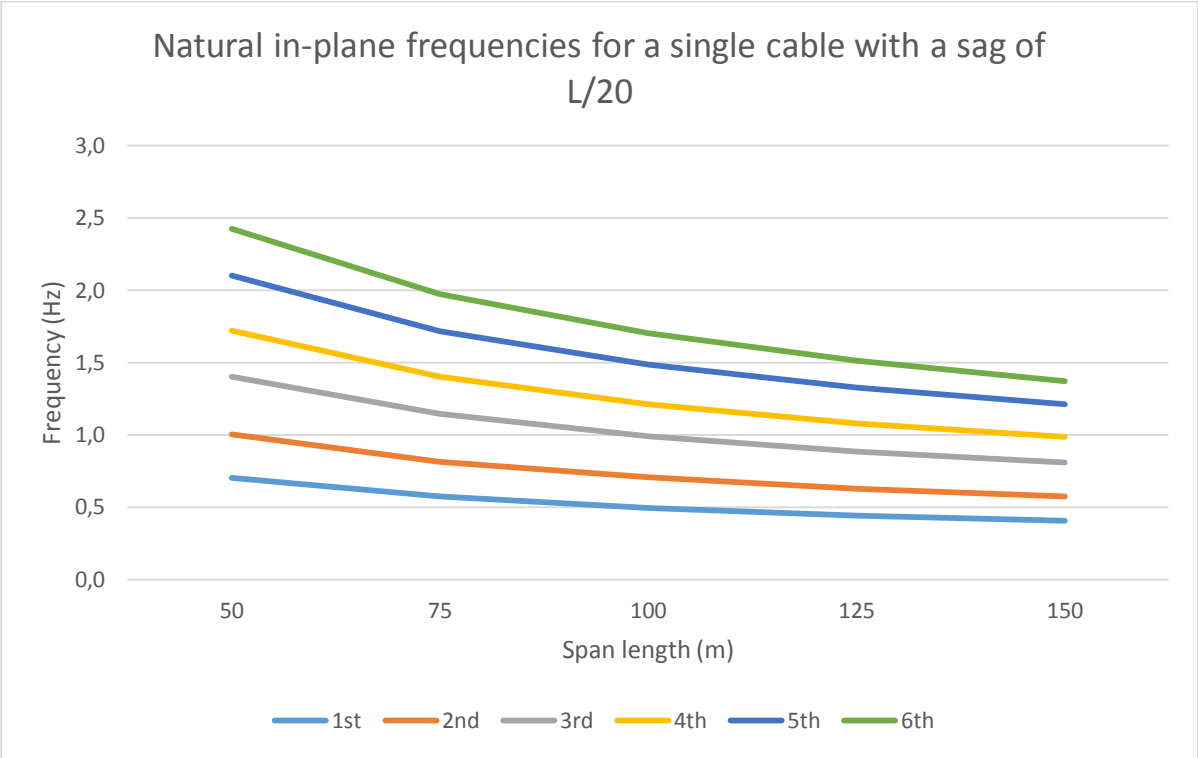

Figure 4.1 Natural in-plane frequencies for a single cable with a sag of L/20

When looking at Figure 4.1, it's easy to get the impression that the natural frequencies of the cable varies with the length of the cable. This is partly true, but the most contributing factor to the reduction of the natural frequencies is the increasing sag of the cable due to the fixed sag/span-ratio, i.e when the span increases, the sag of the cables also increases.

In Figure 4.2 below, a cable with a fixed sag of 5 meter has been analyzed, also this time with hand calculations. The figure clearly shows that it is only the symetric in-plane frequencies that changes when the span increases. The assymetric in-plane frequencies, and also all the out of plane frequencies which aren't showed in the figure, doesn't change with the span length.

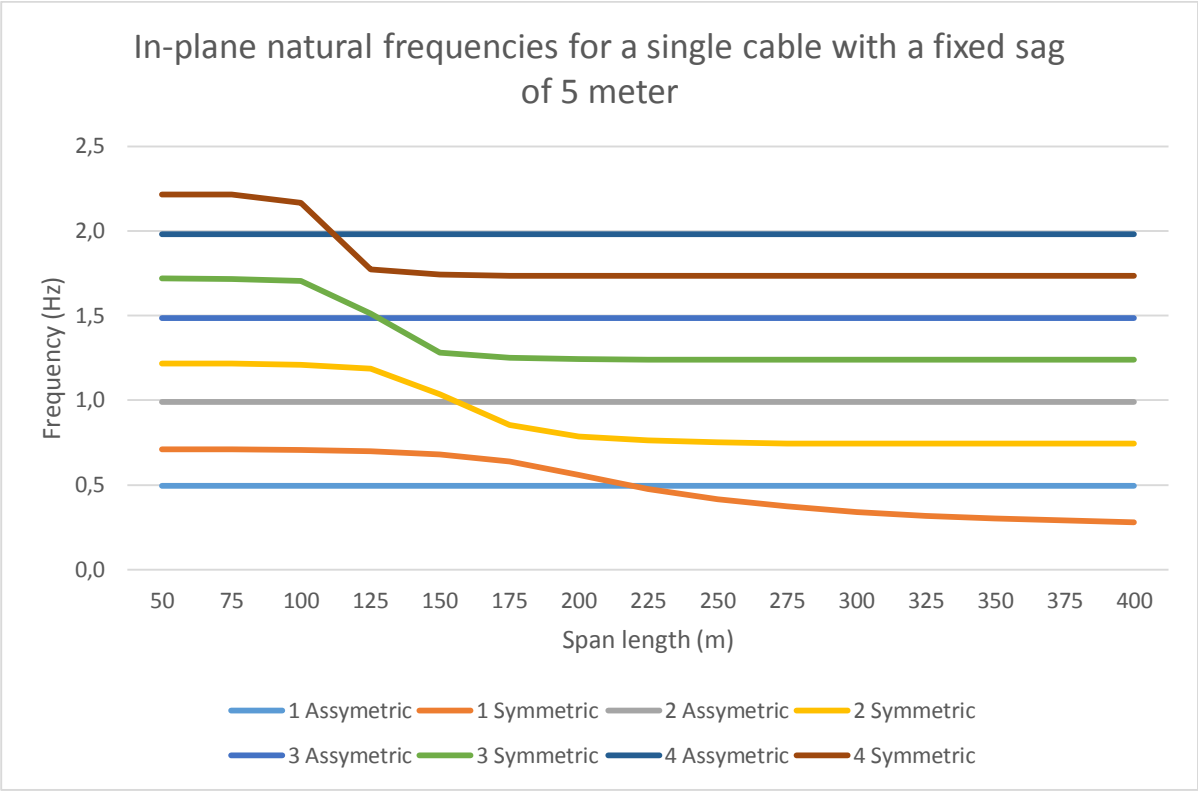

Figure 4.2 In-plane natural frequencies for a single cable with a fixed sag of 5 meter

When the span is shorter than 100 meter, the cable behaves just like the sagging cable it is, but when the span length increases it behaves more and more like a taunt string. The crossover-point for the 4th symetric- and assymetric frequencies take place at around 115 meter. The crossover-points for higher frequencies will take place at smaller spans, but the mode shapes for these frequencies are so small so they are not considered relevant for this report. The remaining crossover-points happens at 130, 160 and 220 meters.

As described in the chapter Dynamics of cables, these crossover-points and the order of the natural modes depends on the value of P_{ge}

$$P_{ge} = \left(\frac{8 \cdot f}{L}\right)^3 \cdot \frac{E \cdot A}{g_a \cdot m \cdot L} \tag{4.1}$$

Where
f is the sag of the cable
E is the Young's modulus of the cable
A is the cross sectional area of the cable
g_a is the acceleration due to gravity
m is the mass per unit length of the string
L is the length between the supports

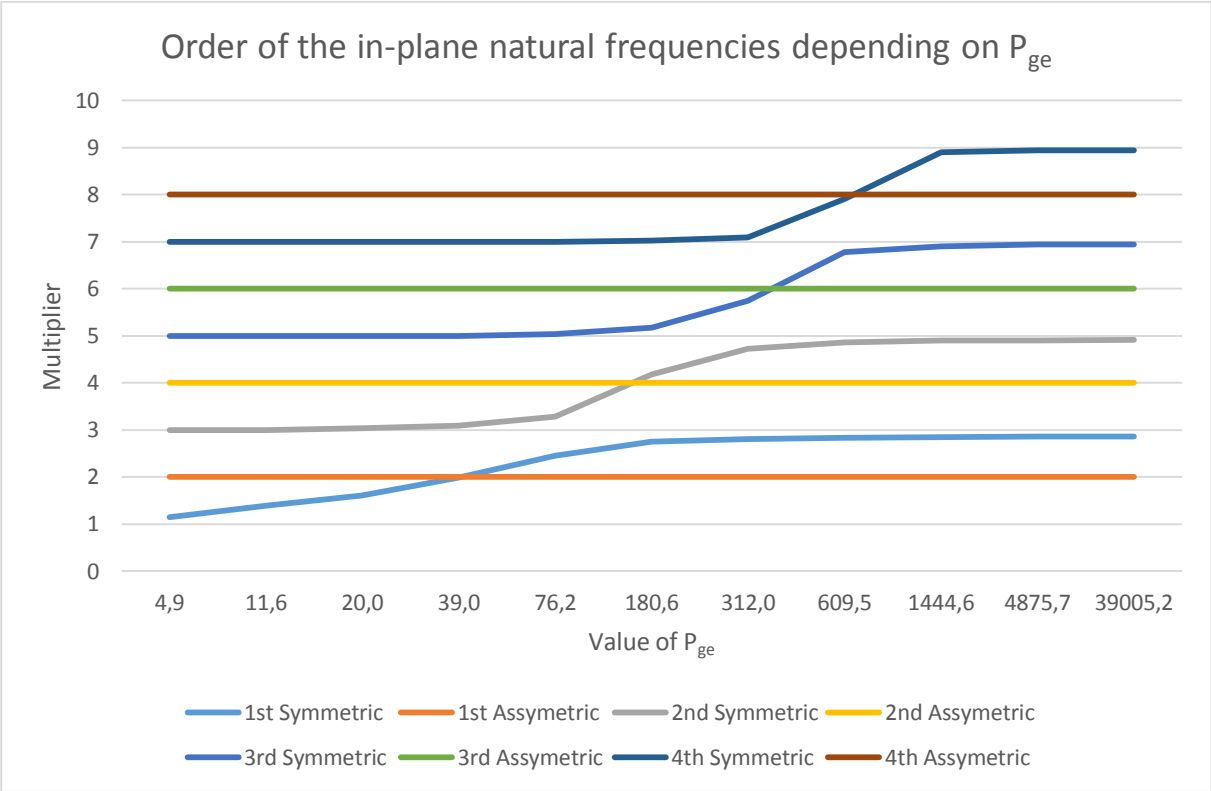

Figure 4.3 Order of the in-plane natural frequencies depending on P_{ge}

The relationship between P_{ge} and the order of the natural in-plane frequencies can be seen in Figure 4.3. This figure is made with the equations from (Irvine, 1981) which were presented in the chapter Dynamics of cables. Figure 4.3 confirms the theory given in Figure 2.16 and it also shows the next two crossover-points. The multiplier on the vertical axis in Figure 4.3 can be used in equation (4.2).

$$frequency = \frac{Multiplier}{2 \cdot L}\sqrt{\frac{H}{m}} \quad Hz \tag{4.2}$$

Where H is the horizontal force component in the cable
m is the mass per unit length of the string
L is the length between the supports

Since the span length L is present in both the denominator and the numerator (L^2 is included in H) in equation (4.2), the frequency for the symmetric modes won't change, due to their constant multiplier, if the length of the span varies.

A more efficient way to manipulate the natural in-plane frequencies is to change the sag of the cable. The relationship between the frequencies and the sag can be seen in Figure 4.4, Figure 4.5 and Figure 4.6. In these figures the span length is fixed and the sag is varying which means that all the natural frequencies, in-plane and out of plane, will be affected by the changes in the sag. In Figure 4.4 the symmetric in-plane natural frequencies can be seen. The sign of the

derivative for the symmetric frequency-curves isn't constant since their "multiplier" is affected by the value of P_{ge}. This is not the case for the asymmetric in-plane

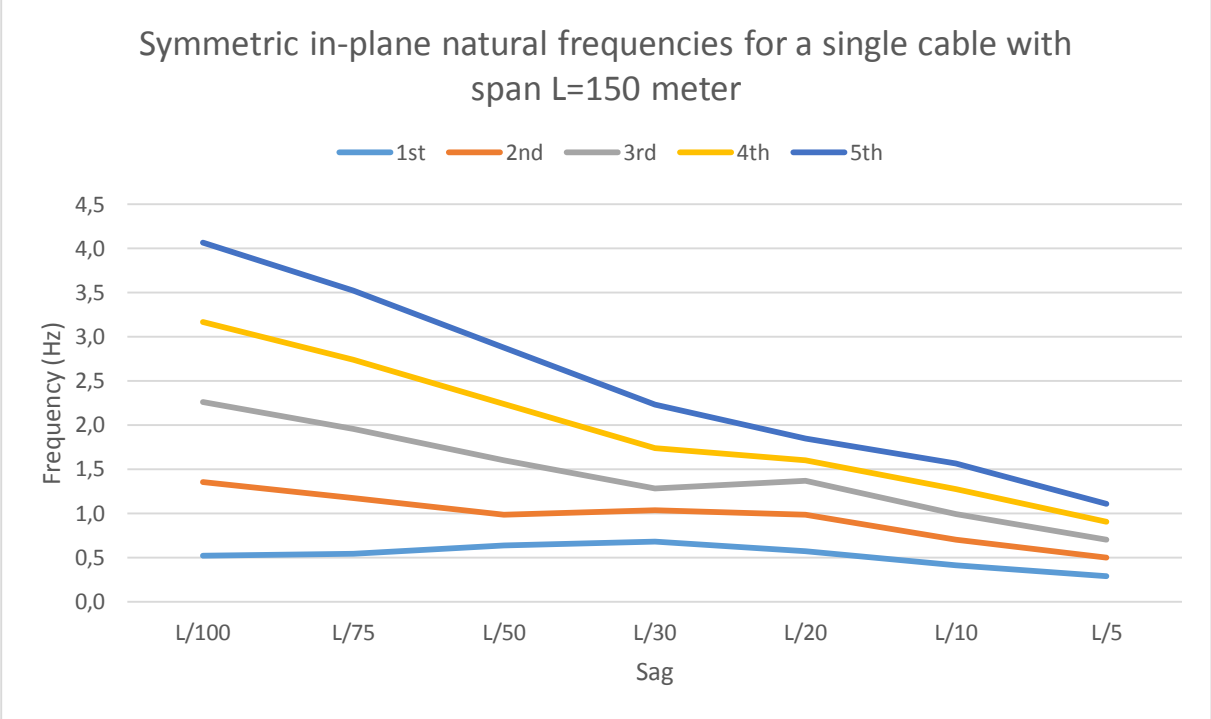

Figure 4.4 Symmetric in-plane natural frequencies for a single cable with span L=150 meter

frequencies. The sign of the derivative is always constant, i.e. if the sag increases the frequencies will always decrease. This can be seen in Figure 4.5 below.

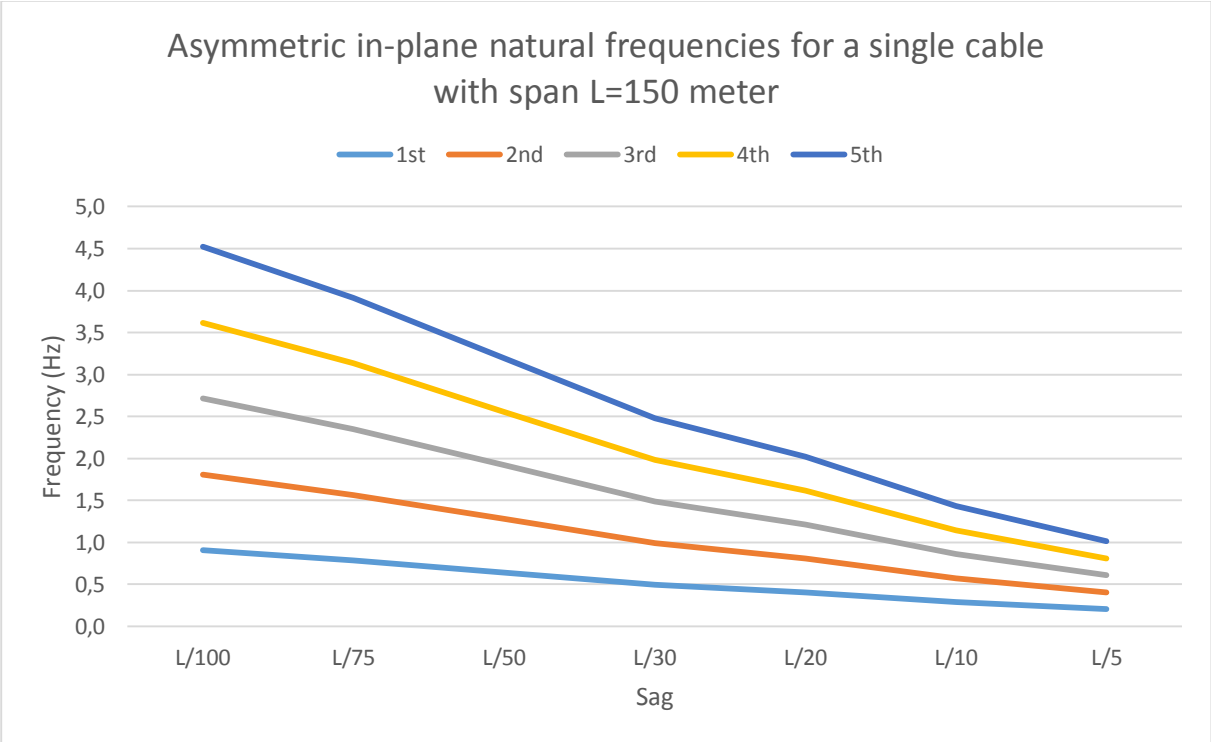

Figure 4.5 Asymmetric in-plane natural frequencies for a single cable with span L=150 meter

The first three symmetric and three antisymmetric in-plane frequencies have been plotted together in Figure 4.6. This figure clearly shows three crossover-points on the way from behaving like a taut string at a sag of L/100 to having like a sagging cable from sag bigger than L/20.

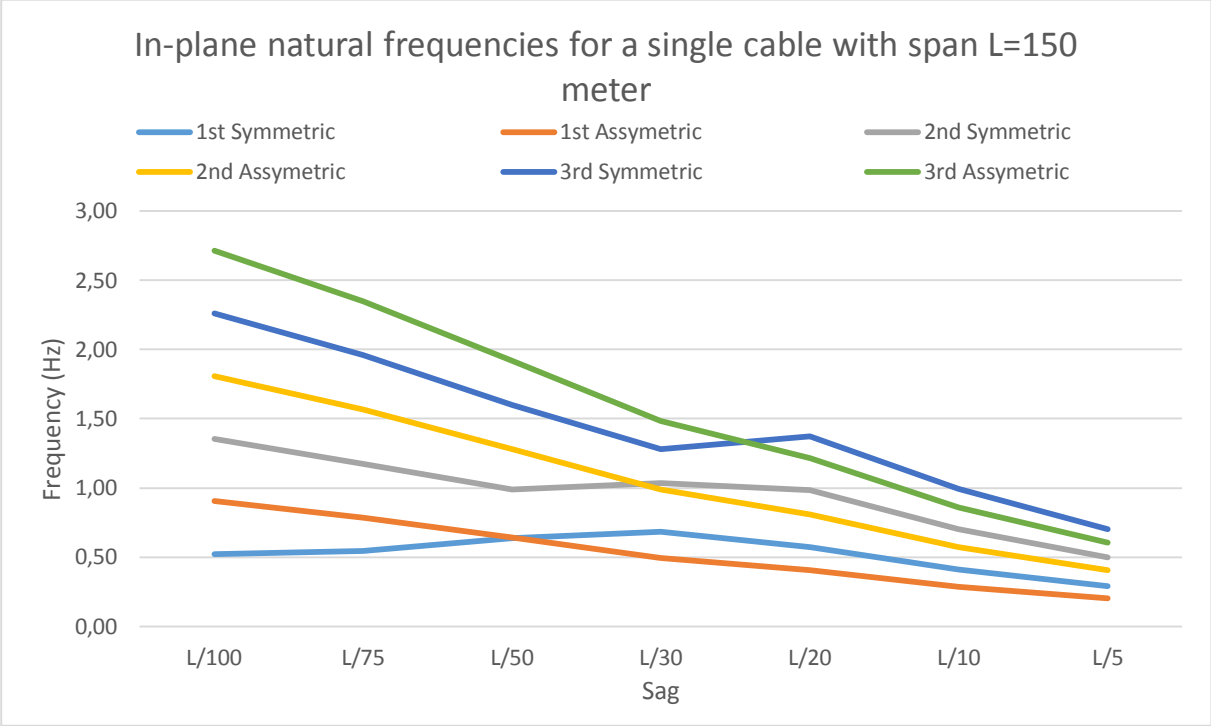

Figure 4.6 In-plane natural frequencies for a single cable with span L=150 meter

Since it's quite easy to calculate the natural frequencies for a single cable, it would be useful if theses frequencies corresponds to the one that's been calculated from the bridge models in Brigade/Plus. This connection will be researched further in chapter 0.

4.2 Modelling of a single cable in Brigade/Plus

As a first step in the modelling of a suspended bridge, a single cable has been modelled. Since it has been shown in chapter 2.7 that it's easy to calculate the natural frequencies by hand, this is a good way to start working with Brigade since it's possible to compare the result from the model with the hand calculated results. This is a good way to check if the results from the model is reasonable. The chosen cable has the diameter of 35 mm which gives an approximate metallic area of 544 mm^2. A rough sketch of the cable can be seen in Figure 4.7 below.

Length L:	60 meter
Sag f:	3 meter
Mass:	4.27 kg/m
E-modulus:	110 GPa
Metallic area:	544 mm^2

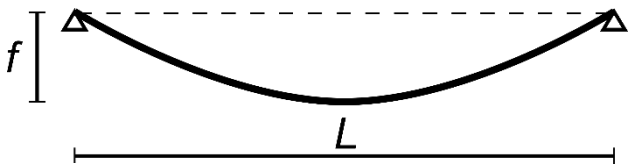

Figure 4.7 Sketch of the cable

The cable in the model is composed of two node beam elements and it's pinned in both ends.

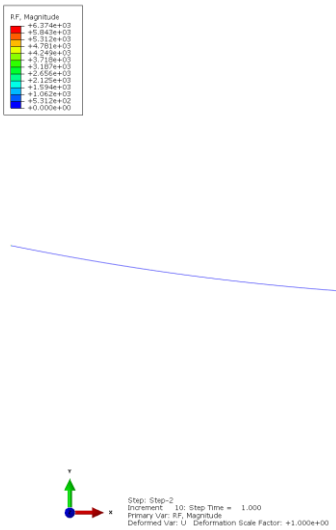

Figure 4.8 Brigade model

The Brigade model can be seen in Figure 4.8 above. The cable force near the supports in the model is 6,37 kN. Since the sag is increased in the cables deformed stadium and the hand calculation estimate the cable force to be 6.41 kN it's seem like a reasonable result.

The eigenmodes and appurtenant frequencies have been calculated for both in plane- and out of plane vibrations. Since the P_{ge}-number is quite high, $P_{ge} \approx 1500$, the cable will act like a sagging cable (which it is) and not like a taut string or anything in between. This causes the first vertical eigenmode to be assymetric, which both the hand calculations and the Brigade model has shown. As seen in the tables below, the frequencies calculated by hand and the ones calculated in the model are very alike.

	1st	2nd	3rd	4th
Direction	Out of plane	Vertical	Out of plane	Vertical
Mode type	Symmetric	Asymmetric	Asymmetric	Symmetric
BRIGADE/Plus (Hz)	0,318	0,631	0,637	0,910
Hand calculations (Hz)	0,320	0,639	0,639	0,914

	5th	6th	7th	8th
Direction	Out of plane	Vertical	Out of plane	Vertical
Mode type	Symmetric	Asymmetric	Asymmetric	Symmetric
BRIGADE/Plus (Hz)	0,957	1,279	1,282	1,578
Hand calculations (Hz)	0,959	1,279	1,279	1,573

Table 4.1 Natural frequencies for a single cable

In Figure 4.9 below, the second natural mode and therefore the first in-plane natural mode of the single cable can be seen.

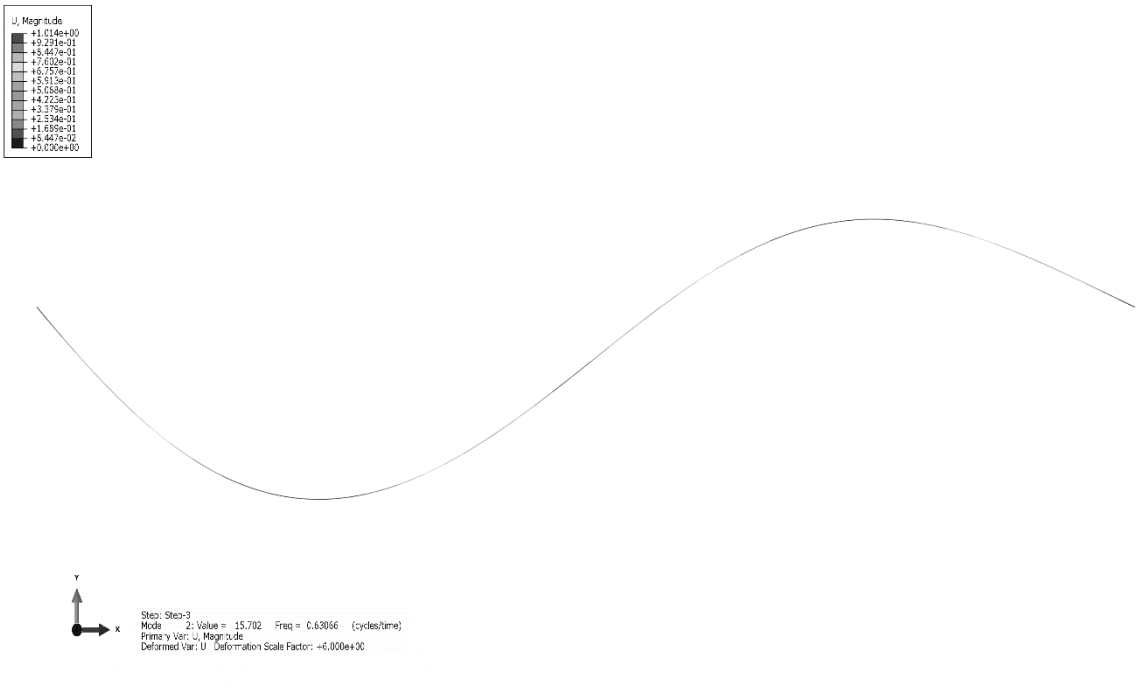

Figure 4.9 The second mode of the single cable, i.e the first vertical mode

4.3 Discussion

The results in this chapter has proven that modifying the sag is an effective way to change the value of the natural frequencies of a single cable. It has also been proven that the hand calculations are very similar to the finite element model when it comes to calculating natural frequencies for a single cable. Since the way to hand calculate the natural frequencies of a single cable is well known, it can be assumed that the FE-modelling of cables is precise so far. This is promising for the modelling in further chapters.

5 Static analysis of the suspended bridge

5.1 Hand calculations

Designing a suspended bridge with regard to only static loads isn't a difficult task for a person with some knowledge of structural engineering. The design procedure can be made systematic which has led to the creation of a design guide in the form of an Excel sheet. The Excel sheet can be used to design a suspended bridge according to both Helvetas and Eurocode and also with or without windguys as lateral stabilization. Since the main and handrail cables in a suspended bridge are the structural members that carries the whole load of the bridge and its users, the main focus in the design guide is to determine the appropriate dimensions for these cables. A design example for a 150 meter long suspended bridge made with this design guide can be seen in the appendix.

Note that unless otherwise stated, all hand calculations presented are calculated with the design guide.

5.2 Modelling

Component	Part	Element
Cable	Wire 3D deformable	B31
Crossbeam	Wire 3D deformable	B31
Suspender	Wire 3D deformable	T3D2

Table 5.1 Properties for components in Brigade/Plus

B31 is a 2 node beam element in 3D space with a linear interpolation function. And T3D1 is a 2 node truss element in 3D space. This means that the connection between the suspender and the crossbeam will be a joint due to the lack of rotational degrees of freedom in the truss element.

5.3 Influence lines

An influence line shows the deflection, moment, shear force etc for a certain position on the bridge due to a force placed somewhere on the bridge. In this case, influence lines showing the deflection for two points on a 150 meter long suspended bridge has been made. The bridge is designed according to Eurocode. The two points are:

- $x = \frac{L}{2} = 75\ m$
- $x = \frac{L}{4} = 37.5\ m.$

The influence lines had been made with the Brigade/Plus model and the recorded displacements has been normalized to achieve a displacement factor η that can be multiplied with an acting force on the bridge. Since the unit of η is m/N, the user of the influence line can multiply the value of the force with the displacement factor η for the location of the force.

One important matter to notice is the nonlinearity in the force-displacement relationship. This nonlinearity is important to have this in mind when using the influence lines. The influence lines in Figure 5.1 and Figure 5.2 has been made by recording the displacement due to a vertical force with a magnitude of 100 newton.

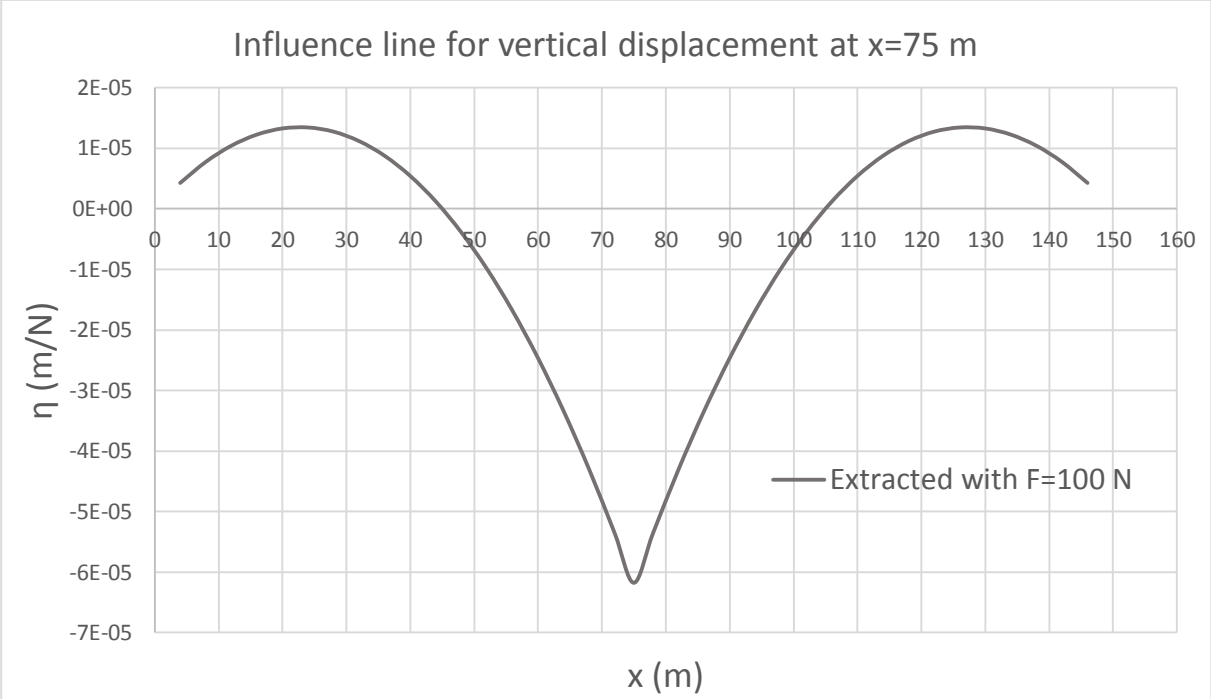

Figure 5.1 Vertical displacements at x=75 meter

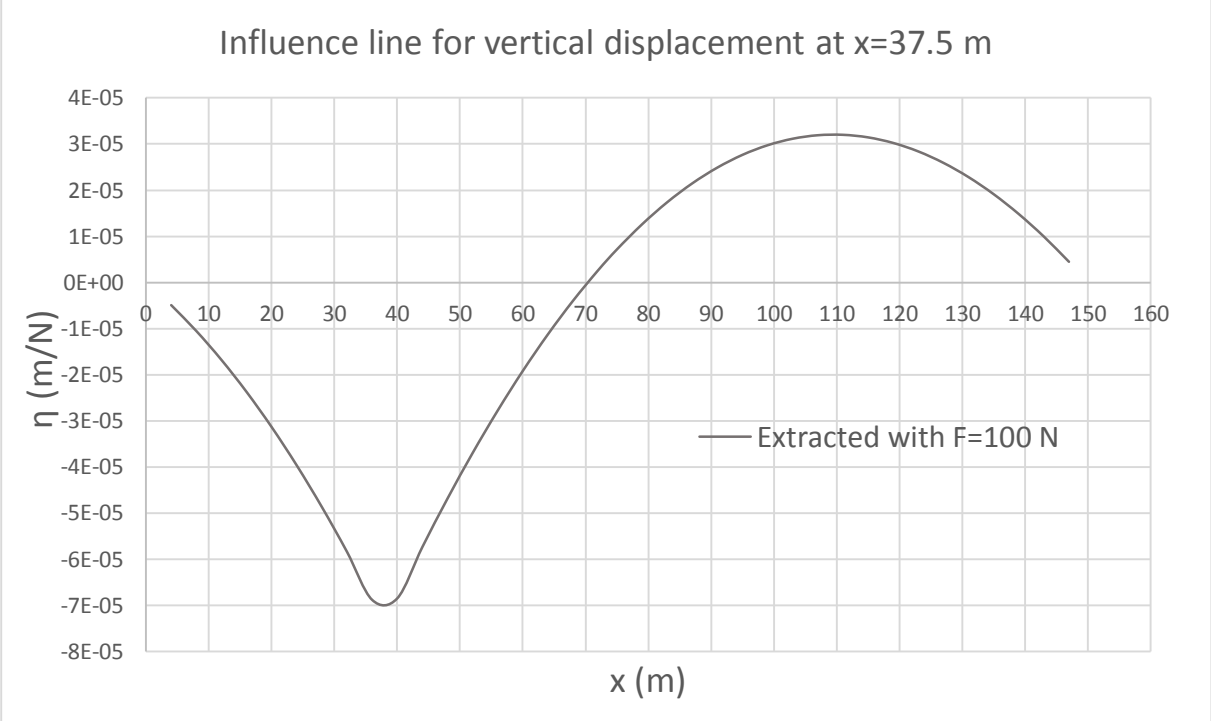

Figure 5.2 Vertical displacement at x=37,5 meter

To investigate the assumption of nonlinearity two another influence lines was made. These two recorded the deflections due to a vertical force of 2000 newton for the same points as the earlier ones. In Figure 5.3 and Figure 5.4 the influence lines for the force of 2000 newton has been inserted. Both of the influence lines in each figure has been normalized and as expected a small difference between the lines can be seen. When using the influence lines, interpolation have to be used even if the difference between the lines isn't big.

If one want to use the influence lines for a uniformly distributed load, the influence line have to be integrated over the length of the uniformly distributed load. For example, if the maximum possible displacement for the midpoint of the bridge should be determined, the influence line should be integrated over the distance $x \approx 43 - x \approx 107$ and then multiplied with the uniformly distributed load that should be placed over the same distance.

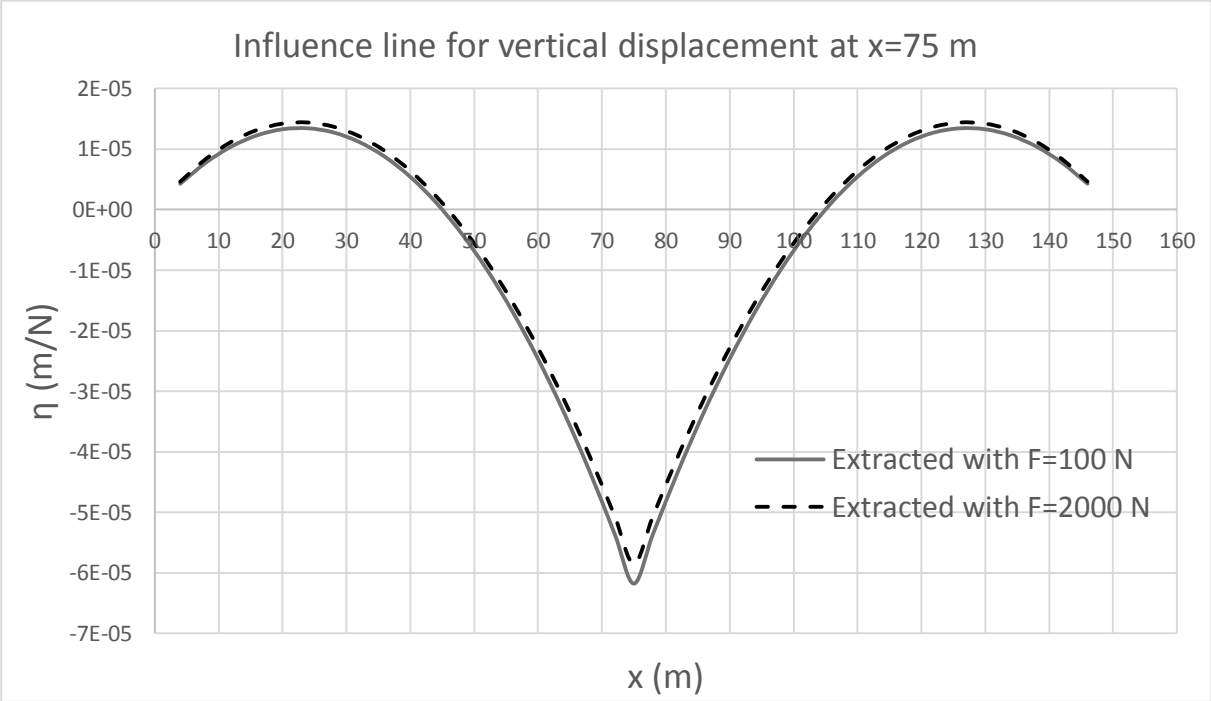

Figure 5.3 Vertical displacements at x=75 meter

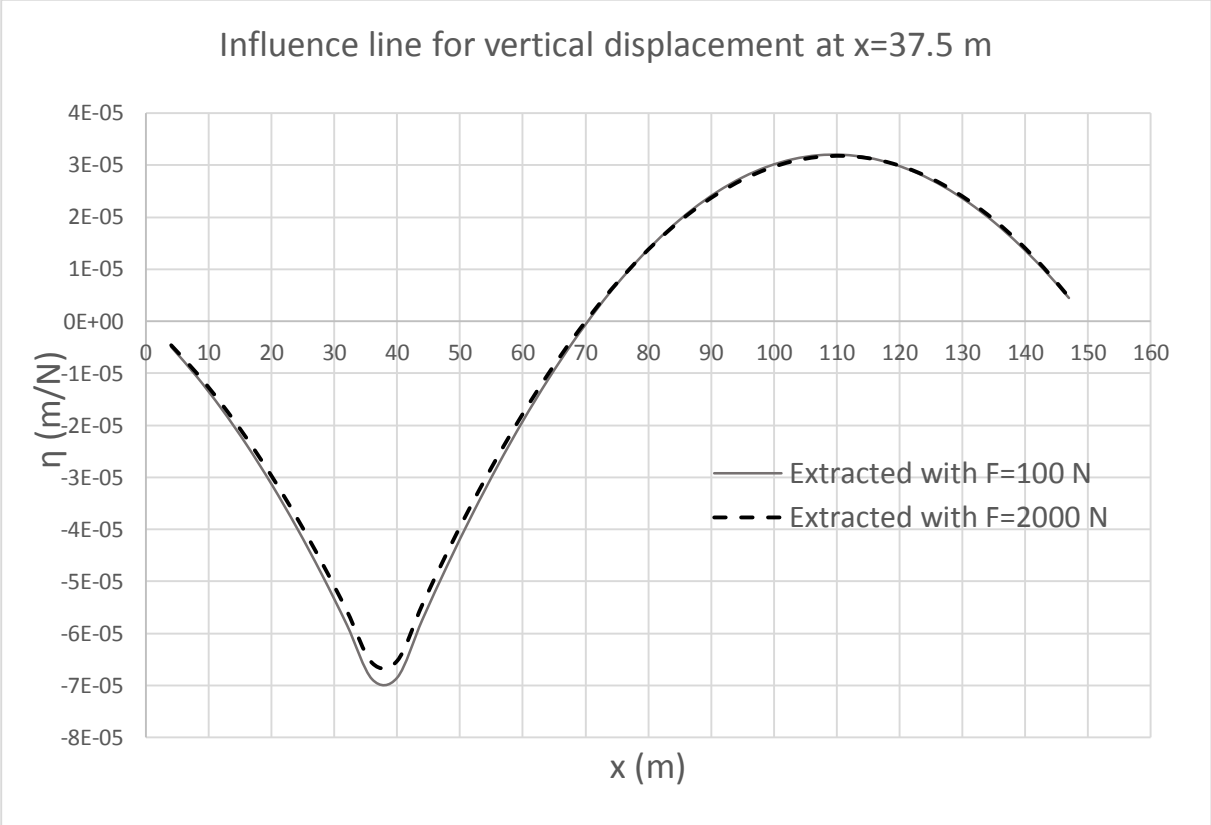

Figure 5.4 Vertical displacement at x=37,5 meter

An example of how to use an influence line can be seen below. A force with a magnitude of 1 kN has been placed at the position $x = 20\ m$. This can be seen in Figure 5.5. The displacement for the two positions can be calculated with interpolation between the two influence lines in Figure 5.3 and Figure 5.4:

Deformation at $x = 37.5\ m$: $v_{37.5} = 1000 \cdot -3{,}1 \cdot 10^{-5} = -31\ mm$

Deformation at $x = 75\ m$: $v_{75} = 1000 \cdot 1{,}35 \cdot 10^{-5} = 13{,}5\ mm$

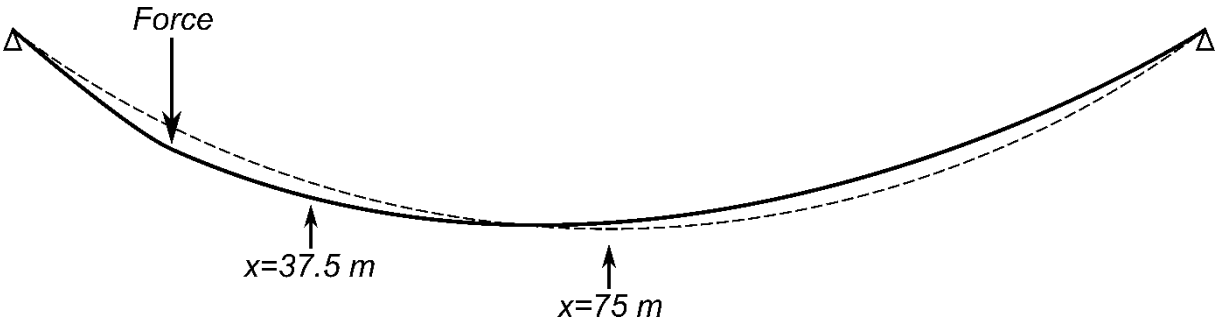

Figure 5.5 Deflection due to a vertical force with the position x=20 meter

Another example can be seen below. A force with a magnitude of 1 kN has been placed at the position $x = 75\ m$. This can be seen in Figure 5.6. The displacement for the two positions can be calculated with interpolation between the two influence lines in Figure 5.3 and Figure 5.4:

Deformation at $x = 37.5\ m$: $v_{37.5} = 1000 \cdot 0{,}75 \cdot 10^{-5} = 7{,}5\ mm$

Deformation at $x = 75\ m$: $v_{75} = 1000 \cdot -6{,}0 \cdot 10^{-5} = -60\ mm$

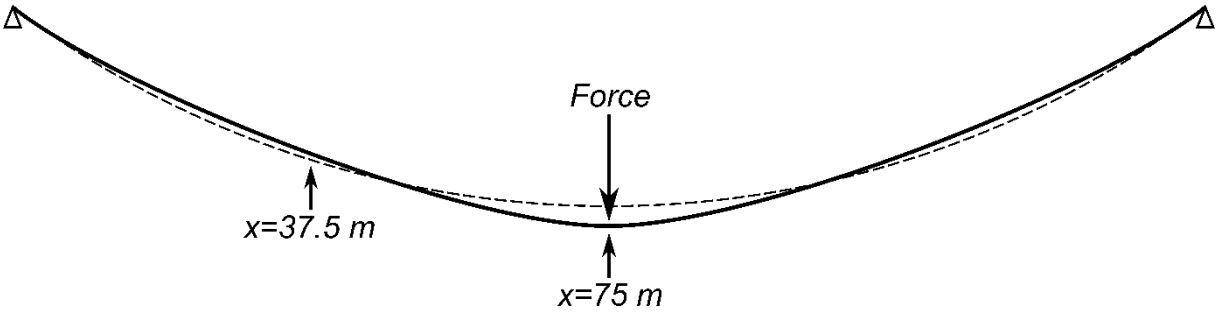

Figure 5.6 Deflection due to a vertical force with the position x=75 meter

5.4 Displacements

Due to their slim and flexible shape, suspended bridges can be subjected to large vertical and lateral displacements. In this chapter, displacements due to static loads will be discussed. Displacements in the vertical direction will always occur, in fact the dead load sag is a displacement from the hoisting sag, i.e. the sag the cables are hoisted to during construction. The vertical displacements for the two investigated bridges can be seen in Table 5.2.

The vertical displacements for the 150 meter long bridge have been determined with Brigade, influence lines and hand calculations. The live load used is the characteristic live load according to Eurocode for a 150 meter long bridge, and this load acts on the whole length of the bridge. The calculated displacements are quite similar and they span from 1,6 – 1,75 meter, which seems like a reasonable result. These displacements won't significantly affect the users of the bridge, with a possible exception for old or disabled people. However, live loads of this magnitude are extremely rare. For a smaller but still large live load, 1000 kN/m, the vertical displacement becomes approximately 0,78 meter.

Vertical	Span (m)	Dead load (N/m)	Live load (N/m)	Total load (N/m)	Displacement (m)
Brigade	150	460	2670	3137	1,65
influence line	150	460	2670	3137	1,6
Hand calculations	150	460	2670	3137	1,75
Brigade	64	490	2670	3167	0,36
Hand calculations	64	490	2670	3167	0,33

Table 5.2 Vertical displacements

The deformed shape of the 150 meter long bridge can be seen in Figure 5.7 below.

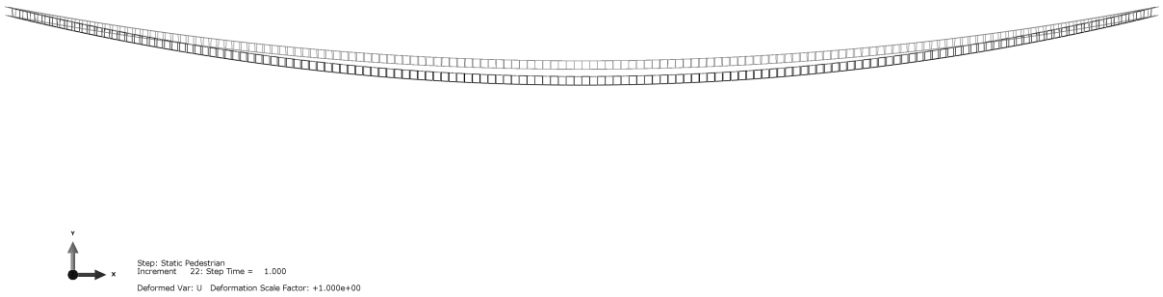

Figure 5.7 Vertical displacements due to a live load of 2,67 kN/m.

Lateral displacements due to wind load are hard to determine in a realistic way. Due to the non-steady state of wind loads, static displacements are more an easy calculated estimation of possible lateral displacements. More lateral displacements due to wind will be presented in the dynamics chapter 0

The lateral displacements in Table 5.3 below are based on wind speeds of 10, 15 and 20 m/s and the wind loads are determined according to equation (2.31. For both the Brigade and the hand calculations, the bridge has only been subjected to its own dead load since this will be the worst case with regard to lateral displacements. Live load would have increases the reference area for the wind load, but since the vertical load is greater than the increased wind load, this would have reduced the lateral displacements.

Lateral	Span (m)	Windguys	Wind (m/s)	Dead load (N/m)	Wind load (N/m)	Displacement (m)
Brigade	150	-	10	460	57	0,99
Brigade	150	Yes	10	460	57	0,18
Hand calculations	150	-	10	460	57	0,92
Brigade	150	-	15	460	129	2,16
Brigade	150	Yes	15	460	129	0,34
Hand calculations	150	-	15	460	129	2,01
Brigade	150	-	20	460	229	3,55
Brigade	150	Yes	20	460	229	0,51
Hand calculations	150	-	20	460	229	3,32

Table 5.3 Lateral displacements

As it can be seen in Table 5.3, the lateral displacements determined with Brigade and hand calculations are very similar. The hand calculations are done with the "pendulum theory" presented in chapter 2.10.5. The lateral displacements determined with the Brigade model

without windguys are approximately 7% bigger than the displacements determined by the hand calculations. It can therefore be stated that quite simple hand calculations are very similar to finite element models when calculating lateral displacement due to static wind load for bridges without windguys.

The lateral displacements due to a wind speed of 20 m/s for the 150 meter long bridge with and without windguys can be seen in Figure 5.8 below.

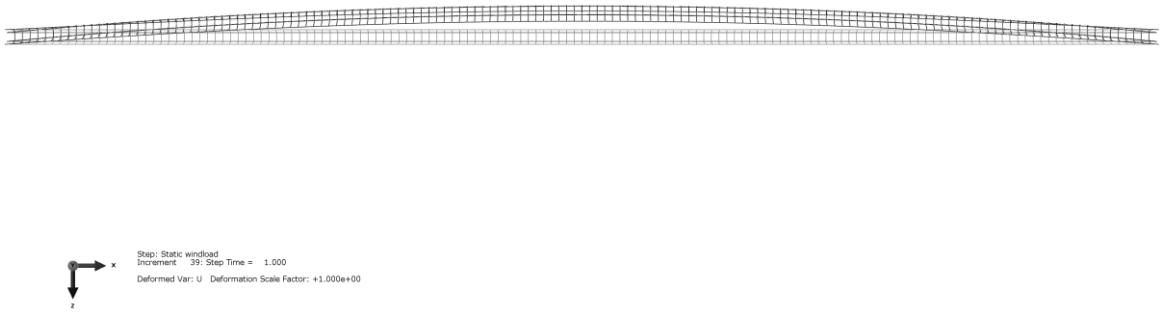

Figure 5.8 Lateral displacements due to a static wind of 20 m/s

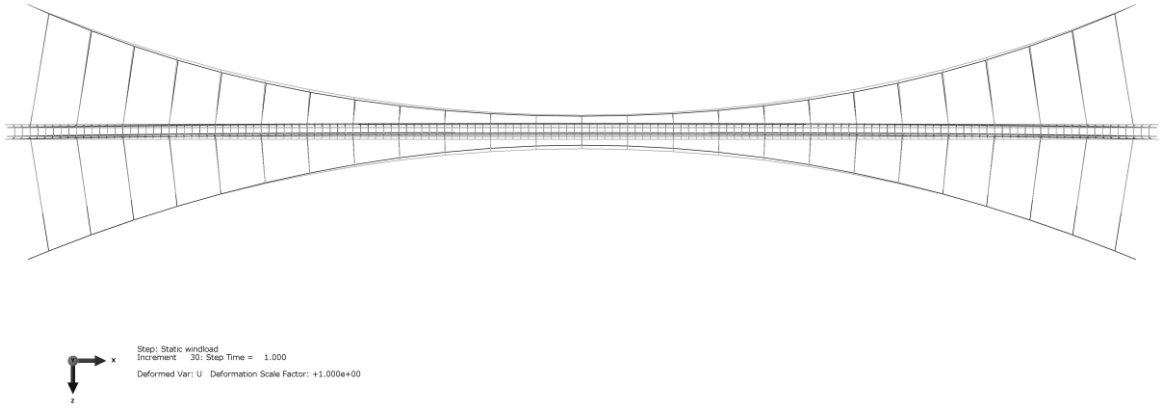

Figure 5.9 Lateral displacements due to a static wind of 20 m/s

5.5 Stress distribution

The main part of the loads on a suspended bridge acts on the walkway deck. If this load shall be uniformly distributed over both the walkway cables and the handrail cables, the suspenders have to be very stiff. Since the suspenders, and therefore the connection, between the handrail

and walkway cables aren't completely stiff, there will be a difference between the forces in these cables.

To be able to investigate the force and the appurtenant stress distribution in the cables, both the models of the Jicaro Bridge and the 150 meter bridge have been analyzed. The cable diameter of the Jicaro Bridge in the model has in this case been changed to a diameter that's recommended by Eurocode. The comparison between the two bridges would otherwise have been poor.

The two bridge models have been subjected to both their design load and their dead load and the stresses in the cables have been measure for these load cases. An additional load step was used for the Jicaro Bridge, which can be seen in Figure 5.10. In this figure, two lines can be seen. The upper line corresponds to the stress in one of the walkway cables and the lower line corresponds to the stress in one of the handrail cables. The stress is plotted against time, where the dead load was applied in steps during the first second and the 1 kN/m load was applied in steps during the second second.

The stress difference starts during the first load steps. Since most of the dead load are situated in the lower parts of the bridge, the stress in the walkway cables will increase first. Since the handrail cables are connected with suspenders to the walkway cables, a vertical displacement of the walkway cables must occur before the suspenders will be tensioned and the lower part of the bridge starts to "hang" in the handrail cables. So if the suspenders aren't pre-tensioned, which seems hard to achieve, the deformation and therefore the stresses on the walkway cables will be greater, at least for small loads.

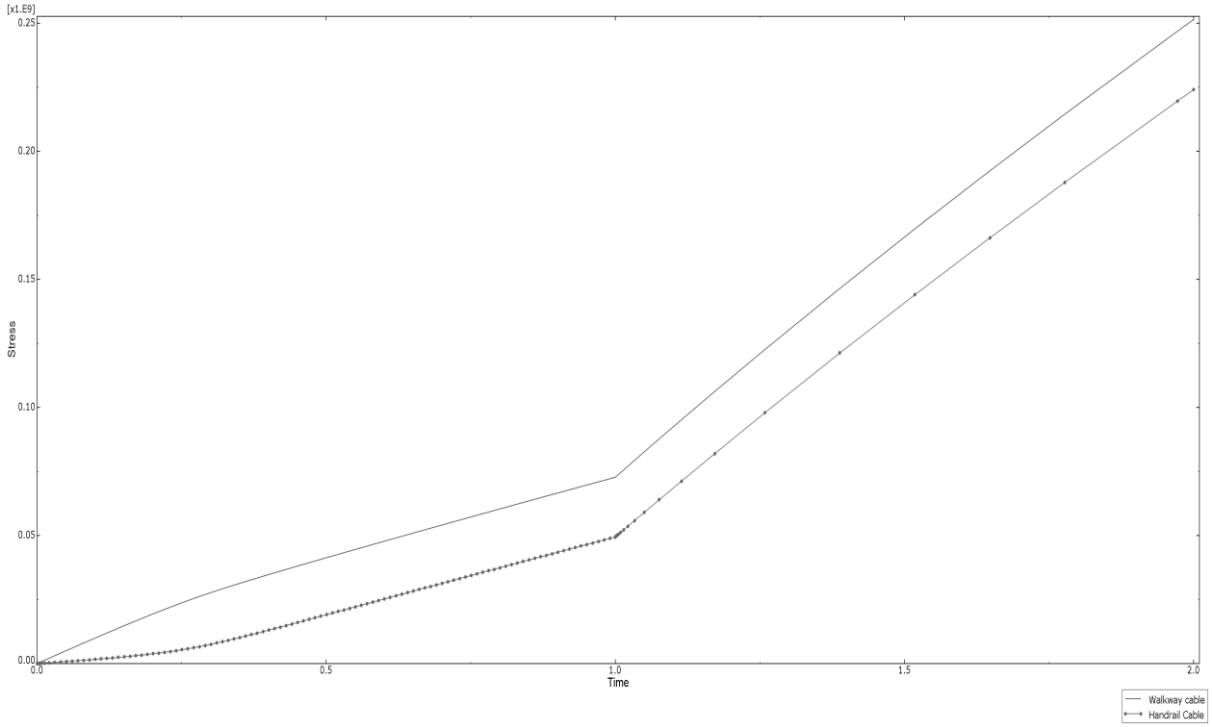

Figure 5.10 Stress distribution for walkway cables and handrail cables for the Jicaro Bridge

When the bridges are subjected to larger loads, the quotient between the stresses in the handrail cables and the walkway cables decreases, which can be seen in Table 5.4 below. It can also be seen that the stress distribution becomes more uniform with an increasing span.

	Jicaro 64 m			Bridge 150 m		
	Handrail (HR)	Walkway (WW)	Quotient WW/HR	Handrail (HR)	Walkway (WW)	Quotient WW/HR
Load	(Mpa)	(Mpa)		(Mpa)	(Mpa)	
Dead load	54,0	78,0	1,44	84,3	92,1	1,09
Dead load + 1 kN/m	230,0	260,0	1,13	-	-	-
Dead load + 5,5 kN/m	850,0	900,0	1,06	888	895	1,01

Table 5.4 Stress distribution between handrail and walkway cables

For the dead load case, the quotient between the walkway cables and the handrail cables are quite high, especially for the shorter Jicaro Bridge. For the longer bridge however, the quotient are quite low even for the dead load case. When the load increases, it's clear that the quotient decreases, which can be seen in Table 5.4. This is due to the increasing interaction between the cables that occurs when the deformation of the cables increases. In the designers viewpoint, this is a positive result since designing in the ultimate limit won't be affected if a uniformly stress distribution among both the handrail cables and the walkway cables is assumed. When the bridge approaches its maximum capacity, the stresses in the handrail cables and the walkway cables are almost identical, which is also assumed in the design sheet used for the hand calculations in this thesis.

If the quotient still would be 1,44 for the Jicaro Bridge when it approaches its maximum capacity, some kind of enlargement factor should be added to the walkway cable dimensions to compensate for the higher stress level. But as seen in Table 5.4, this doesn't seem necessary.

5.6 Cable diameter and span

For a suspended bridge, the length of the span and therefore the size of the sag, has a crucial impact on the necessary size of the load carrying cables. To make the growth of the cables due to an increasing span length clear, two different parameter studies has been made. The first study, which can be seen in Figure 5.11, is based on Eurocode and it's showing the relationship between the span length and the cable diameter for a suspended bridge with 5 load carrying cables and a sag of the span length divided by 21 i.e. L/21. The reason for the choice of the number of cables and the sag is to make a comparison with the reference bridge, i.e. the Jicaro Bridge, possible. As seen in Figure 5.11, the relationship is nonlinear, especially from 30 meter up to around 150, but also for longer spans despite the fact that the relationship looks linear for spans longer than 150 meter.

The cable diameter and the span length of the Jicaro Bridge has been marked in the figure, i.e. five cables with a diameter of 35 mm and a 64 meter long span. It's clear that the cables in the Jicaro Bridge are oversized according to Eurocode. Instead of a diameter of 35 mm, the cables should have a diameter of approximately 21 mm.

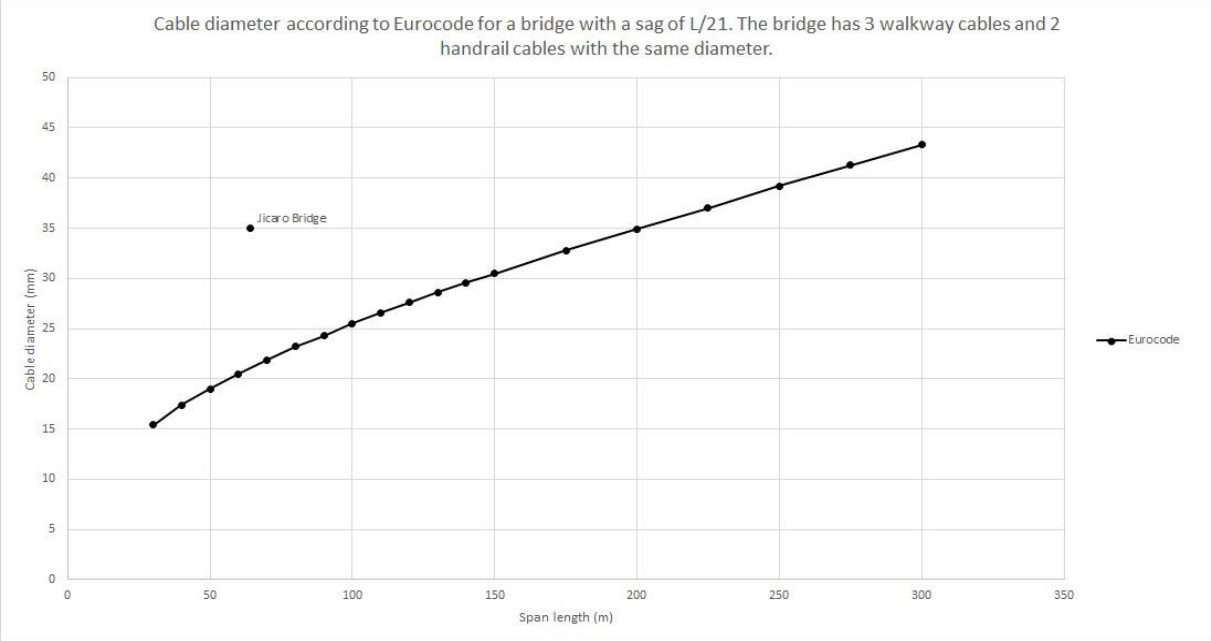

Figure 5.11 Cable diameter according to Eurocode for a bridge with a sag of L/21

A more obvious method to describe the relationship between the span length and the cable size is to use the metallic cross-sectional area instead of the cable diameter, which can be seen in Figure 5.12. The metallic cross-sectional area are direct proportional to the total strength of the cables and it's approximately 55-56 % of the total cross-sectional area of the type of wire rope used in this report. The cables use in the Eurocode design is of rope class 1570 MPa, with $f_u = 1570\ MPa$ and $f_{0.2} = 1370\ MPa$.

In Figure 5.12 it's even clearer that the Jicaro Bridge are oversized according to Eurocode. The metallic cross-sectional area of the Jicaro Bridge is almost three times bigger than the necessary area suggested by Eurocode.

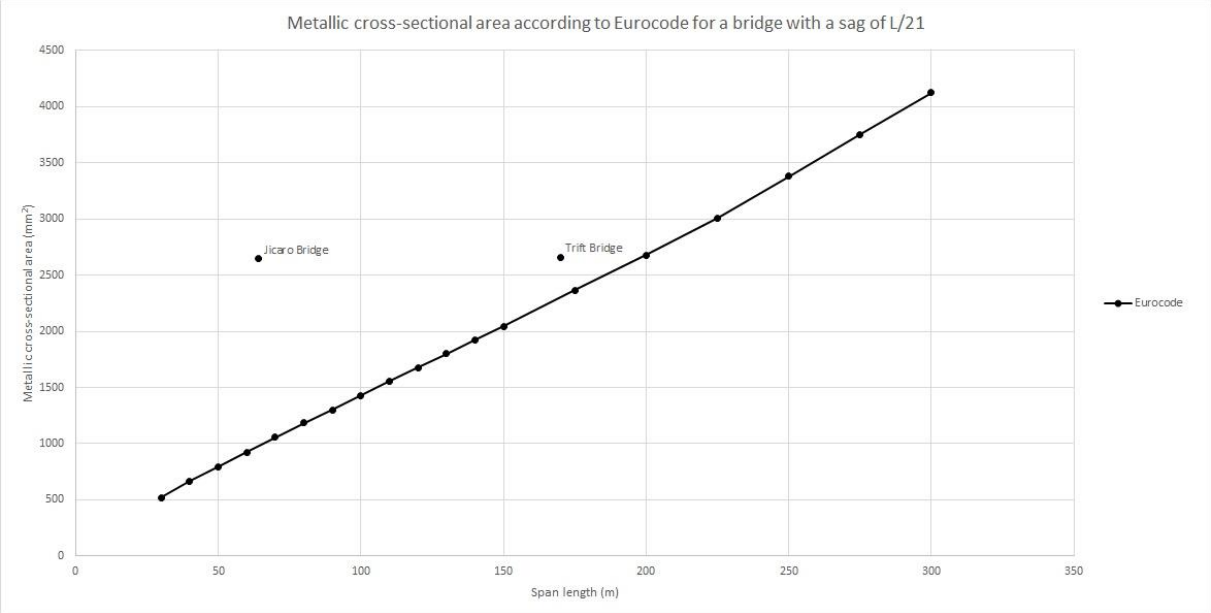

Figure 5.12 Metallic cross-sectional area according to Eurocode for a bridge with a sag of L/21

The other bridge marked in Figure 5.12 is the Trift Bridge, which is a suspended bridge spanning over a gorge close to the Trift glacier in Switzerland. This bridge was opened in 2009 when it replaced a few year older bridge that suffered from wind instability. The Trift Bridge has a similar sag ratio and it's design for a similar load as the load recommended by Eurocode (Pfaffen, Brog, & Van Rooden, 2009). As seen in Figure 5.12, the dimension of the cables in the Trift Bridge are slightly bigger but still close to the dimensions recommended by Eurocode. One reason for the bigger dimension can be the Trift Bridge are fitted with pre-tensioned windguys which creates an extra vertical force since the windguys aren't completely horizontal.

Another reason for using the metallic cross-sectional area as unit for the relationship between span length and cable size is that a comparison between the Jicaro Bridge and the dimensions suggested by Helvetas is possible. When using the Helvetas design guide it recommends different cable combinations depending on the size of the calculated force. Since the number and diameter of the cables used in these combinations varies, it's impossible to use the cable diameter as unit for the cable size. However, the metallic cross-sectional area for each cable combination is given which makes a comparison possible. In Figure 5.13 below, a maximum span for each cable combination has been calculated.

Even according to Helvetas, the cables in the Jicaro Bridge seems to be oversized. If the Jicaro Bridge should have been designed according to Helvetas, the recommended cable combination should have been point number three in the line in Figure 5.13 below, i.e. 4 cables with a diameter of 26 mm under the walkway and 2 cables with a diameter of 26 mm as handrails. This gives a metallic cross-sectional area of 1751 mm^2 even if approximately 1500 mm^2 is necessary.

The cables in the Trift Bridge are undersized according to Helvetas. Since the dimension of the cables where close to the Eurocode dimensions, this result was expected.

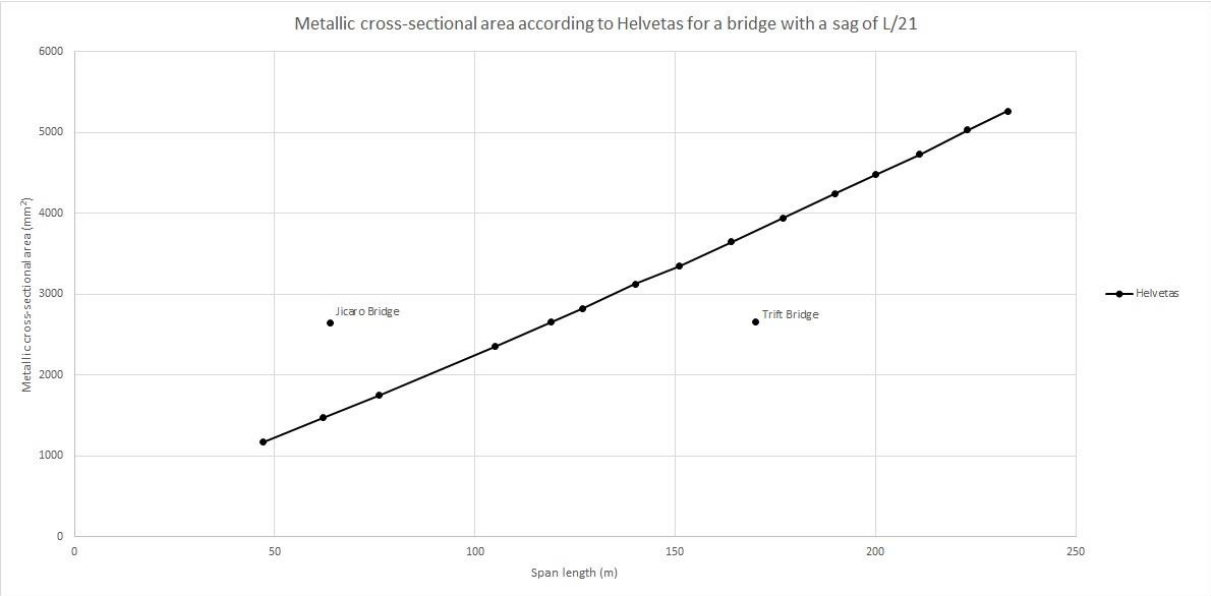

Figure 5.13

Not surprisingly, the curves in Figure 5.12 and Figure 5.13 has a quite constant factor between them, which can be seen in Figure 5.14. The areas calculated according to Helvetas are approximately 60 % bigger than the areas calculated according to Eurocode. However, for a span of 64 meter, both these areas are much smaller than the metallic cross-sectional area of the cables in the Jicaro Bridge. The Trift Bridge positions itself between the Helvetas- and the Eurocode curves. Its metallic cross-sectional area is approximately 400 mm^2 bigger than the Eurocode recommendations and 1000 mm^2 smaller than the Helvetas recommendation.

Note that neither the Helvetas nor the Eurocode curves are calculated with regard to windguys.

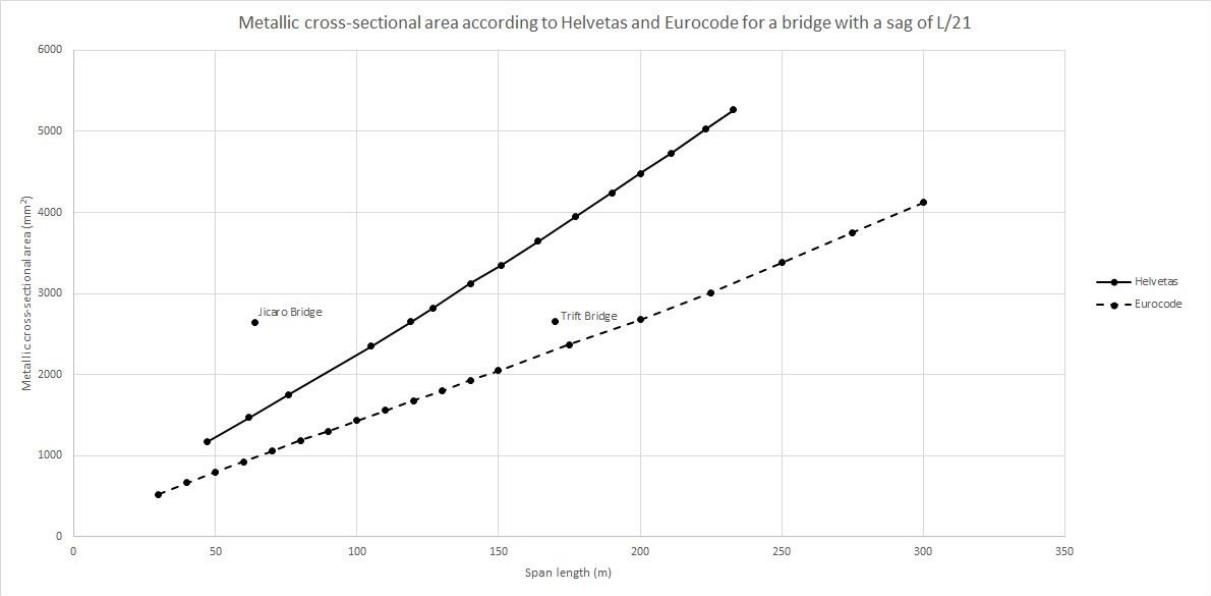

Figure 5.14

5.7 Discussion

The influence lines are a good tool to identify the most crucial load positions for a suspended bridge but they should be used with care. The influence lines presented in chapter 5.3 are created specifically for a 150 meter long bridge designed according to Eurocode and the displacement axis should only be used for this bridge. However, the shape of the influence lines won't differ much from bridges with different span but with the same span/sag-ratio. They can therefore be used with quite good accuracy to determine the displacements for different load positions.

The stress distribution between the handrail and walkway cables showed to be more and more uniformly distributed when the vertical load was increased, i.e. the cables deforms uniformly. The interaction between the handrail and the walkway cables depends on the suspenders connecting them. The difference between the vertical deformations, and therefore the stresses, in the cables will decrease with an increasing load. Since the stresses in the cables are almost similar when the bridge reaches its structural capacity, the design in the ultimate limit state can be made with the assumption of full interaction between the cables.

Hand calculations have proved to be very alike the Brigade-calculations when it comes to displacements due to static loads. The need for time-consuming FEM-models is therefore small when only static loads are used in the design.

The design according to Helvetas must be seen as oversized in comparison with Eurocode since the recommended cable dimensions by Helvetas are approximately 60 % larger than the recommended dimensions by Eurocode. Bridges to Prosperitys design guide is based on the Helvetas design guide, but as it can be seen in Figure 5.14, the design of the Jicaro Bridge is very oversized according to both Helvetas and Eurocode. The cross-sectional area of the cables in the Jicaro Bridge is almost identical with the over 100 meter longer Trift Bridge even if the cable quality can differ between them. It's however determined that damage due to fatigue aren't common on suspended bridges designed according to Helvetas (Schnetzer, 2002). If this is because of the larger dimensions will remain uncertain, but it's clear that the larger dimensions aren't a disadvantage when it comes to reducing fatigue damage.

The available cables sizes on the building site must also be considered in the design. Perhaps it's cheaper to buy a larger cable dimension on site than transport a smaller cable a long way. This could be one reason to the oversized design of the Jicaro Bridge. Since it's only the walkway and handrail cables that are the main load carrying elements, it's quite cheap to increase the cable size and therefore the structural capacity of the bridge.

6 Dynamic Analysis

6.1 Modal superpositioning

6.1.1 Natural Frequencies

The extracting of the natural frequencies is done both by hand calculation for a single cable and it's also treated as an eigenvalue problem in Brigade/plus. The step in Brigade that is used is a linear perturbation step called frequency. When the whole bridge is modelled one can obtain torsion modes in addition to vertical and out of plane modes. The number of natural frequencies and modes extracted is user defined but in theory it's possible to extract a number equal to the number of degrees of freedom. 3 vertical, out of plane and torsional frequencies are extracted both from the Jicaro Bridge and the 150 m span bridge. A few different modes are presented below while the rest can be seen in appendix.

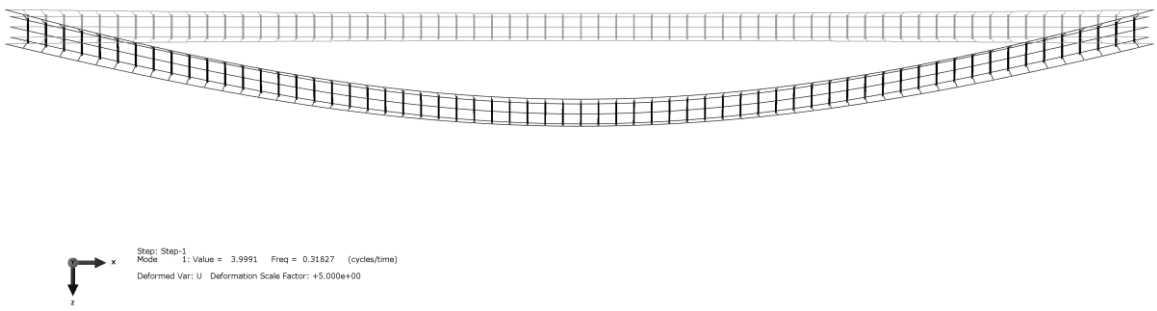

Figure 6.1 First out of plane mode shape for the Jicaro Bridge

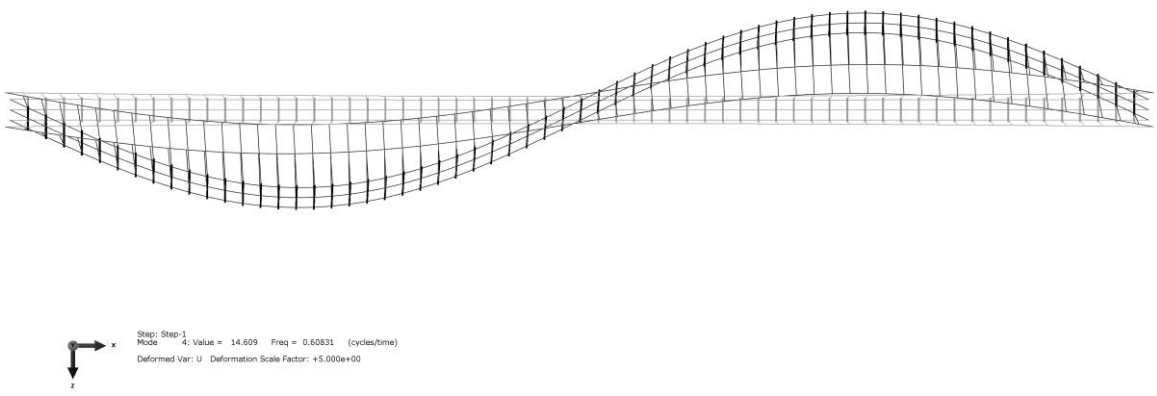

Figure 6.2 Second out of plane mode shape for the Jicaro Bridge

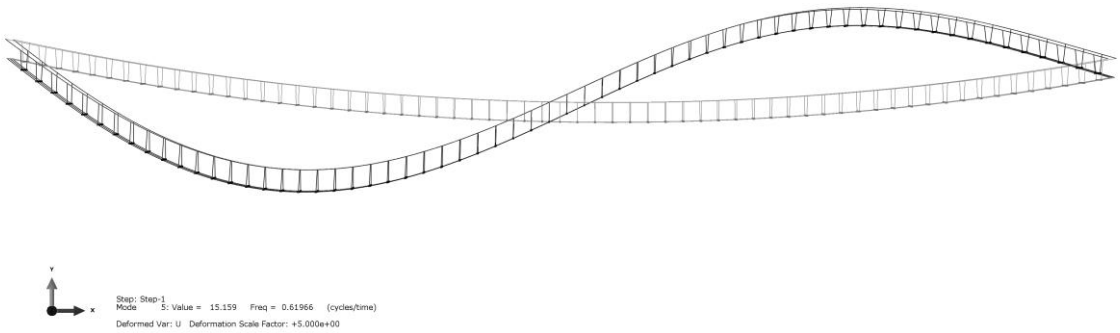

Figure 6.3 First in- plane mode shape for the Jicaro Bridge

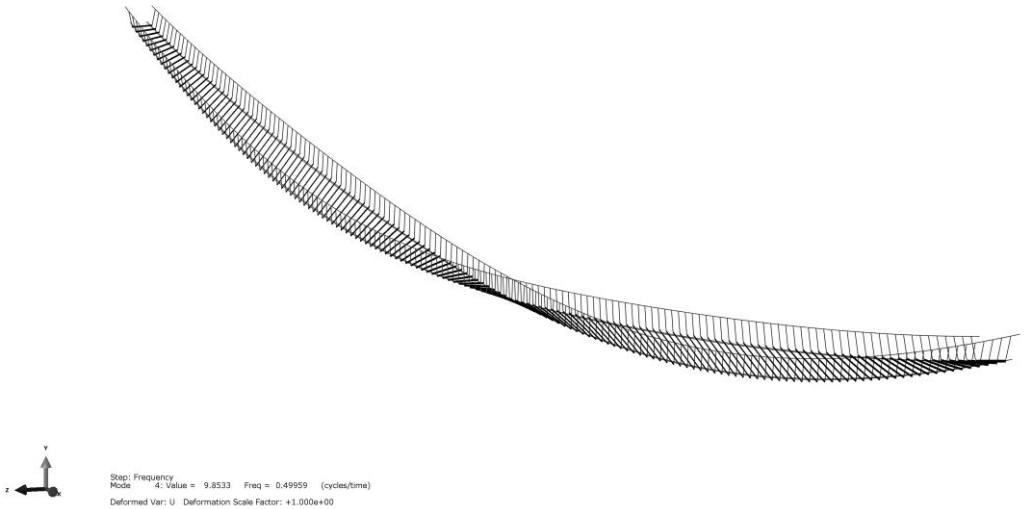

Figure 6.4 First torsional mode shape for the 150 meter span bridge

A comparison between hand calculated and FEM modelled frequencies has been done. The frequencies from these calculations can be seen in Table 6.1 below.

Natural frequencies	Jicaro Bridge 64 meter Brigade/Plus	Single cable 64 meter Hand calculated		Modelled bridge 150 meter Brigade/Plus	Single cable 150 meter Hand calculated
Out of plane	(Hz)	(Hz)		(Hz)	(Hz)
1st	0,318	0,320		0,201	0,209
2nd	0,608	0,639		0,388	0,419
3rd	0,910	0,959		0,567	0,628
In-plane					
1st	0,620	0,639		0,401	0,419
2nd	0,887	0,911		0,563	0,592
3rd	1,249	1,279		0,805	0,837

Table 6.1 Comparison of natural frequencies calculated by FEM-models and by hand

Note that the bridges in the Brigade/Plus-models are subjected to their own dead load, i.e. the weight from cables, suspenders, crossbeams etc. The single cables are only subjected to the dead load of the cable itself.

6.1.2 Excitation / Impulse

To analyse the dynamic response of the bridges, energy need to be added to the system. Consequently the response will be very much dependent on the energy added. The excitation of the bridge in the horizontal direction is based on the wind velocities of 10, 15 and 20 m/s. Since "real" wind loads are very difficult to model, a reference method is used where the load is applied as a line load on the side of the bridge in the out of plane direction. The load is built up under a 2 second period and then decayed under a period of 0.1 second. This will allow free vibration of the bridges in the excited modes when load has decayed to zero. The load is applied with Smooth Step in Brigade. This gives the transition between the input values of the amplitude as a fifth degree polynomial. The first and second derivative will be zero at the start and end value. Figure 6.5 shows the transition of the load between two input values.

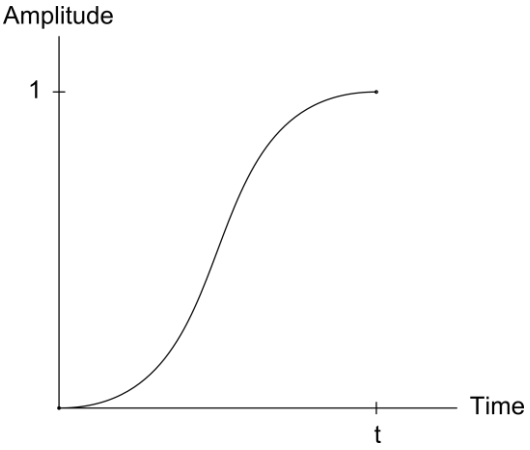

Figure 6.5 Amplitude curve for Smooth Step

6.1.3 Damping

The Rayleigh damping coefficients are extracted from experimental dynamic pluck tests on the Jicaro Bridge in Nicaragua. The pluck tests are performed by Bridges to Prosperity and Maria Gibbs. According to (Austrell, 2015) the damping ratio on lightly damped systems can be given by equation (6.1).

$$\xi = \frac{1}{2\pi j} \cdot \ln\left(\frac{u_i}{u_{i+j}}\right) \tag{6.1}$$

6.2 Modal analysis

In Brigade the modal super positioning analysing step is a linear perturbation step called modal dynamics. This step needs to be preceded by the frequency step where the natural frequencies are extracted. The number of natural frequencies used for the modal analysis is set to 25. Because of the excitation of the bridges is done along the whole span, one can suspect that the dominant mode will be the first mode in the out of plane direction, see Figure 6.1. The results extracted from the analyses will be displacements and accelerations for the midpoints of the three bridges, Jicaro Bridge (64 m), 150 m span bridge and 150 m span bridge with windguys installed.

6.2.1 Displacements

The response in the form of displacements is shown in Figure 6.6, Figure 6.7 and Figure 6.8. Each figure shows the response from the three different wind velocities acting on one of the bridges.

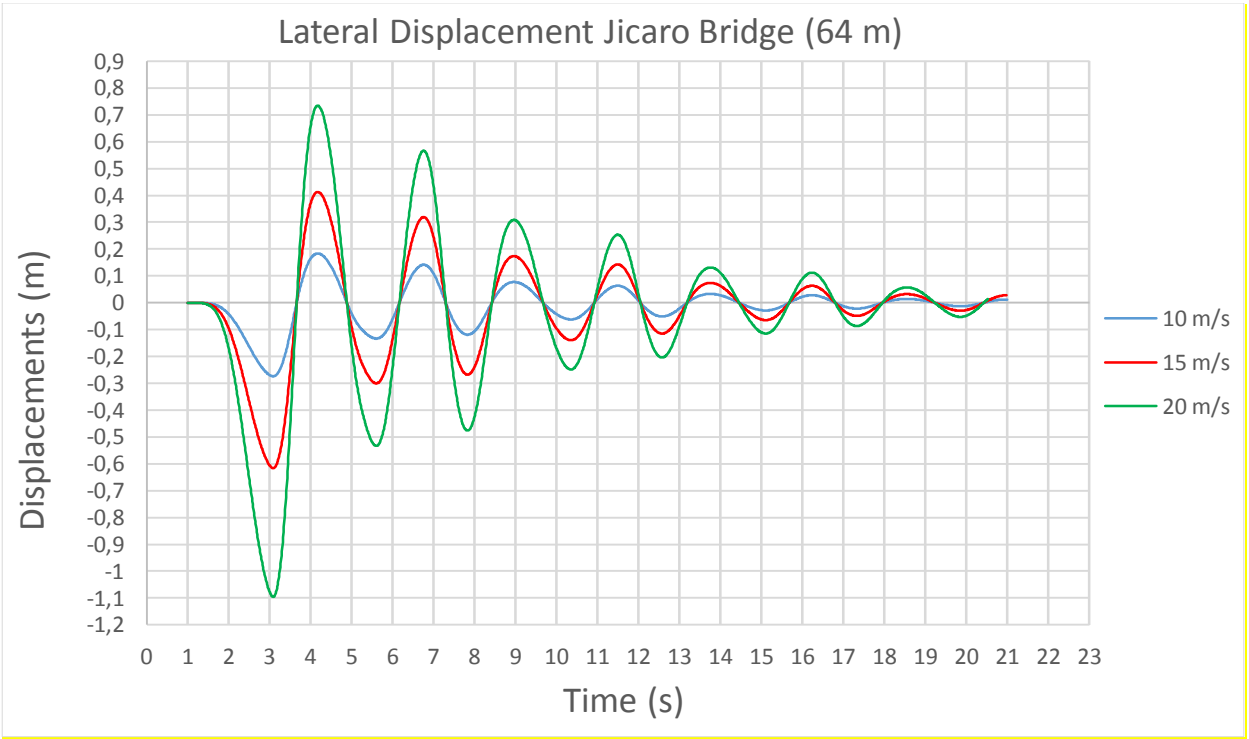

Figure 6.6 Lateral displacement in the center of Jicaro Bridge

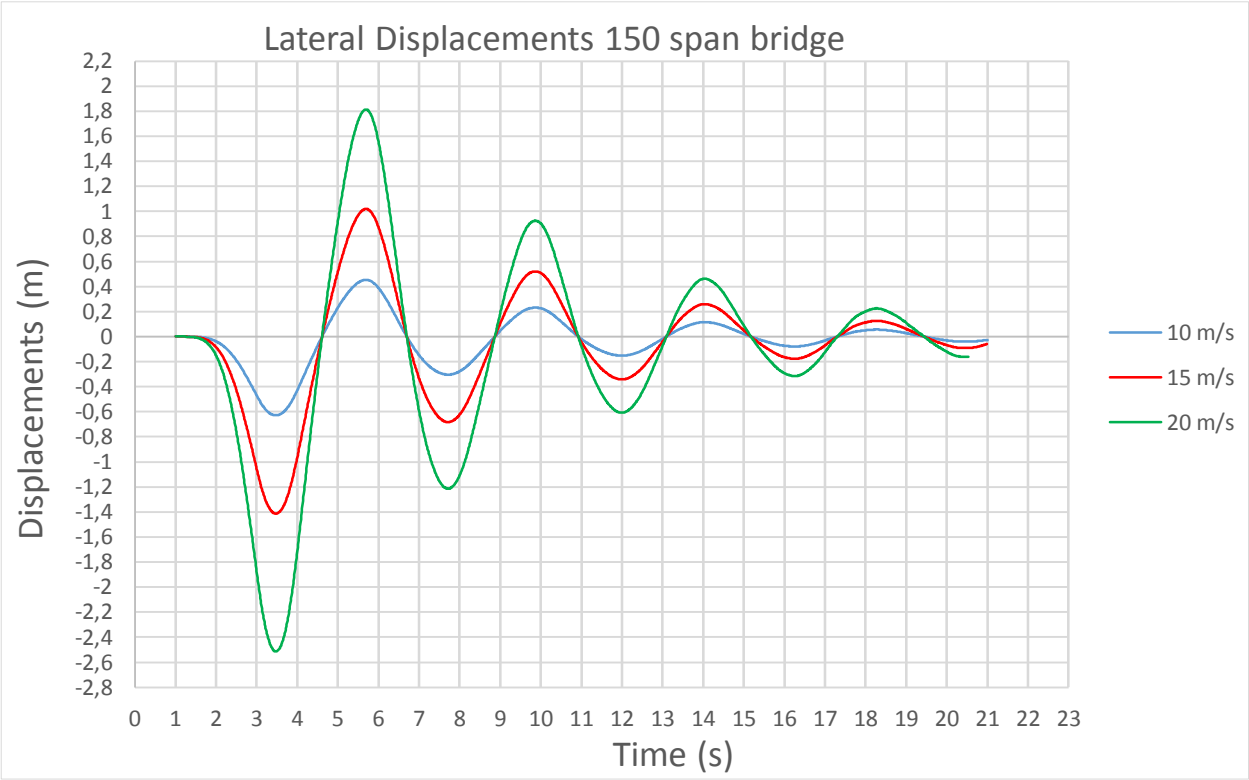

Figure 6.7 Lateral displacement in the center of the 150 m span bridge

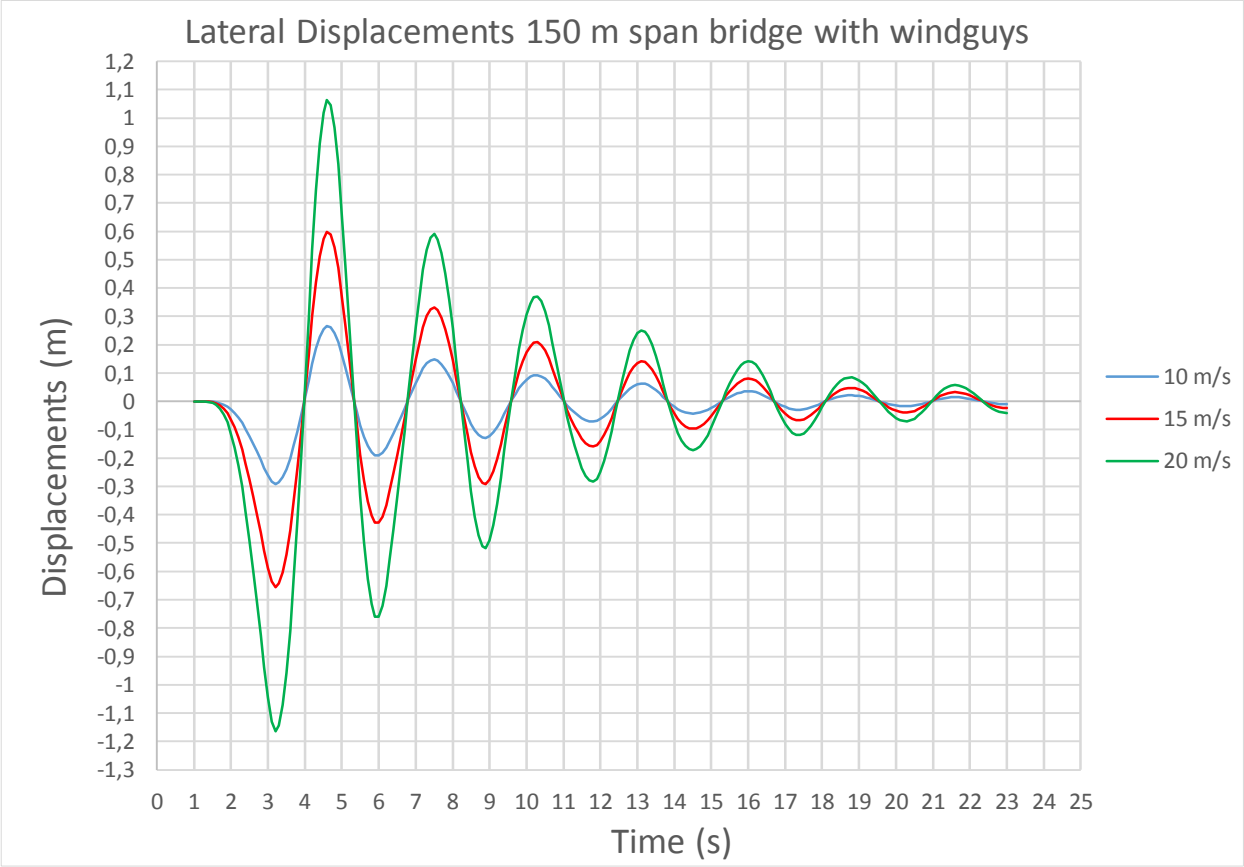

Figure 6.8 Lateral displacement in the center of the 150 m span bridge with windguys

6.2.2 Accelerations

The response in the form of accelerations is shown in Figure 6.9, Figure 6.10 and Figure 6.11. Each figure shows the response from the three different wind velocities acting on one of the bridges.

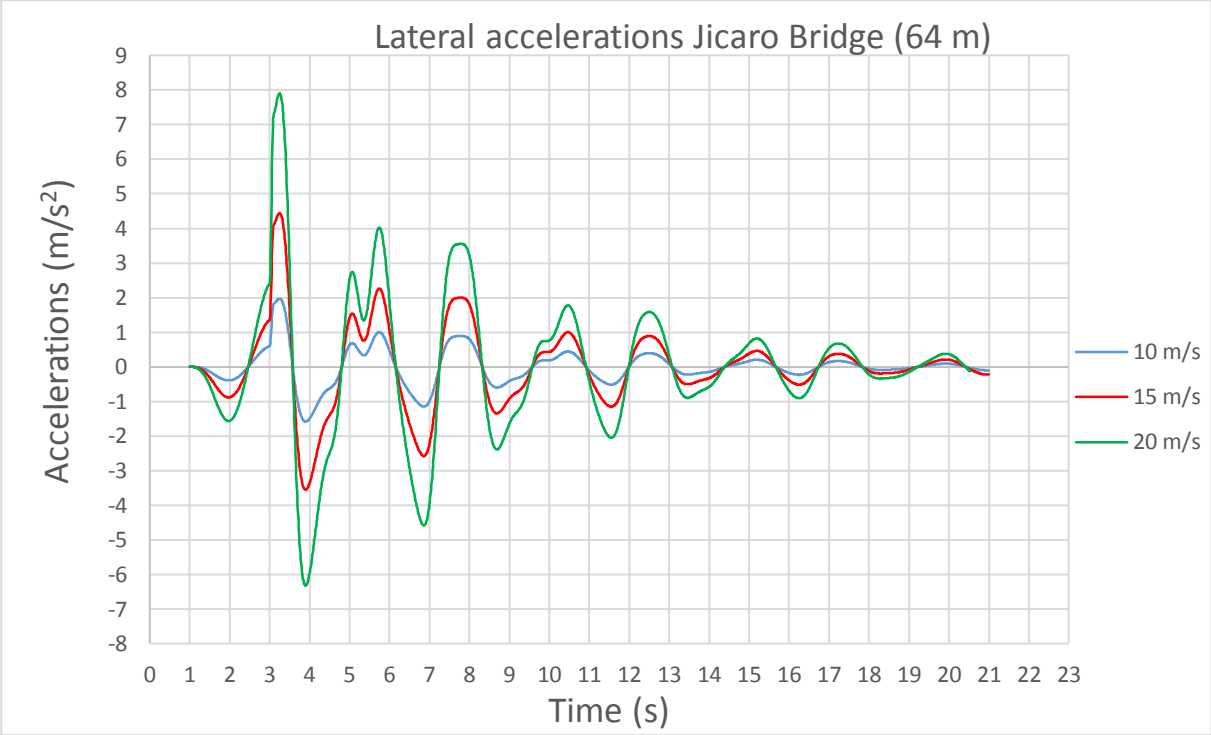

Figure 6.9 Lateral accelerations in the center of Jicaro Bridge

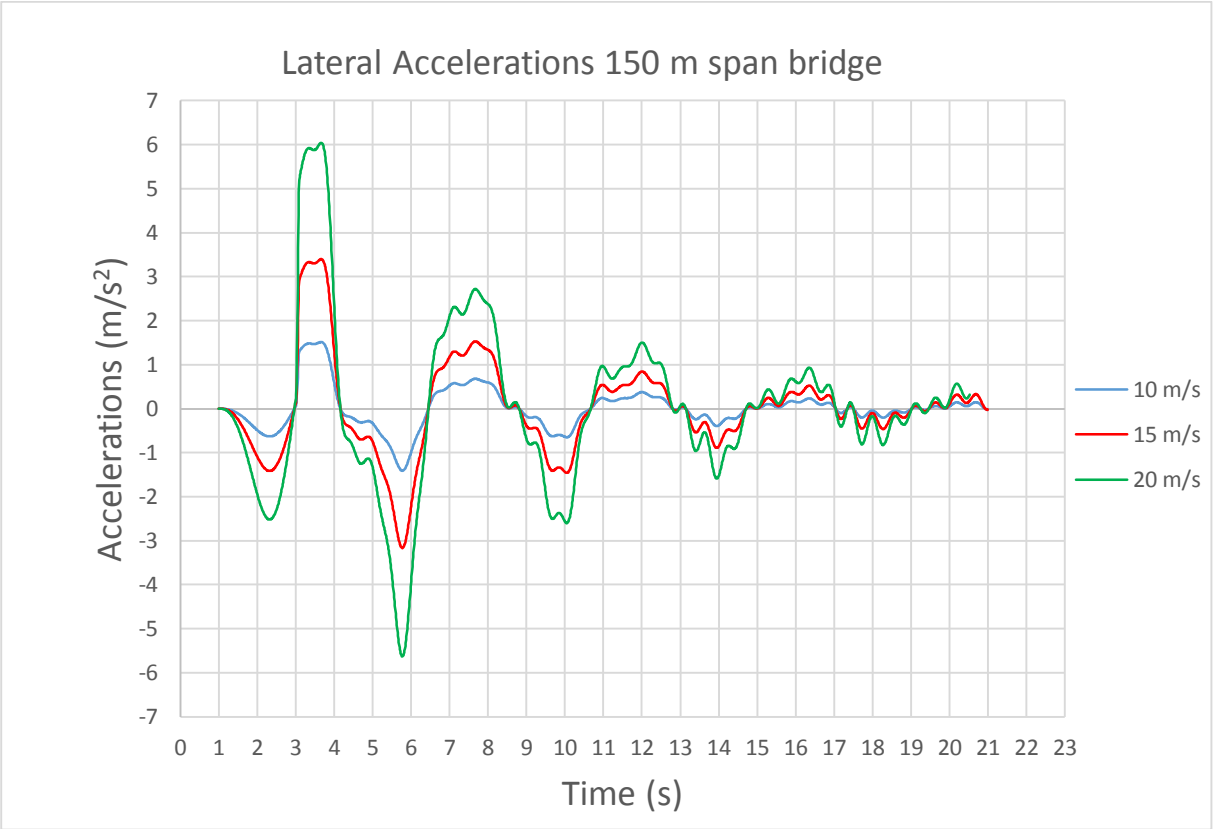

Figure 6.10 Lateral accelerations in the center of the 150 m span bridge

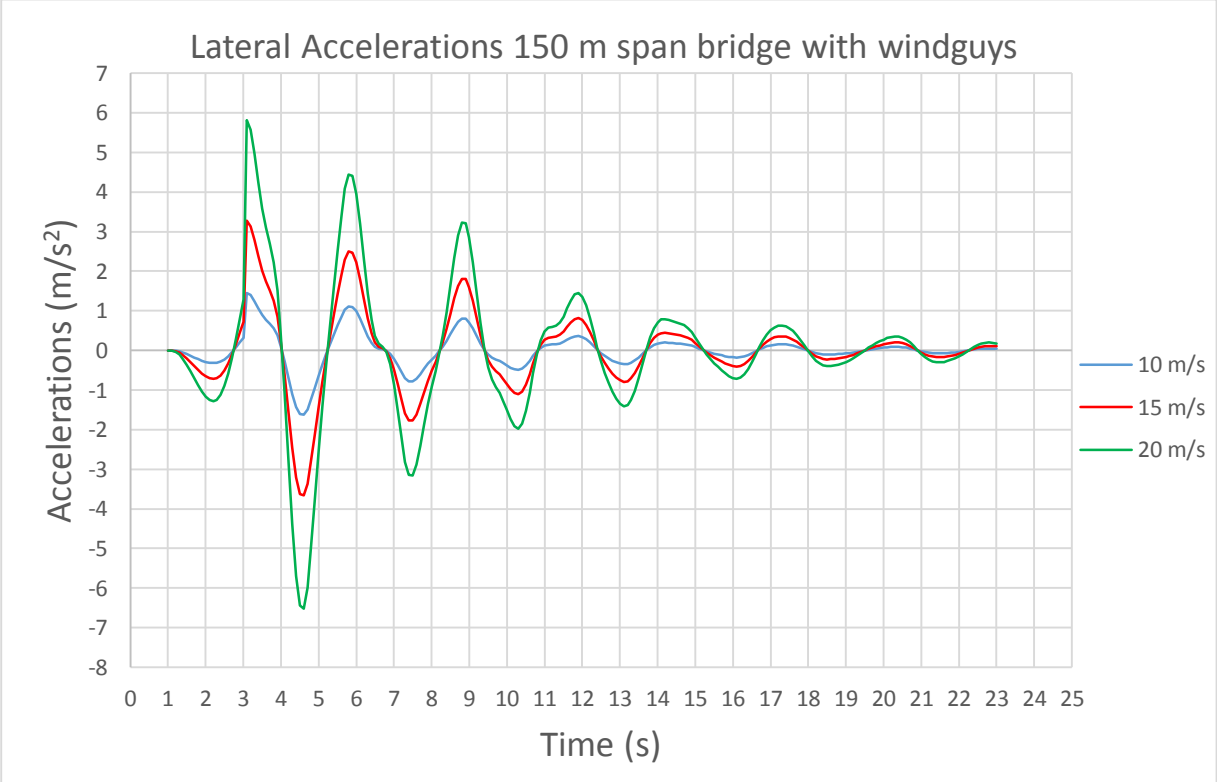

Figure 6.11 Lateral accelerations in the center of the 150 m span bridge with windguys

6.3 Implicit dynamic step

As stated before the cables gives a nonlinearity to the problem. And because a modal analysis only can handle linear problems a comparison is made with an implicit dynamic analysis. The comparison is made on the 150 meter span bridge without windguys and a wind velocity of 10 m/s. It should also be noted that the modal analysis only uses the first 25 modes which also can give a deviation between the different analyses. The response comparison in the form of displacements and accelerations are shown in the figures below.

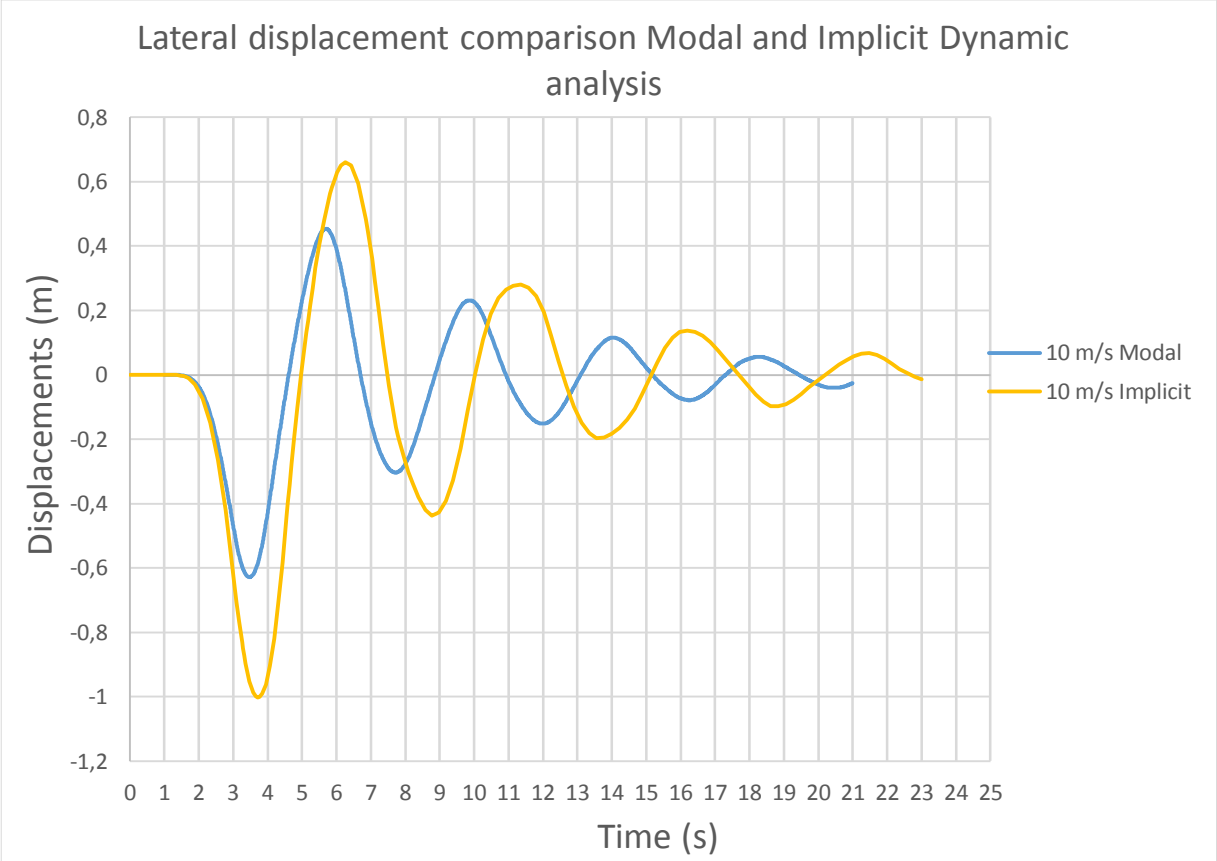

Figure 6.12 Lateral displacement comparison between modal and implicit dynamic analysis

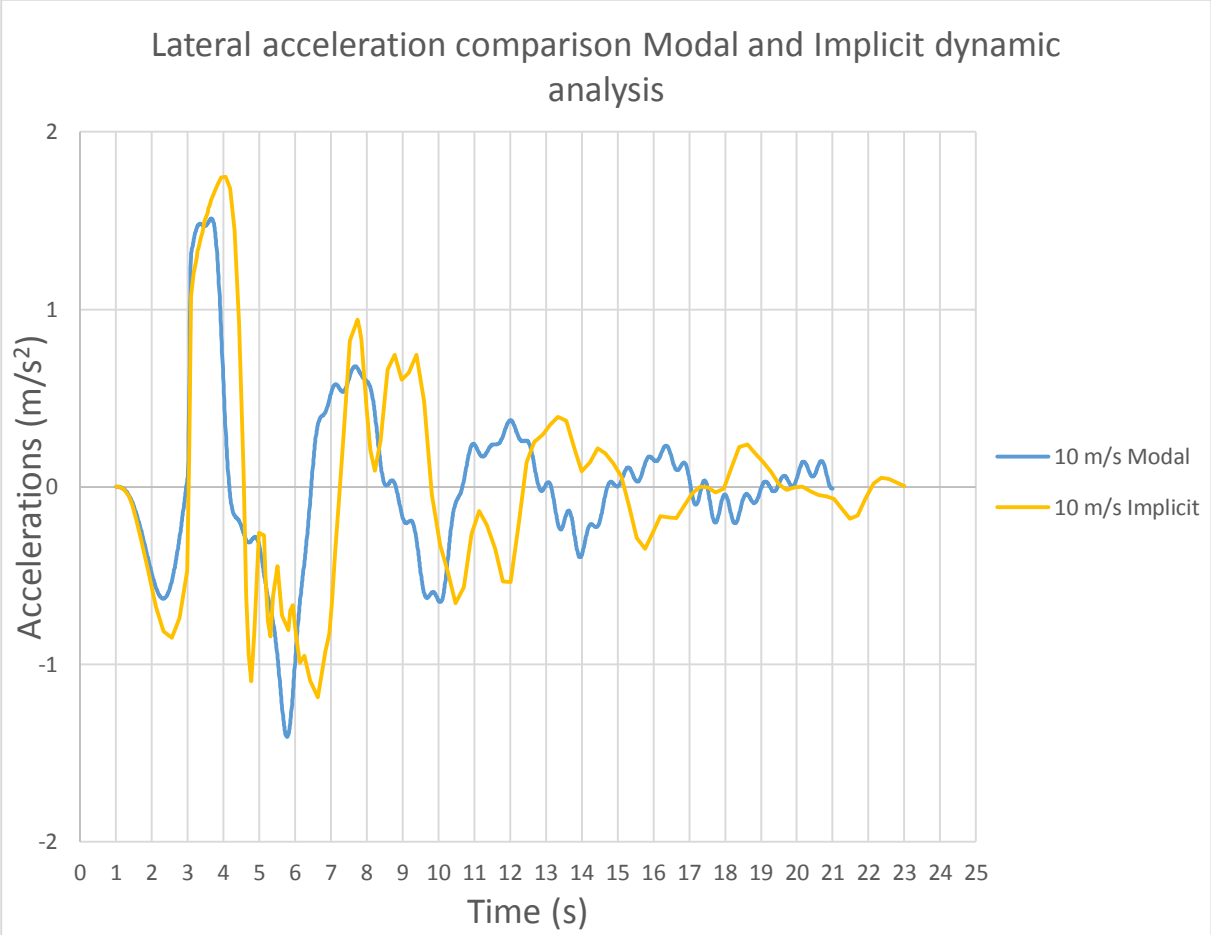

Figure 6.13 Lateral accelerations comparison between modal and implicit dynamic analysis

6.4 Discussion

One must first mention that hand calculations and FE-models aren't the only way to identify the dynamic behavior of bridges. Wind tunnel tests are still in use when designing larger bridges since computer models haven't replaced this method as a way of identifying the dynamic behavior. This fact must be considered with respect.

The natural frequencies that are extracted from Brigade seems to conform with the hand calculations for a single cable with the same sag and span and only its own self weight acting on it. This means that hand calculations is a good way to approximate the first few natural frequencies in the in-plane and out of plane directions for this type of bridges without the need to use more advanced FE-models. With the Brigade model, torsional modes can be identified which can be useful if further investigation is done on wind effects. One conclusion of this chapter is that a good way to affect the natural frequencies of a suspended bridge is to modify the size of its sag.

The response for different type of bridges follows its first out of plane frequency. The displacement of the midpoint increases with a larger span which also has been concluded in chapter 5.4. With windguys installed the displacement again decreases. The acceleration peak values on the other hand decreases with a larger span but seems to be unchanged with or without

the windguys. One can make the conclusion that the design criteria for using windguys is based on allowed lateral displacement rather than allowed accelerations of the bridge.

The acceleration values for the three bridge types are relative large compared to the suggested accelerations by Nakamura. The choice of excitation parameters that are put into the system is of great importance for the response of the bridge and will greatly influence the values. It's possible that it's more important in this case to analyse the change in behavior with greater span and windguys rather than analysing the actual peak values.

In the comparison between a modal analysis and an implicit analysis in Figure 6.12 and Figure 6.13, a difference can be distinguished in the early peak values for the displacements. The implicit analysis gives larger displacements than the modal analysis. The peak values for the accelerations seems to conform in a better way. A small difference in frequency of the response can also be seen. The modal analysis gives overall a good approximation of the response of the bridge but to fully analyse the nonlinearities that occur with cables, an implicit analysis is needed. Note that the modal analysis requires less calculation time than the implicit dynamic analysis.

7 Conclusions

Since all the results have been discussed in each chapter, this chapter will summarize them shortly.

Modifying the sag is the best way to affect the natural frequencies.

The Brigade model and hand calculations gives very alike result for both vertical and lateral displacements due to static loads.

The stress distribution between the handrail and the walkway cables is not a problem for designing in ultimate limit state. The stress distribution becomes more uniformly distributed between the cables when the vertical load increases, i.e. the cables will deform uniformly.

When analyzing the natural frequencies of a suspended bridge, a good approximation will be to evaluate a single cable with the same sag and span subjected to its self weight.

The criteria for using windguys should rather be based on displacements than accelerations. It could also be a combination of the two.

In Brigade/plus the cables, and therefore the whole bridge, will have no stiffness before the dead load is applied which means that the sag will get larger than what it's initially modeled as. This needs to be accounted for when modelling a suspended bridge in Brigade/plus.

Bridges designed with design guides from Helvetas and Bridges to Prosperity requires larger cable dimensions compared with bridges designed according to Eurocode.

When determining the lateral dynamic response from wind loads, a modal dynamics analysis gives a good approximation of the behavior of the bridge. However, a full implicit dynamic analysis is preferred.

7.1 Further investigations

In this section a number of suggestions are made for further investigations and analyses that have not been included in this thesis.

- More full dynamic implicit analyses should be done to fully understand the nonlinear behavior of the dynamic response.

- If possible make experimental tests on existing suspended bridges for calibrating models. This can for instance be a simple pluck test to identify natural frequencies.

- Try to find a criteria depending on displacements, accelerations and span length for when windguys should be installed.

- The effect of temperature changes. Very low temperature will lead to a temporary shortening of the cables which will increase the stress levels.

- Corrosion protection of the cables.

8 References

Austrell, P. E. (2015, 06 08). *VSMN10 Strukturdynamiska Beräkningar*. Retrieved from VSMN10 Strukturdynamiska Beräkningar: http://www.byggmek.lth.se/fileadmin/byggnadsmekanik/SDOF_with_damping_mod.pdf

BBC. (2015, 11 7). *BBC*. Retrieved from BBC: http://www.bbc.com/news/magazine-33291373

Certex. (n.d.). *Certex*. Retrieved 01 29, 2015, from Certex: http://www.certex.co.uk/steelwirerope/steelwireropes/technicalinformation/properties-of-extension-of-steel-wire-ropes

COWI. (2015, 05 18). *COWI*. Retrieved from COWI: http://www.cowi.com/menu/NewsandMedia/News/Newsarchive/Pages/italytohavetheworldslargestbridge.aspx

Dylan Thuras; Atlas Obscura. (2015, 05 18). *Atlas Obscura*. Retrieved from Atlas Obscura: http://www.atlasobscura.com/places/last-handwoven-bridge

Dyrbye, C., & Hansen, S. O. (1997). *Wind Loads on Structures.* Chichester: John Wiley & Sons Ltd.

Ekantipur. (2015, 05 18). *Ekantipur*. Retrieved from Ekantipur: http://www.ekantipur.com/photo-gallery/2010-03-03/218/2494

Gimsing, N. J. (1997). *Cable supported bridges* (Second Edition ed.). Baffins Lane, Chichester: John Wiley & Sons Ltd.

Hanes Supply. (2015, Mars 19). *Hanes Supply*. Retrieved from Hanes Supply: http://www.hanessupply.com/content/pdfs/wireRope101.pdf

Heinemeyer et al. (2009). *Design of leightweight footbridges for human induced vibrations.* JRC-ECCS cooperation.

Helvetas. (2004). *Long span trail bridge manual*. Kathmandu: His Majesty's Government of Nepal, Helvetas Nepal.

Helvetas. (2015, 05 22). *Helvetas*. Retrieved from Helvetas: http://www.helvetas.org/about_us/at_a_glance/

Irvine, H. M. (1974). *Studies in the statics and dynamics of simple cable system.* Pasadena, California: Californina Institute of Technology.

Irvine, H. M. (1981). *Cable Structures.* Cambridge, Massachusetts: MIT Press.

LTH, Structural Engineering. (2014, 12 10). *Structural Engineering, Advanced Course, Design of Bridges*. Retrieved 01 29, 2015, from Structural Engineering, Advanced

Course, Design of Bridges: http://www.kstr.lth.se/fileadmin/kstr/pdf_files/vbk041/forelas/7_Suspension.pdf

Marti, P. (2012). *Baustatik.* Berlin: Wilhelm Ernst & Sohn.

Nakamura, S.-I. (2003). *Field measurements of lateral vibration on a pedestrian suspension bridge.* The Structural Engineer.

OPAC Consulting Engineers. (2015, 05 18). *OPAC Consulting Engineers*. Retrieved from OPAC Consulting Engineers: http://www.opacengineers.com/projects/Cangrejillo

Pfaffen, H., Brog, W., & Van Rooden, C. (2009). Hochseilakt. *Tec21*, pp. 23-32.

Ramiro Matos, Smithsonian. (2015, 01 23). *Smithsonian*. Retrieved from Smithsonian: http://newsdesk.si.edu/photos/inka-suspension-bridge

Ryall, M., Parke, G., & Harding, J. (2000). *The Manual of Bridge Engineering.* London: Thomas Telford Publishing.

Schnetzer, D. H. (2002). *Expertise on windguy arrangement for BBLL standard bridges.* Basel: WGG Schnetzer Puskas Ingenieure AG.

Sétra. (2006). *Footbridges, Assessment of vibrational behaviour of footbridges under pedestrian loading.* Paris.

SIS. (2010). *SS-EN 1990.* Swedish Standard Institute.

Storebaelt Publications. (1998). *East Bridge*. Köbenhavn: A/S Storebaeltsforbindelsen.

Zivanovic et al. (2005). *Vibration serviceability of footbridges under human-induced excitation: a literature review.* Journal of sound and vibration.

9 Annex

9.1 Design guide

This part gives a short guidance on how to use the excel design sheet. All formulas and labels are based on the design guides made by Helvetas, especially the Long Span Trail Bridge Standard, but the loads and the safety criteria has been adjusted to also fit Eurocode. The excel sheet has five different parts, each for different design situations, for example if the bridge should be fitted with windguys or not, or if it should be designed according to Eurocode or Helvetas. Note that the authors don't take responsibility for any design created with this excel sheet. It's only a guideline and reasonable check should always be done after the use of this sheet.

In the design example below, a suspended bridge with a span of 150 meter will be designed according to Eurocode. Since the span length exceeds 120 meter, the sheet *>120 Eurocode* is chosen. The first step is to determine the basic geometry of the bridge. This is done in the first part of the sheet which can be seen in Figure 9.1 below. A green cell means that a value must be given. A white cell will be calculated automatically.

Geometrical properties			
Design span	l	150	m
Sag dead load	b_d	7,2	m
Sag hoisting	b_h	6,11	m
Sag full load	b_f	9,55	m
Height difference between saddles	h	0	m
Cable lenght	L	150,9	m
Lowest point from highest point	f_d	7,20	m
Distance lowest point from highest point	e	75,00	m

	Mean	Low	High
Recommended	**7,2**	6,52	7,89

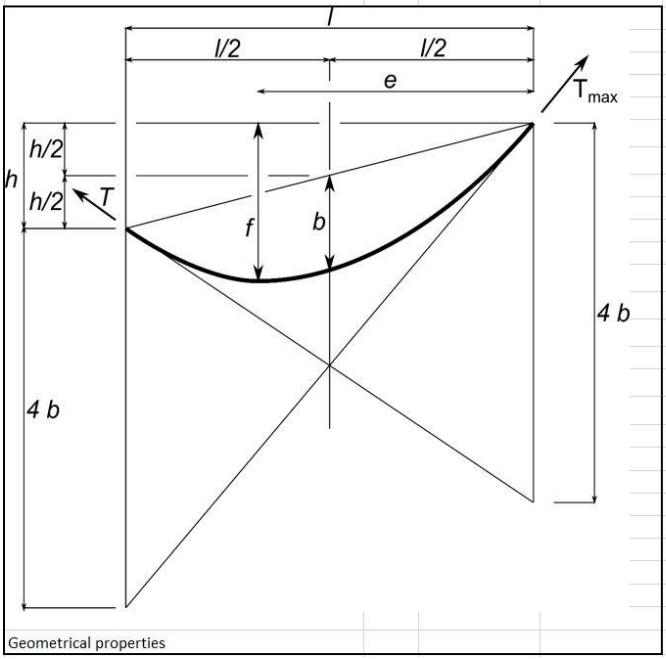

Figure 9.1 Geometry

l The *design span* is the horizontal distance between the two saddles.

b_d The *dead load sag* is the sag of the bridge when it's subjected to its own dead load. The recommended min-, max-, and mean dead load sag is given in the cells to the right.

b_h The *hoisting sag* is the sag the cables should be hoisted to during construction. When suspenders, crossbeams, walkway etc. are installed, the cables will sink to their dead load sag.

b_f The *full load sag* is the sag of the bridge when it's subjected to its maximal vertical load. Note that if a certain freeboard is required for a bridge, the full load sag must be checked against the height requirement for the freeboard.

Note that the prefixes d, b, f stands for dead load, hoisting load and full load.

h The height difference between the saddles which can be seen in Figure 9.1.

L The cable length is the total length of the cable.

f_d The vertical distance between the lowest point on the cable and the highest saddle. f_d is marked with an f in Figure 9.1.

e The horizontal distance between the lowest point on the cable and the highest saddle.

The next part concerns the properties of the main load carrying cables. This part is very important since many cells have to be filled in and it's important to get the right information from the cable manufacturer.

Cables			
Young's modulus	E	1,1E+11	Pa
Rope grade	R_r	1570	MPa
Minimum breaking strength (one cable)	F_{min}	430,81	kN
Diameter of the rope	d	28	mm
Number of handrail cables		2	
Number of main cables		4	
Metallic Cross-sectional area cables	A_m	2 069	mm^2
Minimum breaking force factor	K	0,35	
Loss factor	k_e	1	
Fill factor	f	0,56	
Ultimate strenght characteristic (all cables)	F_{uk}	2584,85	kN
Characteristic proof strength (all cables)	$F_{0,2k}$	2834,43	kN
Partial factor	Υ_R	1	
Design strength all cables	F_{Rd}	1723,23	kN

Figure 9.2 Cable properties

E The Young's modulus for the cable. Note that Young's modulus for cables is always lower than the modulus for steel. In this case it's 110 GPa.

R_r The rope grade is a level of breaking force requirement given in N/mm^2, i.e. MPa, for example 1570, 1770 or 1960 N/mm^2. The rope grade does not necessary correspond to the tensile strength of the wires in the rope.

F_{min} The minimum breaking force for one cable is calculated according to SS-EN 1993-1-1 1.3.9.

d The diameter of the rope should be chosen from standard manufacturing dimensions. For simplicity the diameter will be the same for all the cables in the bridge. The number of handrail cables is fixed to two, the main cables under the walkway can be chosen with a minimum of two.

A_m The metallic cross-sectional area is calculated by multiplying the fill factor with the cross-sectional area of all the cables.

K The breaking force factor is an empirical factor used to determine the minimu breaking force for a cable. Should be given by the manufacturer. If not, it can be calculated with SS-EN 1991-1-11 1.3.8.

k_e The loss factor for end terminations is given in Table 6,3 in SS-EN 1993-1-11.

f The fill factor is the percent of metal area in the cross-sectional area of a cable.

F_{uk} The characteristic value of breaking strength is calculated according to equation 6,4 in SS-EN 1993-1-11.

$F_{0,2k}$ The characteristic proof strength is the maximum strength of the cable without exceeding a permanent strain of 0,2 %.

γ_R The partial factor used in equation 6,2 in SS-EN 1993-1-11.

F_{Rd} The total design strength for all cables is calculated with equation 6,2 in SS-EN 1993-1-11. The equation can be seen below:

$$F_{Rd} = min\left\{\frac{F_{uk}}{1{,}5 \cdot \gamma_R}; \frac{F_k}{\gamma_R}\right\} \tag{9.1}$$

In Figure 9.3 below, the loads acting on the bridge can be seen. These loads are the same as the loads presented in chapter 2.10.3. The only load that has to be given is the horizontal wind load for the current bridge. The other loads, both dead load and live load, will be calculated automatically. The load combination creating the worst load situation will be the design load. In almost all cases, load combination 6,10b will be the design load combination.

In this sheet, the windguys are assumed to carry all the horizontal wind load. In the sheet for spans under 120 meter, an enlargement factor will be added to the vertical loads to compensate for the displacement caused by the wind load, as described in chapter 2.10.5. This enlargement factor will be calculated and added automatically.

Loads		**Design**	**Caracteristic**	**6,10a**	**6,10b**	
Cables (from table) (kN/m)		0,23	0,19	0,26	0,23	Ekv 2.1 SS-EN 1993-1-11
Walkway (1 meter width) (kN/m)		0,55	0,46	0,62	0,55	
Walkway support (kN/m)		0,26	0,22	0,30	0,26	
Fixation cables (kN/m)		0,01	0,01	0,01	0,01	
Wiremesh netting (kN/m)		0,07	0,06	0,08	0,07	
Windguy cables (kN/m)		0,10	0,08	0,11	0,10	
Windties (average) (kN/m)		0,04	0,03	0,04	0,04	
Live load (kN/m)		4,00	2,667	1,60	4,00	SS-EN 1991-2 (5,1)
Design load		5,27		3,03	5,27	
Wind load ultimate (kN/m)		1,695	1,13	0,5085	1,695	SS_EN 1991-1-4 8.3.2
Load combinations						
Hoisting load	g_h	0,23	kN/m			
Dead load	g_d	1,27	kN/m			
Full load	g_f	5,27	kN/m			

Figure 9.3 Loads

When the loads and load combinations are determined the hoisting sag and the full load sag can be determined. This is done in an iterative way for both the hoisting sag and the full load sag. The numbers of iterations varies depending on the loads.

Load combinations					
Hoisting load	g_h	0,23	kN/m		
Dead load	g_d	1,27	kN/m		
Full load	g_f	5,27	kN/m		
Hoisting sag, iteration procedure		The hoisting sag must be determined in an iterativ manner. The iterations must proceed untill Δg1 ≤ 0,01			
1:st iteration					
Cable length	L_d	150,92	m		
Constant factor	C	0,01			
Sag primary, hoisting load	$b_h{}^*_{start}$	6,70	m		
Load primary	g*	0,73	kN/m		
New sag primary, hoisting load	$b_h{}^*$	6,22	m		
Load difference	Δg_1	-0,5020	kN/m	Not OK	[Δg1] ≤ 0,01
2:nd iteration					
Load primary	g*	0,32	kN/m		
New sag primary, hoisting load	$b_h{}^*$	6,13	m		
Load difference	Δg_2	-0,0884	kN/m	Not OK	[Δg1] ≤ 0,01
3:rd iteration					
Load primary	g*	0,25	kN/m		
New sag primary, hoisting load	$b_h{}^*$	6,11	m		
Load difference	Δg_3	-0,0181	kN/m	Not OK	[Δg1] ≤ 0,01
4:th iteration					
Load primary	g*	0,23	kN/m		
New sag primary, hoisting load	$b_h{}^*$	6,11	m		
Load difference	Δg_4	-0,0038	kN/m	OK	[Δg1] ≤ 0,01
Final hoisting sag	b_h	6,11	m	Choose $b_h{}^*$ from the iteration when [Δg1] ≤ 0,01	

$$C = \frac{64E \cdot A}{3\ell^3 \cdot L_d}$$

$$g^* = C \cdot b^* \cdot \left(b^{*2} - b_d^2\right) + \frac{b^*}{b_d} g_d$$

$$b^* = b_d + \left(b_{old}^* - b_d\right) \cdot \frac{g_i - g_d}{g_{old}^* - g_d}$$

Figure 9.4 Hoisting sag iteration procedure

L The cable length is the total length of the cable.

C The constant factor gather all the constants in the iteration procedure. The formula used can be seen in Figure 9.4.

$b_{h_{start}}^*$ The primary hoisting sag is the starting value for the hoisting sag in the iteration procedure. The starting value is set to 93 % of the dead load sag.

g^* The primary hoisting load is the load used for calculating the primary hoisting sag in every iteration. Will with every iteration move closer to the real hoisting load.

b_h^* The primary hoisting sag is the sag determined with the primary hoisting load in the current iteration.

Δg_i The load difference is the difference between the primary hoisting load and the real hoisting load, i.e. $\Delta g_i = g_h - g^*$. The condition to be fulfilled is that $|\Delta g_i| \leq 0{,}01\ kN/m$. If this condition is fulfilled, the cell to the right will sign OK.

b_h The final hoisting sag is set to the b_h^* in the first iteration that fulfills the condition $|\Delta g_i| \leq 0{,}01\ kN/m$. For example, in Figure 9.4 above, the 4th iteration fulfilled the condition and b_h is therefore set to 6,11 meter.

When the hoisting sag has been determined, the same procedure is followed to determine the full load sag. The same unit are used as in the hoisting sag procedure. The only difference is that the prefixes are changed from h to d, which can be seen in FIGURE XXX

Full load sag, iteration procedure		The full load sag must be determined in an iterativ manner. The iterations must proceed untill Δg1 ≤ 0,01			
1:st iteration					
Cable length	L_d	150,87	m		
Constant factor	C	0,01			
Sag primary, full load	b_f*	8,54	m		
Load primary	g*	3,83	kN/m		
New sag primary, full load	b_f*	9,44	m		
Load difference	Δg_1	1,4761	kN/m	Not OK	[Δg1] ≤ 0,01
2:nd iteration					
Load primary	g*	5,90	kN/m		
New sag primary, full load	b_f*	9,12	m		
Load difference	Δg_1	-0,6012	kN/m	Not OK	[Δg1] ≤ 0,01
3:rd iteration					
Load primary	g*	5,11	kN/m		
New sag primary, full load	b_f*	9,23	m		
Load difference	Δg_1	0,1893	kN/m	Not OK	[Δg1] ≤ 0,01
4:th iteration					
Load primary	g*	5,37	kN/m		
New sag primary, full load	b_f*	9,19	m		
Load difference	Δg_1	-0,0652	kN/m	Not OK	[Δg1] ≤ 0,01
5:th iteration					
Load primary	g*	5,28	kN/m		
New sag primary, full load	b_f*	9,20	m		
Load difference	Δg_1	0,0211	kN/m	Not OK	[Δg1] ≤ 0,01
6:th iteration					
Load primary	g*	5,31	kN/m		
New sag primary, full load	b_f*	9,20	m		
Load difference	Δg_1	-0,0073	kN/m	OK	[Δg1] ≤ 0,01
When [Δg1] ≤ 0,01, Calculate the maximum full load tension in the cable					
Sag full load, choose b* from above	b_f	9,20	m	Choose b_f* from the iteration when [Δg1] ≤ 0,01	
Maximum tension	T_{max}	1669,37	kN		
Calculate the safety factor					
Safety factor	F	1,18	OK	If F ≥ 1 ok	

Figure 9.5 Full load sag iteration procedure

As it can be seen in Figure 9.5, the maximum tension in the cables due to the full load, is calculated with the full load sag. In the figure above, the full load sag is determined to be 9,2 meter and the tension in the cables 1,67 MN. In the bottom of the figure is the structural capacity for the cables checked against the maximum tension. If the capacity is greater than the maximum tension in the cables, the safety factor, i.e. the capacity divided by the maximum tension, is larger than 1. If this condition is fulfilled, the cell to the right will sign "OK". If the condition isn't fulfilled, it will sign "Not OK". When this condition is fulfilled, the design of the load carrying cables of the bridge is done.

Windguys

Designing the windguys is a more complicated task. Four different anchors have to be installed. Hopefully, the ground conditions are favorable so a symmetric position of the anchors is possible. Otherwise a more detailed design procedure have to be done.

But let's assume favorable ground conditions and a bridge with no height difference between its saddles. This means that the windguys will be symmetric and that it's enough to design only one of the windguys. This has been assumed in the design guide, and otherwise the Helvetas Long San Trail Bridge Standard should be used. Note that the design guide contains many pictures explaining the geometric properties of the windguys. These picture has not been included in this document due to publicity rights. The figure below contains the geometric properties, the wind load and the resulting tension in the windguy cable/cables.

Windguys			
The design of the windguys are very dependent on the ground conditions on the building site.			
The design below are quite adjustable and it will work for the most conditions.			
Design span bridge	l	150	m
Distance vertex - bridge abbutment	v_R	75,0	m
Horizontal distance vertex-right bridge abbutment	f_w	15	m
Elevation highest bridge saddle	H_1	100	m
Elevation windguy cable foundation right	H_R	88,55	m
Elevation windguy cable foundation left	H_L	88,55	m
Horizontal distance windguy at abbutments	h_w	0	m
Sag at mid-span	b_w	15	m
Distance between windties in plan	d	6	m
Distance bridge axis-wintie connection on crossbeam	k	0,66	m
Wind load	w	1,695	kN/m
Windguy horisontal cable tension	H_w	317,8	kN
Windguy cable tension right side	T_R	342,3	kN
Windguy cable tension left side	T_L	342,3	kN
Maximum tension in cable	$T_{w,max}$	342,3	kN

Figure 9.6 Windguy geometry

Note that when the term *in-plane* is used here it mean as viewed in plan.

l The *design span* is the horizontal distance between the two saddles.

v_R The horizontal distance from the right abutment to the in-plane vertex for the windguy cable. For a bridge with abutments at the same height, v_R has the same value as e for the bridge.

f_w The in-plane sag of the windguy cable measured from the right abutment of the bridge.

H_1 Elevation of the highest bridge abutment. In this case the elevation is the same for both the abutments.

H_R Elevation of the right windguy foundation.

H_L Elevation of the left windguy foundation.

h_w The horizontal in-plane distance between the crossing points between the windguy cable and the abutments, i.e. the in-plane distance from the windguy cable to the bridge axis at the left abutment minus the same distance at the right abutment. For a symmetric windguy, this distance is zero.

b_w The in-plane sag of the windguy cable at midspan. If $h_w = 0$, i.e. a symmetric windguy, $b_w = f_w$.

d The distance between the windties, i.e. the cables connection the windguy to the bridge. d should be equal to 6 meter for suspended bridges.

k The distance from the midpoint of the crossbeam to the connection with the windtie.

w The wind load, which is determined in the earlier parts of the design guide.

H_w The horizontal force in the windguy cable

T_R The force in the windguy cable at the right foundation

T_L The force in the windguy cable at the left foundation

$T_{w,max}$ The largest of T_R and T_L.

In the figure below, the cables are designed in the same way as in the earlier part. The only difference is that one have to choose the number of cable in each windguy, n_w, which most often is one or two. For example,in the figure below it was enough with one.

Number of cables on one side of the bridge	n_w	1	
Cable diameter	$ø_w$	32	mm
Metallic Cross-sectional area cables	A_m	450	mm^2
Rope grade	R_r	1570	MPa
Minimum breaking force factor	K	0,35	
Loss factor	k_e	1	
Fill factor	f	0,56	
Ultimate strenght characteristic	F_{uk}	562,69	kN
Characteristic proof strength (all cables)	$F_{0,2k}$	617,02	kN
Partial factor	Y_R	1	
Design strength one windguy	F_{Rd}	375,13	kN
Weight / load of one whole windguy		0,042	kN/m
Location of first windtie right side	B_R	3,0	m
Location of first windtie left side	B_L	3,0	m
Inclination windguy - bridge axis Right	α_R	22,0	deg
Inclination windguy - bridge axis left	α_L	22,0	deg
Horizontal Distance windguy foundation - bridge axis Right	C_R	17,24	m
Horizontal Distance windguy foundation - bridge axis Left	C_L	17,24	m
Horizontal Distance windguy - bridge axis at the bridge saddle Right	C_{Ro}	17,24	m
Horizontal distance windguy - bridge axis at the bridge saddle Left	C_{Lo}	17,24	m
Distance windguy foundation - bridge saddle Right	D_R	0	m
Distance windguy foundation - bridge saddle Left	D_L	0	m
Calculate the safety factor			
Safety factor	F	1,10	OK

Figure 9.7 Windguy porperties

B_R The horizontal distance from the right abutment to the first windtie.

B_L The horizontal distance from the left abutment to the first windtie.

α_R The in-plane inclination between the windguy and the bridge axis at the right abutment.

α_L The in-plane inclination between the windguy and the bridge axis at the left abutment.

C_R The in-plane, orthogonal to the bridge axis, distance between the right bridge abutment and the right windguy foundation.

C_L The in-plane, orthogonal to the bridge axis, distance between the left bridge abutment and the left windguy foundation.

C_{Ro} The in-plane, orthogonal to the bridge axis, distance between the right bridge abutment and the windguy.

C_{Lo} The in-plane, orthogonal to the bridge axis, distance between the left bridge abutment and the windguy.

D_R The in-plane, along the bridge axis, distance between the right bridge abutment and the right windguy foundation. Negative if the windguy foundation is closer than the abutment to the midpoint of the span.

D_L The in-plane, along the bridge axis, distance between the left bridge abutment and the right windguy foundation. Negative if the windguy foundation is closer than the abutment to the midpoint of the span.

F The safety factor is finally determined by dividing the structural capacity of the windguy, f_{Rd} with the maximum force $T_{w,max}$. If the safety factor exceeds 1, the design is correct.

Windties

The windties connects the bridge to the windguy. The length of the windties can be determined with a series of parabolas that describes the shape of the bridge and the windguy in both plan and elevation.

Windties			
	tan(γ)	0,268	
Inclination parabola plane - horizontal plane	γ	15,02718544	deg
Horizontal distance windguy - windtie connection at walkway vertex	y_{lp}	1,54	m
Vertical distance windguy - windtie connection at walkway vertex	Δh_{lp}	0,413425009	m
Parabola 4			
	a_4	0,002666667	
	c_4	1,54	
Parabola 1			
	a_1	0,001244444	
	c_1	0,413425009	
Parabola 2			
	a_2	-0,000717613	
	c_2	0	
Parabola 3			
	a_3	-0,000717613	
	c_3	0	

Figure 9.8 Windties properties

γ The inclination between the windtie at the walkway vertex and the horizontal plane.

y_{lp} The horizontal distance from the windguy to the wintie connecting bolt at the vertex of the walkway.

Δh_{lp} The vertical distance from the windguy to the wintie connecting bolt at the vertex of the walkway.

$Parabola\ 1$ The parabola that describes the elevation of the suspended bridge.

$Parabola\ 2$ The parabola that describes the elevation of the windguy to the right side of the walkway vertex.

$Parabola\ 3$ The parabola that describes the elevation of the windguy to the left side of the walkway vertex.

$Parabola\ 4$ The parabola that describes the plan of the windguy.

The parabola equation used is:

$$y\ or\ z = a_i \cdot x^2 + c_i$$

where x is parallel to the bridge axis. The parabolas and the geometry can be seen in the design guide.

Finally the length of the windties is determined.

				Length of winties		
windtie	Horizontal distance from vertex	Δh_i	y_i	c/c_i		
1	72,0	10,58	15,36	18,66		
2	66,0	8,96	13,16	15,92		
3	60,0	7,48	11,14	13,42		
4	54,0	6,13	9,32	11,15		
5	48,0	4,93	7,68	9,13		
6	42,0	3,87	6,24	7,35		
7	36,0	2,96	5,00	5,81		
8	30,0	2,18	3,94	4,50		
9	24,0	1,54	3,08	3,44		
10	18,0	1,05	2,40	2,62		
11	12,0	0,70	1,92	2,05		
12	6,0	0,48	1,64	1,71		
13	0,0	0,41	1,54	1,59	Remember to shift from parabola 2	
14	-6,0	0,48	1,64	1,71	to parabola 3 when x < 0	
15	-12,0	0,70	1,92	2,05		
16	-18,0	1,05	2,40	2,62		
17	-24,0	1,54	3,08	3,44		
18	-30,0	2,18	3,94	4,50		
19	-36,0	2,96	5,00	5,81		
20	-42,0	3,87	6,24	7,35		
21	-48,0	4,93	7,68	9,13		
22	-54,0	6,13	9,32	11,15		
23	-60,0	7,48	11,14	13,42		
24	-66,0	8,96	13,16	15,92		
25	-72,0	10,58	15,36	18,66		

Figure 9.9 Length of windties

As it can be seen in the figure above, it's important to use parabola 2 for values x>0 and parabola for values x<0.

Finally, note that if a non-symmetric bridge is designed, formulas might need to be changed. Please check the Long Span Trail Bridge Standard in this case.

9.2 Natural frequencies and appurtenant modes

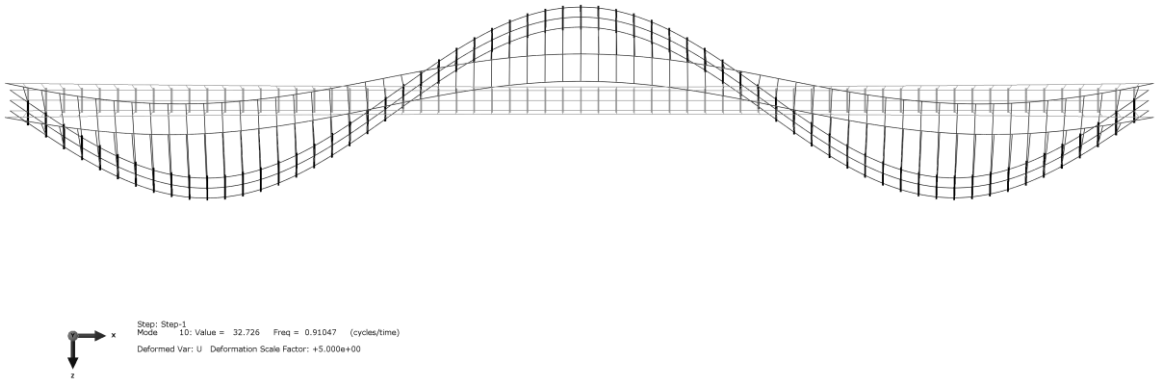

Figure 9.10 Third out of plane mode shape for Jicaro Bridge

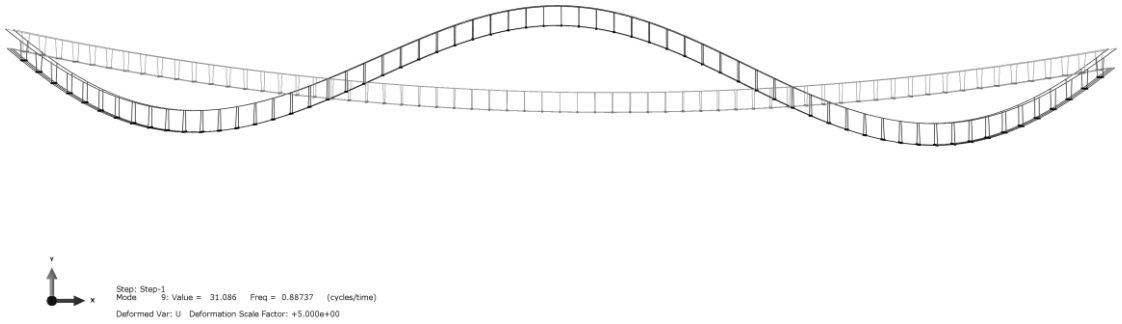

Figure 9.11 Second in-plane mode shape for Jicaro Bridge

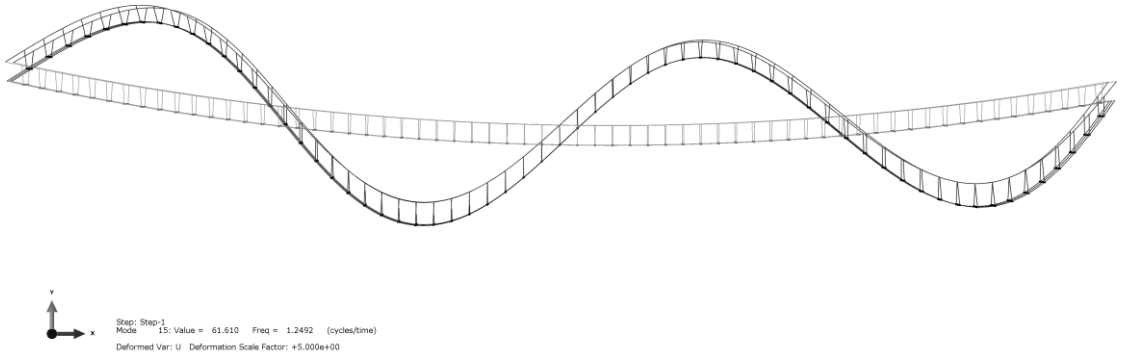

Figure 9.12 Third in-plane mode shape for Jicaro Bridge

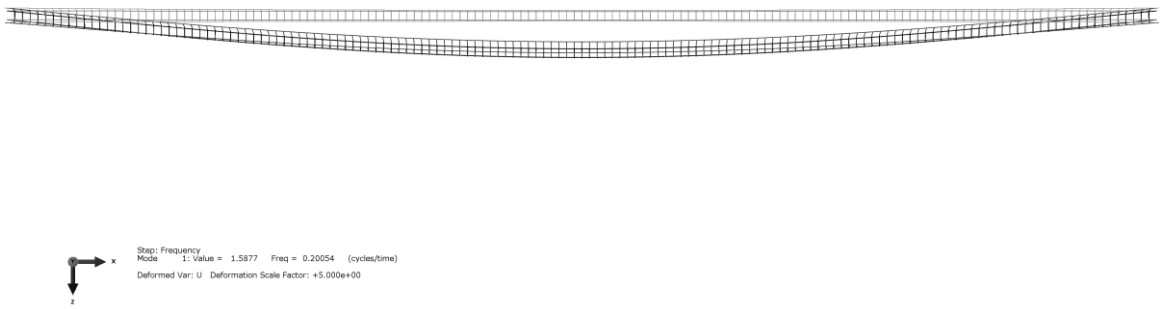

Figure 9.13 First out of plane mode shape for 150 m span bridge

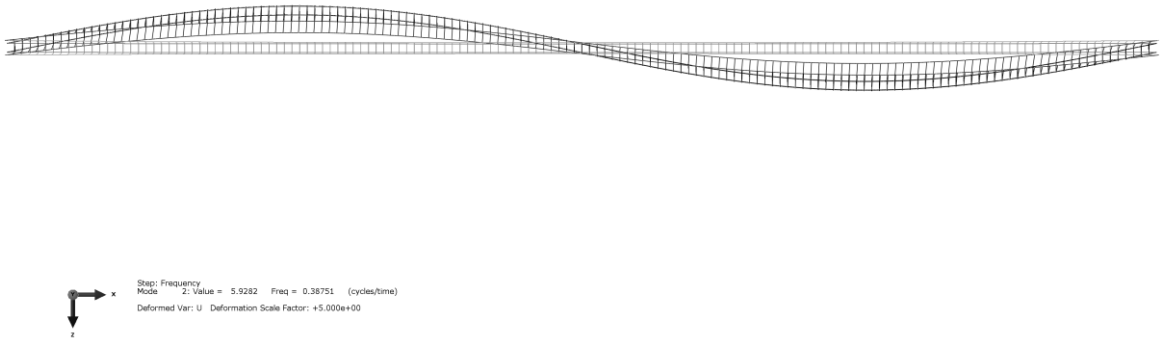

Figure 9.14 Second out of plane mode shape for 150 m span bridge

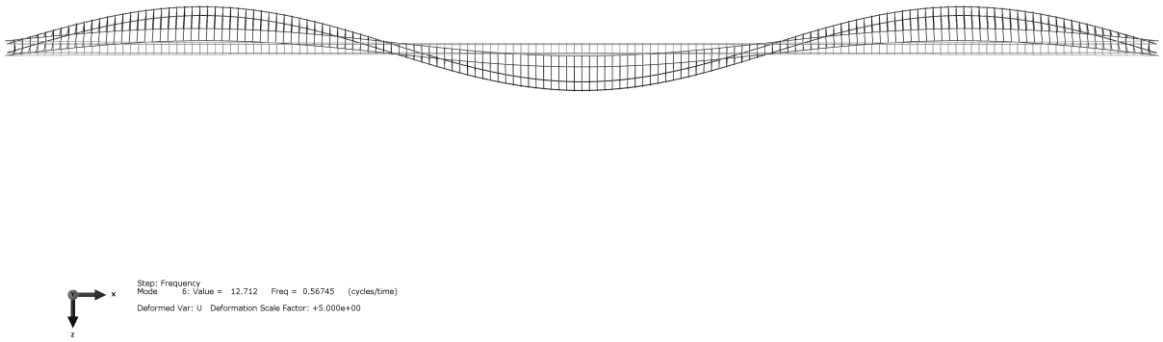

Figure 9.15 Third out of plane mode shape for 150 m span bridge

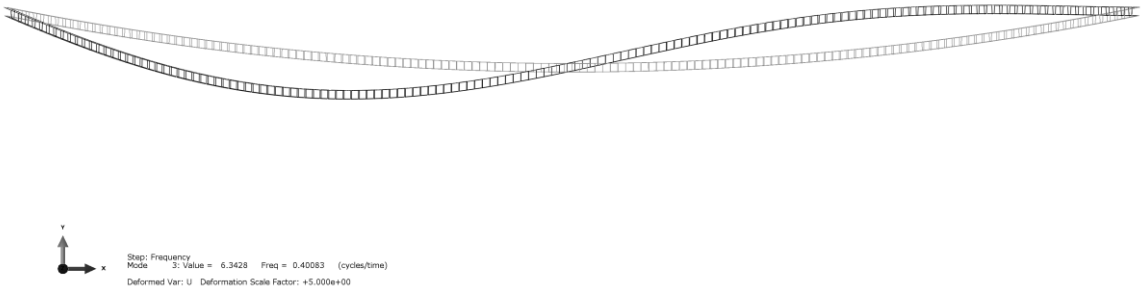

Figure 9.16 First in-plane mode shape for 150 m span bridge

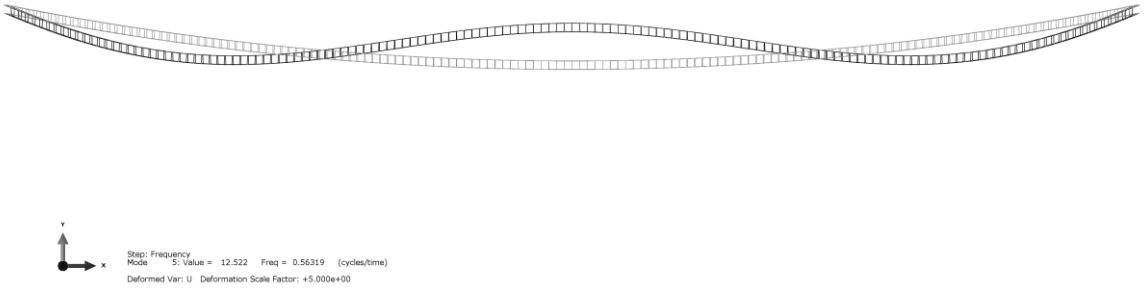

Figure 9.17 Second in-plane mode shape for 150 m span bridge

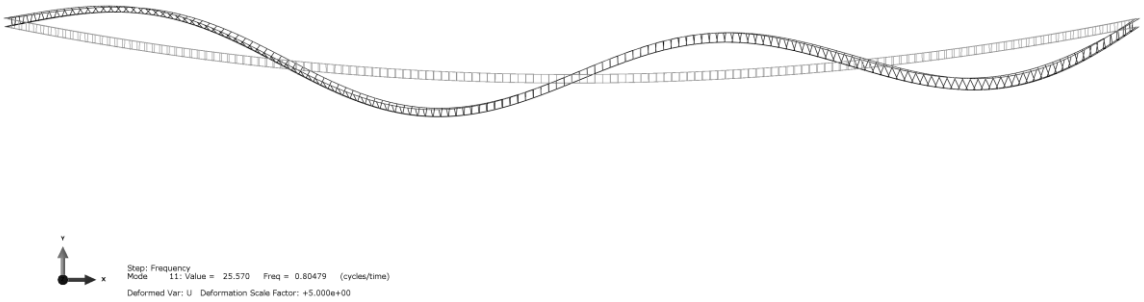

Figure 9.18 Third in-plane mode shape 150 m span bridge

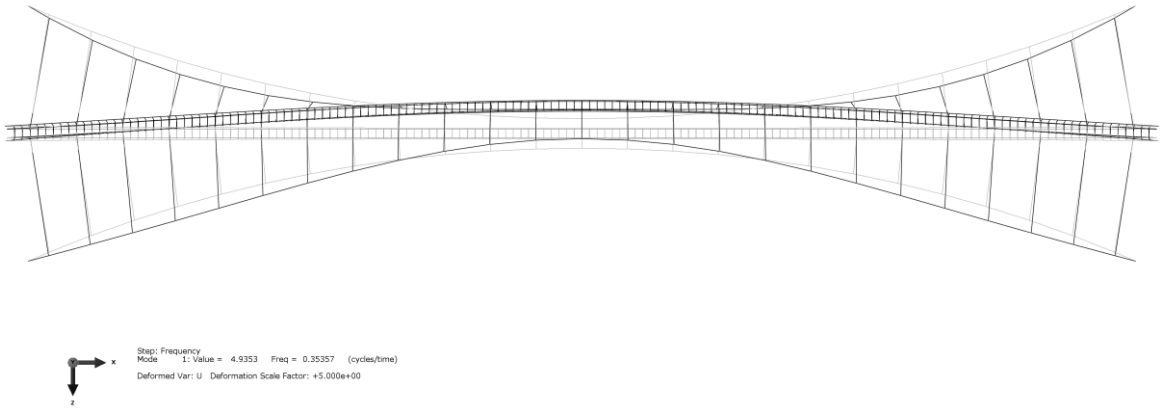

Figure 9.19 First out of plane mode shape 150 m span bridge with windguys

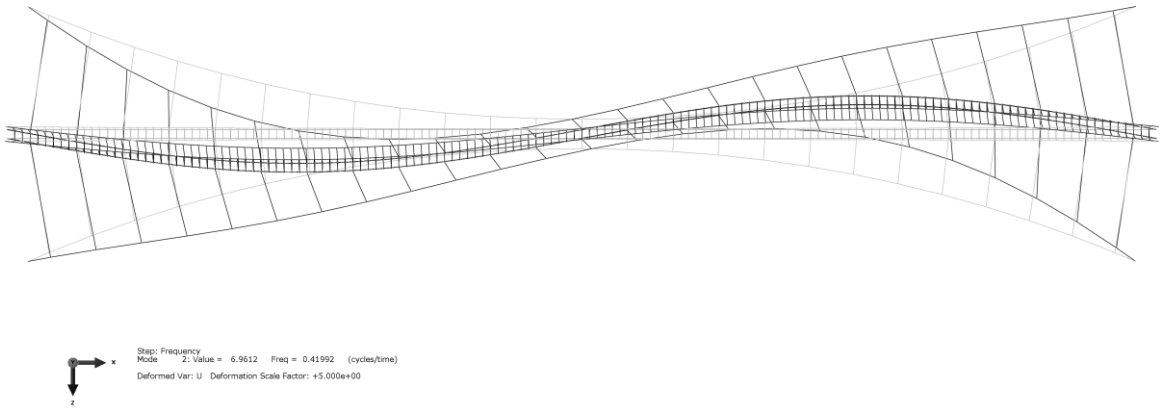

Figure 9.20 Second out of plane mode shape 150 m span bridge with windguys

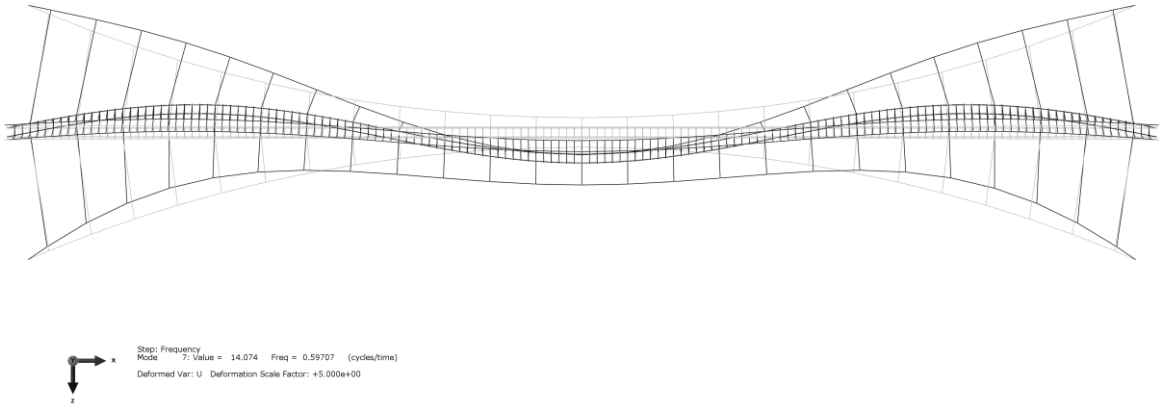

Figure 9.21 Third out of plane mode shape 150 m span bridge with windguys

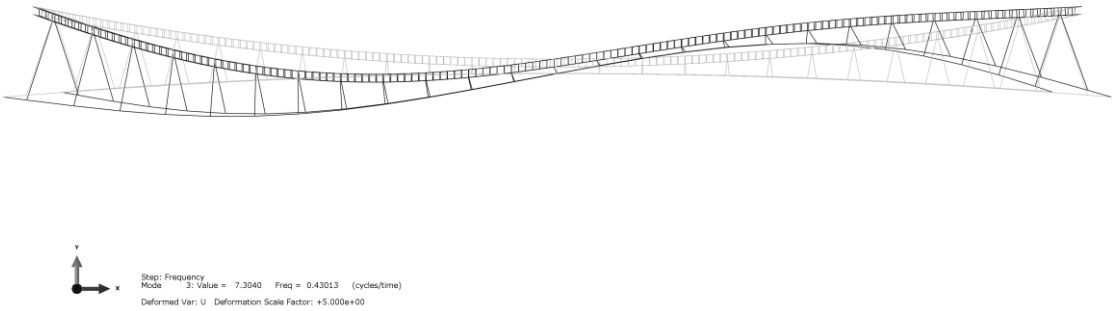

Figure 9.22 First in-plane mode shape 150 m span bridge with windguys

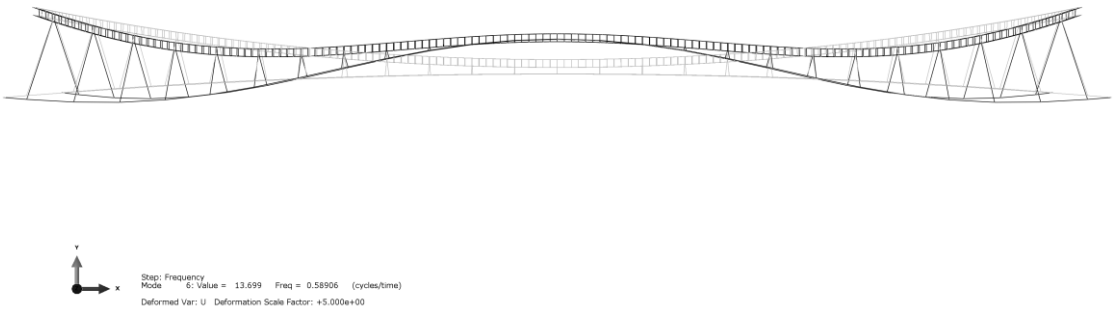

Figure 9.23 Second in-plane mode shape 150 m span bridge with windguys

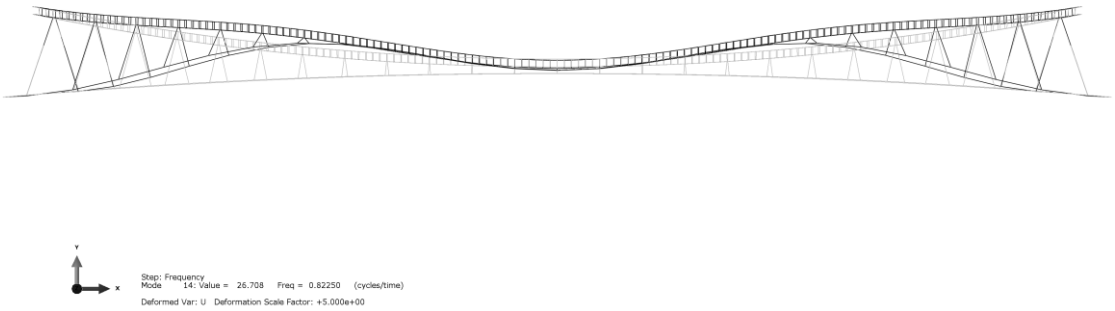

Figure 9.24 Third in-plane mode shape 150 m span bridge with windguys

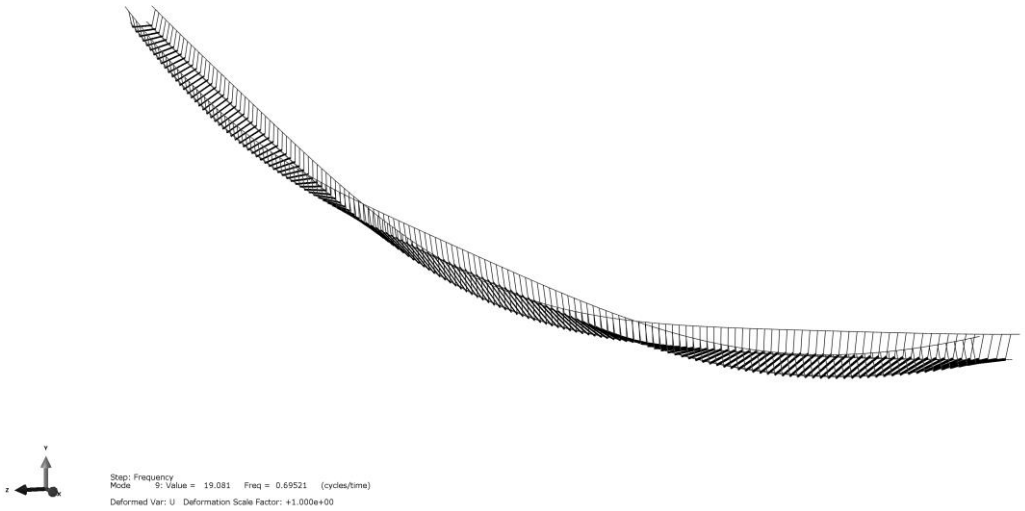

Figure 9.25 Second torsional mode shape 150 m span bridge

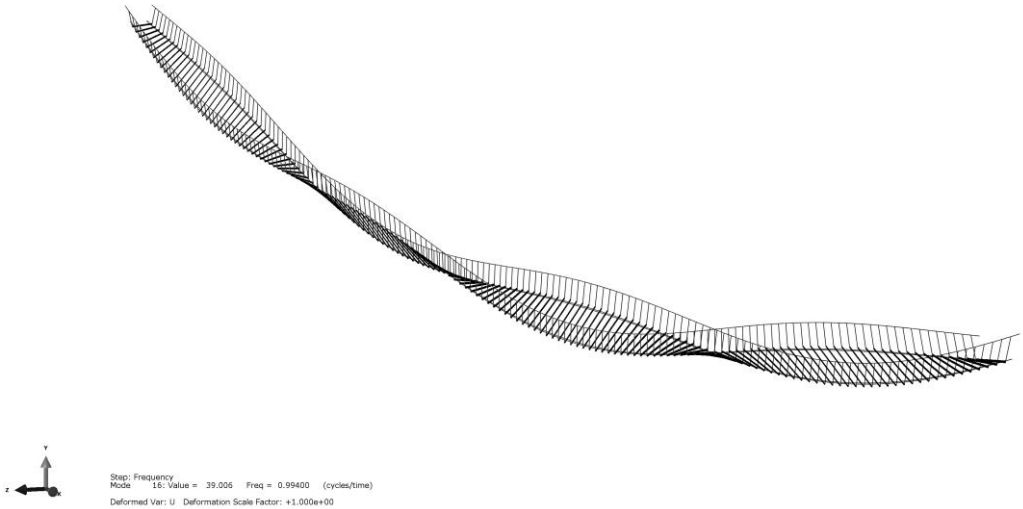

Figure 9.26 Third torsional mode shape 150 m span bridge